
Correlation of C_v and K_{Ic}/K_{Jc} Transition Temperature Increases Due to Irradiation

Prepared by A. L. Hiser

Materials Engineering Associates, Inc.

Prepared for
U.S. Nuclear Regulatory
Commission

8512270355 851130
PDR NUREG
CR-4395 R PDR

NOTICE

This report was prepared as an account of work sponsored by an agency of the United States Government. Neither the United States Government nor any agency thereof, or any of their employees, makes any warranty, expressed or implied, or assumes any legal liability of responsibility for any third party's use, or the results of such use, of any information, apparatus, product or process disclosed in this report, or represents that its use by such third party would not infringe privately owned rights.

NOTICE

Availability of Reference Materials Cited in NRC Publications

Most documents cited in NRC publications will be available from one of the following sources:

1. The NRC Public Document Room, 1717 H Street, N.W.
Washington, DC 20555
2. The Superintendent of Documents, U.S. Government Printing Office, Post Office Box 37082,
Washington, DC 20013-7082
3. The National Technical Information Service, Springfield, VA 22161

Although the listing that follows represents the majority of documents cited in NRC publications, it is not intended to be exhaustive.

Referenced documents available for inspection and copying for a fee from the NRC Public Document Room include NRC correspondence and internal NRC memoranda; NRC Office of Inspection and Enforcement bulletins, circulars, information notices, inspection and investigation notices; Licensee Event Reports; vendor reports and correspondence; Commission papers; and applicant and licensee documents and correspondence.

The following documents in the NUREG series are available for purchase from the GPO Sales Program: formal NRC staff and contractor reports, NRC-sponsored conference proceedings, and NRC booklets and brochures. Also available are Regulatory Guides, NRC regulations in the *Code of Federal Regulations*, and *Nuclear Regulatory Commission Issuances*.

Documents available from the National Technical Information Service include NUREG series reports and technical reports prepared by other federal agencies and reports prepared by the Atomic Energy Commission, forerunner agency to the Nuclear Regulatory Commission.

Documents available from public and special technical libraries include all open literature items, such as books, journal and periodical articles, and transactions. *Federal Register* notices, federal and state legislation, and congressional reports can usually be obtained from these libraries.

Documents such as theses, dissertations, foreign reports and translations, and non-NRC conference proceedings are available for purchase from the organization sponsoring the publication cited.

Single copies of NRC draft reports are available free, to the extent of supply, upon written request to the Division of Technical Information and Document Control, U.S. Nuclear Regulatory Commission, Washington, DC 20555.

Copies of industry codes and standards used in a substantive manner in the NRC regulatory process are maintained at the NRC Library, 7920 Norfolk Avenue, Bethesda, Maryland, and are available there for reference use by the public. Codes and standards are usually copyrighted and may be purchased from the originating organization or, if they are American National Standards, from the American National Standards Institute, 1430 Broadway, New York, NY 10018.

Correlation of C_v and K_{Ic}/K_{Jc} Transition Temperature Increases Due to Irradiation

Manuscript Completed: September 1985
Date Published: November 1985

Prepared by
A. L. Hiser

Materials Engineering Associates, Inc.
9700-B George Palmer Highway
Lanham, MD 20706-1837

Prepared for
Division of Engineering Technology
Office of Nuclear Regulatory Research
U.S. Nuclear Regulatory Commission
Washington, D.C. 20555
NRC FIN B8900

ABSTRACT

Reactor pressure vessel (RPV) surveillance capsules contain Charpy-V (C_v) specimens, but many do not contain fracture toughness specimens; accordingly, the radiation-induced shift (increase) in the brittle-to-ductile transition region (ΔT) is based upon the ΔT determined from notch ductility (C_v) tests. Since the ASME K_{IC} and K_{IR} reference fracture toughness curves are shifted by the ΔT from C_v , assurance that this ΔT does not underestimate ΔT associated with the the actual irradiated fracture toughness is required to provide confidence that safety margins do not fall below assumed levels.

To assess this behavior, comparisons of ΔT 's defined by elastic-plastic fracture toughness and C_v tests have been made using data from RPV base and weld metals in which irradiations were made under test reactor conditions. Using "as-measured" fracture toughness values (K_{JC}), average comparisons between $\Delta T(C_v)$ and $\Delta T(K_{JC})$ are:

- (a) All data: $\Delta T(K_{IC} @ 100 \text{ MPa}\sqrt{\text{m}}) = \Delta T(C_v @ 41 \text{ J}) + 9^\circ\text{C}$
- (b) Plates only: $\Delta T(K_{JC} @ 100 \text{ MPa}\sqrt{\text{m}}) = \Delta T(C_v @ 41 \text{ J}) + 22^\circ\text{C}$
- (c) Welds only: $\Delta T(K_{JC} @ 100 \text{ MPa}\sqrt{\text{m}}) = \Delta T(C_v @ 41 \text{ J}) - 5^\circ\text{C}$

When the fracture toughness data are adjusted to account for specimen size using a " β_{IC} correction," average comparisons are:

- (a) All data: $\Delta T(K_{\beta C} @ 75 \text{ MPa}\sqrt{\text{m}}) = \Delta T(C_v @ 41 \text{ J}) \pm 0^\circ\text{C}$
- (b) Plates only: $\Delta T(K_{\beta C} @ 75 \text{ MPa}\sqrt{\text{m}}) = \Delta T(C_v @ 41 \text{ J}) + 10^\circ\text{C}$
- (c) Welds only: $\Delta T(K_{\beta C} @ 75 \text{ MPa}\sqrt{\text{m}}) = \Delta T(C_v @ 41 \text{ J}) - 11^\circ\text{C}$

Comparison of ΔT 's at various index levels implies that the C_v curve for irradiated material tends to be shallower than that for unirradiated material. However, the shape of the K_{JC} curve for irradiated and unirradiated material is the same, but the $K_{\beta C}$ curve for irradiated material is steeper than that for unirradiated material.

Comparisons between measured $\Delta T(C_v)$ and values predicted using various correlations or models are also made. In this case, correlations give accurate-to-slightly-nonconservative average estimates of the measured $\Delta T(C_v @ 41 \text{ J})$ for base metals. For welds, the predicted ΔT values average more than 15°C above the measured $\Delta T(C_v @ 41 \text{ J})$.

CONTENTS

	<u>Page</u>
ABSTRACT.....	iii
LIST OF FIGURES.....	vii
LIST OF TABLES.....	ix
ACKNOWLEDGEMENT.....	xi
 1. INTRODUCTION.....	 1
2. MATERIALS.....	2
3. DATA ANALYSIS PROCEDURES.....	2
3.1 Notch Ductility (C_v).....	2
3.2 Fracture Toughness (K_{Jc}).....	4
3.3 Fracture Toughness Data with the Irwin β_{Ic} Adjustment ($K_{\beta c}$).....	5
4. TEST METHOD COMPARISONS.....	7
4.1 Charpy-V vs. K_{Jc}	7
4.2 Charpy-V vs. $K_{\beta c}$	8
4.3 K_{Jc} vs. $K_{\beta c}$	16
4.4 Curve-Fit vs. Eyeball.....	16
4.5 Other Comparisons.....	21
5. COMPARISONS OF CHARPY-V SHIFTS WITH CORRELATIONS.....	31
5.1 Guthrie Trend Curves - 1983.....	31
5.2 Odette/Perrin Correlations - 1984.....	32
5.3 Metal Properties Council - 1983.....	32
5.4 ASTM E 900 - 1983.....	33
5.5 Varsik - 1983.....	33
5.6 Varsik and Byrne - 1979.....	35
5.7 Heller and Lowe - 1984.....	36
5.8 Berggren and Stallman - 1983.....	36
5.9 Regulatory Guide 1.99 Rev. 1 - 1977.....	37
5.10 Draft Revision 2 to Regulatory Guide 1.99 - 1985.....	37
5.11 NRC Screening Criteria - 1982.....	37
5.12 C_v Comparisons.....	38
5.13 K_{Jc} Comparisons.....	38
5.14 $K_{\beta c}$ Comparisons.....	41
6. DISCUSSION.....	41
7. SUMMARY AND CONCLUSIONS.....	43
REFERENCES.....	45
Appendix A Comparison Plots of Measured and Predicted $\Delta T(C_v @ 41 J)$	A-1
Appendix B Comparison Plots of Measured $\Delta T(K_{Jc} @ 100 MPa/\sqrt{m})$ and Predicted $\Delta T(C_v @ 41 J)$	B-1

LIST OF FIGURES

<u>Figure</u>		<u>Page</u>
1	Comparison of ΔT 's from C_v at 41 J and K_{Jc} at 100 MPa \sqrt{m} , for base metals.....	9
2	Comparison of ΔT 's from C_v at 41 J and K_{Jc} at 100 MPa \sqrt{m} , for weld metals.....	9
3	Comparison of ΔT 's from C_v at 41 J and K_{Jc} at 100 MPa \sqrt{m} , for all of the data.....	10
4	Comparison of C_v and K_{Jc} data for the A508-2 forging.....	12
5	Comparison of ΔT 's from C_v at 41 J and K_{Bc} at 75 MPa \sqrt{m} , for base metals.....	13
6	Comparison of ΔT 's from C_v at 41 J and K_{Bc} at 75 MPa \sqrt{m} , for weld metals.....	13
7	Comparison of ΔT 's from C_v at 41 J and K_{Bc} at 75 MPa \sqrt{m} , for all of the data.....	15
8	Comparison of ΔT 's from K_{Jc} at 100 MPa \sqrt{m} and K_{Bc} at 75 MPa \sqrt{m} , for base metals.....	17
9	Comparison of ΔT 's from K_{Jc} at 100 MPa \sqrt{m} and K_{Bc} at 75 MPa \sqrt{m} , for weld metals.....	17
10	Comparison of C_v temperatures at 41 J determined from manual fits to the data and computerized fits.....	20
11	Comparison of $\Delta T(C_v @ 41 J)$ determined from manual and computerized fits to the data.....	20
12	Comparison of C_v upper shelf level determined from manual and computerized fits to the data.....	22
13	Comparison of C_v upper shelf drop determined from manual and computerized fits to the data.....	22
14	Comparison of K_{Jc} temperature at 100 MPa \sqrt{m} from manual and computerized fits to the data.....	23
15	Comparison of $\Delta T(K_{Jc} @ 100 MPa\sqrt{m})$ determined from manual and computerized fits to the data.....	23
16	Comparison of K_{Bc} temperature at 75 MPa \sqrt{m} determined from manual and computerized fits to the data.....	24
17	Comparison of $\Delta T(K_{Bc} @ 75 MPa\sqrt{m})$ determined from manual and computerized fits to the data.....	24
18	Comparison of $\Delta T(C_v)$ as determined at 41 J and 68 J.....	25

LIST OF FIGURES

<u>Figure</u>		<u>Page</u>
19	Comparison of $\Delta T(K_{Jc})$ determined at 75 MPa/ \sqrt{m} and 100 MPa/ \sqrt{m}	28
20	Comparison of $\Delta T(K_{Jc})$ at 100 MPa/ \sqrt{m} and 150 MPa/ \sqrt{m}	28
21	Comparison of $\Delta T(K_{Bc})$ at 75 MPa/ \sqrt{m} and 100 MPa/ \sqrt{m}	30

LIST OF TABLES

<u>Table</u>		<u>Page</u>
1	Chemistry and Fluence Values for the Subject Heats....	3
2	Statistical Comparisons Between $\Delta T(C_v)$ and $\Delta T(K_{JC})$	11
3	Statistical Comparisons Between $\Delta T(C_v)$ and $\Delta T(K_{\beta C})$	14
4	Statistical Comparisons Between $\Delta T(K_{JC})$ and $\Delta T(K_{\beta C})$	18
5	Comparison of Manual-Fit and Computerized-Fit Results....	19
6	Statistical Comparisons Between $\Delta T(C_v)$ at Indices of 41 J and 68 J.....	26
7	Statistical Comparisons Between $\Delta T(K_{JC} @ 100 \text{ MPa}/\sqrt{\text{m}})$ with Alternate Indices of 75 and 150 $\text{MPa}/\sqrt{\text{m}}$	27
8	Statistical Comparisons Between $\Delta T(K_{\beta C})$ at Indices of 75 and 100 $\text{MPa}/\sqrt{\text{m}}$	29
9	Constants for MPC Mean ΔT Equation (Ref. 11)....	34
10	Constants for MPC Upper Bound ΔT Equation (Ref. 11)....	34
11	Constants for Varsik ΔT Equation (Ref. 13).....	35
12	Comparison of Measured $\Delta T(C_v @ 41 \text{ J})$ with Correlation Predictions.....	39
13	Comparison of Measured $\Delta T(K_{JC} @ 100 \text{ MPa}/\sqrt{\text{m}})$ with Correlation Predictions of $\Delta T(C_v @ 41 \text{ J})$	40
14	Comparison of Measured $\Delta T(K_{\beta C} @ 75 \text{ MPa}/\sqrt{\text{m}})$ with Correlation Predictions of $\Delta T(C_v @ 41 \text{ J})$	42

ACKNOWLEDGEMENT

The assistance of G. M. Callahan in compiling data, curvefitting and plotting the data is appreciated, along with J. L. Phillips and J. Kneipp for typing the manuscript.

The support of M. Vagins of the NRC is gratefully appreciated.

1. INTRODUCTION

As a nuclear power plant operates, the reactor pressure vessel (RPV) is exposed to neutron irradiation caused by the fission process. The effect of this neutron irradiation on the materials constituting the RPV (plates, welds and forgings) is generally to degrade the material properties. The extent of degradation is highly dependent on the chemical composition, product form, and processing history of the material, as well as the fluence and the irradiation temperature. Generally the degradation is demonstrated through increases in tensile properties (both yield and ultimate), decreases in upper shelf toughness, and increases in the brittle-to-ductile transition temperature, i.e., the temperature at which the material failure mode changes from brittle (cleavage) fracture to a ductile behavior, characterized by tearing of the material. Of these three responses of the material to the irradiation, the increase in the transition temperature is of prime consideration in assessing the potential for failure due to a pressurized thermal shock (PTS) or any other scenario under which relatively low RPV temperatures (much less than the operating temperature of 288°C) may be accompanied by significant pressure in the vessel.

In recognition of such concerns, Appendix G of 10CFR50 (Title 10, Part 50 of the Code of Federal Regulations) has established a PTS screening criterion of 270°F for plates, forgings and axial weld materials, and 300°F for circumferential weld materials. In each case, the criterion gives upper limits on the reference temperature, RT_{NDT} , as defined in the ASME code. RT_{NDT} is also used in an analytical sense to index the K_{IR} (reference stress intensity factor) curve in Appendix G of Section III of the ASME Code. Prior to operation of the RPV, determination of RT_{NDT} is a relatively simple task, involving tests of drop weight and Charpy-V notch (C_v) specimens. RT_{NDT} is defined in the ASME code as the greater of T_{NDT} (the nil-ductility transition temperature of drop-weight tests) and $T_{Cv} - 60^\circ F$, where T_{Cv} is either the index at which each C_v test (of three) "shall exhibit at least 35 mils lateral expansion and not less than 50 ft-lb absorbed energy" or the temperature at which the lower bound C_v curve exhibits 50 ft-lb and 35 mils. To account for irradiation effects, Appendix G of 10CFR50 states that "adjusted reference temperature" means the reference temperature as adjusted for irradiation effects by adding to RT_{NDT} the temperature shift (ΔT), measured at the 30-ft-lb (41-J) level, in the average Charpy curve for the irradiated material relative to that for the unirradiated material.

As with the determination of RT_{NDT} , the pre-operation critical stress intensity factor (K_{IC}) curve can be determined in a straight-forward manner for the RPV materials, assuming that the large test specimens required are available. After irradiation, it is difficult to measure the K_{IC} curve directly because the large specimens which would be required are prohibited in the space available for surveillance capsules. For calculation of pressure-temperature (P-T) curves, Appendix G of the 10 CFR 50 assumes that the K_{IC} curve of the irradiated material is defined by shifting the K_{IR} curve as indexed by the "adjusted reference temperature" mentioned above. (For accident

analyses, the K_{IC} curve in Appendix A of the Section XI of the ASME Code is used as the reference curve which is indexed at the "adjusted reference temperature.") However, it is necessary to establish whether or not the shift in the C_v curve at 41 J is an accurate or conservative estimation of the temperature shift in the K_{IC} curve in order to ensure that overestimation of the material toughness does not occur. This study combines the available fracture toughness and Charpy-V data (from the same material irradiation conditions), to assess the relationship between ΔT 's measured by each test type. [Since very large specimens are required to give valid K_{IC} data, the fracture toughness data used are from an elastic-plastic analysis (K_{JC}) and from a " β_{IC} correction" to the K_{JC} data ($K_{\beta c}$).] In this way, an assessment can be made of the degree of conservatism (or lack thereof) afforded by using ΔT from C_v to estimate ΔT for K .

2. MATERIALS

The materials used in this study have been characterized over several years, initially at the Naval Research Laboratory (NRL), and more recently at MEA. Included in the study are an A 508 forging, several heats of A 533-B and A 302-B plate, and submerged-arc welds made with Linde 80, Linde 0091 and Linde 124 fluxes. A listing of the material chemistries and fluences for the subject conditions is given in Table 1. All of the irradiations were conducted in test reactors, under accelerated flux conditions, at nominal temperatures of 288°C.

The four heats listed in Table 1 for which fluence data are not available (67C, 68A, 68C and 6A2) have variations in phosphorous, nickel and copper contents, and will be characterized to give more information about chemistry effects on ΔT comparisons.

3. DATA ANALYSIS PROCEDURES

3.1 Notch Ductility (C_v)

Notch ductility was determined using Charpy-V impact specimens. The Charpy-V energy ($C_v E$) data for each heat and condition (irradiated or unirradiated) were fit to a hyperbolic tangent function:

$$C_v E = A_0 + A_1 \tanh \left[\frac{T - T_0}{A_2} \right] \quad (1)$$

where A_0 , A_1 , A_2 and T_0 are determined through a nonlinear regression analysis. Both shelf (upper and lower) and transition data were included in the same fit to Eq. 1, as opposed to using only transition data for a transition region fit, etc. Since few data were determined in a lower shelf region, some of the fits drop to negative C_v levels at low temperatures. A non-negative lower shelf was not forced, since the purpose for using the chosen equation was to model the data and not to force the data to a model. (The "negative" C_v levels given by some of these fits do not have any impact on the results used here.)

Table 1 Chemistry and Fluence Values for the Subject Heats

Material	Code	Fluence (10^{19} n/cm ² , E > 1 MeV)	C	Mn	P	S	Si	Cr	Ni	Mo	Cu	V	Au	Sn	N	B
A 508-2 Forging	BCB ^c	2.8	0.212	0.63	0.006	0.012	0.26	0.38	0.55	0.62	0.036	0.002	0.006	0.011	0.013	0.0002
A 513-B Plate	CAB ^c	1.2, 1.7, 2.1	0.25	1.41	0.008	0.014	0.26	0.11	0.46	0.49	0.12	0.003	0.012	0.008	0.008	0.0007
	CBC ^c	4.4	0.21	1.45	0.006	0.009	0.23	0.05	0.55	0.64	0.013	0.003	0.035	0.015	0.014	0.0004
	3P ^d	2.66, 5.2, 5.2, 2.7, 1.3	0.20	1.26	0.011	0.018	0.25	0.10	0.56	0.45	0.12	a	a	a	a	a
	02C ^e	1.81	0.23	1.55	0.009	0.014	0.20	0.04	0.67	0.53	0.16	0.003	a	a	a	a
	67C	b	0.23	1.31	0.025	0.018	0.20	< 0.003	0.70	0.51	0.002	a	a	< 0.004	0.009	0.0004
	68A	b	0.23	1.31	0.003	0.017	0.22	< 0.003	0.70	0.52	0.30	a	a	0.004	0.010	0.0006
A 302-B Plate	N ^c F23 ^{c,d} 6A2	2.7 3.7, 2.87, 5.6, 5.6, 2.9, 1.4	0.24 0.24 0.23	1.34 1.34 1.29	0.011 0.011 0.002	0.023 0.023 0.013	0.23 0.23 0.22	0.11 0.11 a	0.18 0.18 0.045	0.51 0.51 0.53	0.20 0.20 0.28	0.001 0.001 a	a	0.037 0.037 0.004	0.008 a a	0.0001 a a
Welds (Linde 80 φ)	E19 ^c	0.1, 0.8, 2.3	0.12	1.37	0.007	0.013	0.53	0.04	0.59	0.44	0.43	a	a	0.01	0.011	0.01
	E23 ^c	0.7	0.11	1.36	0.008	0.013	0.52	0.04	0.60	0.44	0.24	a	a	0.01	0.013	0.01
	71A ^e	1.79	0.124	1.58	0.011	0.011	0.54	0.12	0.63	0.45	0.046	0.005	a	a	a	a
	W8A ^f	1.5, 2.2, 2.1	0.083	1.33	0.011	0.016	0.77	0.12	0.59	0.47	0.39	0.003	0.001	0.002	a	0.000
(Linde 0091 φ)	E2A ^c	0.7	0.16	1.25	0.005	0.009	0.17	0.04	0.59	0.44	0.37	a	a	0.01	0.011	0.01
	68A ^e	1.36	0.15	1.38	0.006	0.009	0.16	0.06	0.13	0.60	0.04	0.007	a	a	a	a
	69A ^e	1.19	0.14	1.19	0.010	0.009	0.19	0.09	0.10	0.54	0.12	0.005	a	a	a	a
	W9A ^f	1.5, 2.2, 2.1	0.19	1.24	0.010	0.008	0.23	0.10	0.70	0.49	0.39	a	a	0.003	a	a
(Linde 124 φ)	70A ^e	1.95	0.10	1.48	0.011	0.011	0.44	0.13	0.63	0.47	0.056	0.004	a	a	a	a
	E4 ^c	2.4	0.08	1.38	0.013	0.018	0.49	0.10	0.65	0.44	0.16	0.005	0.008	0.004	0.001	0.001

a Not determined

b Not available

c Ref. 1

d Ref. 2

e Ref. 3

f Ref. 4

A nonsloping upper shelf fit was used since justification for a sloping upper shelf was not evident for cases in which sufficient characterization of the upper shelf trends was available.

Once a given set of data had been fit to Eq. 1, the upper shelf level and the transition temperatures at various C_v indices were determined from:

$$\text{Upper Shelf Energy (USE)} = A_0 + A_1 \quad (2)$$

$$T_{\text{Index}} = T_0 + A_2 \tanh^{-1} \left[\frac{C_v E_{\text{Index}} - A_0}{A_1} \right] \quad (3)$$

where $C_v E_{\text{Index}}$ was selected as 41 J (30 ft-lb per Appendix G of 10CFR50) and 68 J (50 ft-lb).

3.2 Fracture Toughness (K_{Jc})

The fracture toughness data of interest here are only those within the brittle-to-ductile transition region. No data with stable crack growth of more than 0.15 mm are included.

The static fracture toughness data were determined using compact toughness (CT) specimens. These specimens were full thickness 1T- and 0.5T-CT designs, with several differences from the standard ASTM E 399 design. The major difference was in enlargement of the notch region to permit placement of razor blades on the "load line" for mounting of a displacement transducer. The enlargement of the notch forced an increased spacing of the pin holes and in some cases a reduction in the pin hole diameter. The pin hole changes were required to maintain sufficient ligaments above and below the holes to prevent bending or bulging of the ligaments.

Because of the small specimen size forced by the constraints of the test reactor irradiation facility, the maximum K_{Ic} levels which could be obtained by ASTM E 399 were below 50 MPa \sqrt{m} ($\sim 45 \text{ ksi}\sqrt{\text{in.}}$), much too low to provide a meaningful result. For cases in which only a K_Q number was obtainable, the J integral, an elastic-plastic fracture parameter, was used for data analysis. Specifically, the J value at test termination was taken to be J_{Crit} , since by definition that was the J value at the initiation of "crack growth," albeit fast cleavage fracture. A K_{Jc} value was then calculated from:

$$K_{Jc} = \sqrt{EJ_{\text{Crit}} / (1 - \nu^2)} \quad (4)$$

where E is Young's modulus at the test temperature, and ν is Poisson's ratio, taken as 0.3 for all of these data. For cases in which a K_{Ic} value could be determined from the test record, the K_{Jc} value from Eq. 4 (with $\nu = 0.3$) matched the K_{Ic} value within 5%.

As with the C_v data, the K_{Jc} data were modeled with a mathematical expression, in this case:

$$K_{Jc} = B_0 + B_1 e^{(T/B_2)} \quad (5)$$

where B_0 , B_1 , and B_2 are determined through a nonlinear regression analysis. Since the regression results were not restricted to $B_0 > 0$, in many cases the resultant curve will give negative K_{Jc} values at low temperatures.

The transition temperatures at various indices were determined from Eq. 5 in the following form:

$$T_{Index} = B_2 \ln \left[\frac{K_{Index} - B_0}{B_1} \right] \quad (6)$$

with K_{Index} values of 75, 100 and 150 MPa \sqrt{m} used. For comparisons with C_v data at 41 J (30 ft-lb), K_{Index} of 100 MPa \sqrt{m} was used. This use is supported by correlations from Rolfe and Novak (Ref. 5) and Sailors and Corten (Ref. 6). From Reference 5,

$$K_{Ic} = \sqrt{0.00022 E} (C_v)^{0.75} \quad (7)$$

and, with $E = 206800$ MPa and $C_v = 41$ J, then

$$K_{Ic} = 109 \text{ MPa}\sqrt{m}$$

From Reference 6,

$$K_{Ic} = 14.6 (C_v)^{0.5} \quad (8)$$

and with $C_v = 41$ J,

$$K_{Ic} = 93 \text{ MPa}\sqrt{m}$$

The average of these two is then ~ 100 MPa \sqrt{m} .

3.3 Fracture Toughness Data with the Irwin β_{Ic} Adjustment ($K_{\beta c}$)

For cases in which a K_{Ic} value could not be obtained from a fracture toughness test, an approximation to K_{Ic} better than K_{Jc} was sought. For such cases, Merkle (Ref. 7) has recommended use of the Irwin β_{Ic} adjustment (Ref. 8), to give small specimen fracture toughness values which "consistently vary within the same range as the values determined from larger valid LEFM specimens and large structural tests" (Ref. 7). Caveats to the use of this adjustment procedure are that

cleavage fracture should be the failure mechanism and not ductile tearing, the correct critical conditions are at the onset of unstable cleavage fracture and not the maximum load point and, finally, the testing should be performed in displacement control to accurately locate the cleavage point on the load-displacement record. The data used in this study were limited to the transition region, with cleavage fracture the failure mechanism, as preceded by no more than 0.15 mm of stable crack growth or blunting. All of these tests were conducted in displacement control, and the J value at the onset of cleavage fracture, termed J_{Crit} here, was used to calculate the K_{Jc} values. Therefore, all of the necessary conditions for using the β_{Ic} adjustments appear to be met.

From Reference 7,

$$\beta_c = \beta_{Ic} + 1.4 \beta_{Ic}^3 \quad (9)$$

$$\text{where } \beta_c = \frac{1}{B} \frac{K_c^2}{\sigma_{ys}}$$

$$\beta_{Ic} = \frac{1}{B} \frac{K_{\beta c}^2}{\sigma_{ys}}$$

and B = the specimen thickness
 σ_{ys} = the 0.2% offset yield stress at temperature
 $K_{\beta c}$ = "non-plane strain fracture toughness" = K_{Jc}
 $K_{\beta c}$ = to be solved for (this is differentiated from K_{Ic} since these are not true K_{Ic} values but simply approximations to K_{Ic} values).

Rearranging Eq. 9 gives:

$$\beta_{Ic}^3 + (5/7) \beta_{Ic} - (5/7) \beta_c = 0 \quad (10)$$

Several calculated parameters can be defined:

$$m = (5/14) \beta_c \quad (11)$$

$$A_1 = \sqrt{m^2 + \frac{(5/7)^3}{27}} + m \quad (12)$$

$$A_2 = A_1 - 2m \quad (13)$$

β_{Ic} can be calculated from:

$$\beta_{Ic} = A_1^{1/3} - A_2^{1/3} \quad (14)$$

and finally,

$$K_{\beta c} = \sigma_{ys} \sqrt{B \beta_{Ic}} \quad (15)$$

By definition, K_{Ic} values were not adjusted using this β_{Ic} procedure.

As with the K_{Jc} data, the $K_{\beta c}$ data were modeled with an exponential function:

$$K_{\beta c} = C_0 + C_1 e^{(T/C_2)} \quad (16)$$

with C_0 , C_1 and C_2 determined through a nonlinear regression analysis. Since C_0 is not limited to non-negative values, the best-fit curves may yield negative values at low temperatures.

The transition temperature at various indices was determined from Eq. 16 as follows:

$$T_{Index} = C_2 \ln \left[\frac{K_{Index} - C_0}{C_1} \right] \quad (17)$$

with K_{Index} values of 75 and 100 MPa \sqrt{m} . Since many of the $K_{\beta c}$ curves did exceed 75 MPa \sqrt{m} but few exceeded 100 MPa \sqrt{m} , comparisons with $C_v = 41$ J and $K_{Jc} = 100$ MPa \sqrt{m} were made at $K_{\beta c} = 75$ MPa \sqrt{m} .

4. TEST METHOD COMPARISONS

The focus in this section is on the change in temperature (ΔT) at a specific index due to irradiation, as opposed to the absolute temperature at the index level. Comparisons between ΔT 's from notch ductility and fracture toughness are based on product form, with comparisons at a C_v energy level of 41 J and fracture toughness levels from 75 to 150 MPa \sqrt{m} .

4.1 Charpy-V vs. K_{Jc}

Comparison of ΔT 's from C_v at 41 J [$\Delta T(C_v @ 41 J)$] and K_{Jc} at 100 MPa \sqrt{m} [$\Delta T(K_{Jc} @ 100 MPa\sqrt{m})$] reveals an interesting trend. In Fig. 1 for base metals, only three of the eighteen base metal points represent conservative estimates of $\Delta T(K_{Jc} @ 100 MPa\sqrt{m})$ by $\Delta T(C_v @ 41 J)$. All three of these points are from a single heat of A 533-B plate (the HSST 03 plate) tested as a part of the LWR-PV Dosimetry Improvement Program (Ref. 2). The largest deviation is for the A 508-2 forging, with $\Delta T(K_{Jc}) = 102^\circ C$ and $\Delta T(C_v) = 19^\circ C$. The base metals (excluding the A 508-2 forging which will be discussed later) have a $\Delta T(C_v)$ which averages $22^\circ C$ less than $\Delta T(K_{Jc})$.

In contrast to the base metal results, the welds (Fig. 2) illustrate good correspondence between $\Delta T(C_v)$ and $\Delta T(K_{Jc})$, at all ΔT levels. Here, $\Delta T(C_v)$ averages 5°C higher than $\Delta T(K_{Jc})$.

Combining both data sets (Fig. 3) illustrates the differences in the behavior of the two product forms. At high $\Delta T(K_{Jc})$ levels, the corresponding $\Delta T(C_v)$ for base metals is much less than the weld metal $\Delta T(C_v)$ levels. The A 508-2 forging point far exceeds any reasonable scatter band which one would draw around these data.

Table 2 gives linear least-squares fits to three different equations relating $\Delta T(C_v)$ to $\Delta T(K_{Jc})$:

$$\Delta T(K_{Jc}) = \Delta T(C_v)K_0 + K_1 \quad (18)$$

$$\Delta T(K_{Jc}) = \Delta T(C_v) + K_2 \quad (19)$$

$$\Delta T(K_{Jc}) = \Delta T(C_v)K_3 \quad (20)$$

with $\pm 1-\sigma$ levels also given. (These analyses were made excluding the A508-2 forging point, which is the only forging data in this data base.) While the latter two equations are simply less general subsets of the first, they are less complicated ways for adjusting non-conservative ΔT estimates.

Similar conclusions about $\Delta T(C_v)$ and $\Delta T(K_{Jc})$ can be made at K_{Jc} levels of 75 and 150 MPa \sqrt{m} (Table 2). For example, $\Delta T(C_v)$ for base metal tends to average 22°C less than $\Delta T(K_{Jc})$ while $\Delta T(C_v)$ for weld metal averages 6°C greater than $\Delta T(K_{Jc})$. In fact, the closeness of the K_2 values at each K_{Jc} level implies that on average the K_{Jc} curve for irradiated material is very similar in curvature to that for unirradiated material.

The C_v and K_{Jc} data available for the A 508-2 forging are illustrated in Fig. 4. While variations in the C_v data are such that the unirradiated and irradiated data overlap, the K_{Jc} data exhibit a distinct difference between unirradiated and irradiated specimen behavior. One cautionary note required here is that there are few irradiated K_{Jc} data points (only four) and these few points do exhibit considerable variability. Regardless of the variability consideration, major differences between C_v and K_{Jc} indications of the irradiation degradation are apparent.

4.2 Charpy-V vs. K_{Bc}

Comparison of $\Delta T(C_v)$ and that from K_{Bc} , i.e., $\Delta T(K_{Bc})$, reveals different behavior from the prior K_{Jc} comparisons. As illustrated in Fig. 5 for base metals, $\Delta T(K_{Bc} @ 75 \text{ MPa}\sqrt{m})$ is generally much closer to $\Delta T(C_v @ 41 \text{ J})$, than was $\Delta T(K_{Jc} @ 100 \text{ MPa}\sqrt{m})$. On average, $\Delta T(C_v)$ is only 10°C less than $\Delta T(K_{Bc})$ (Table 3), vs. 22°C less when compared to $\Delta T(K_{Jc})$. For weld metals (Fig. 6), the overall variation is significantly higher, with $\Delta T(C_v)$ averaging 11°C greater than $\Delta T(K_{Bc})$. With both plates and welds combined (Fig. 7), $\Delta T(C_v)$ is within 1°C of $\Delta T(K_{Bc})$, on average.

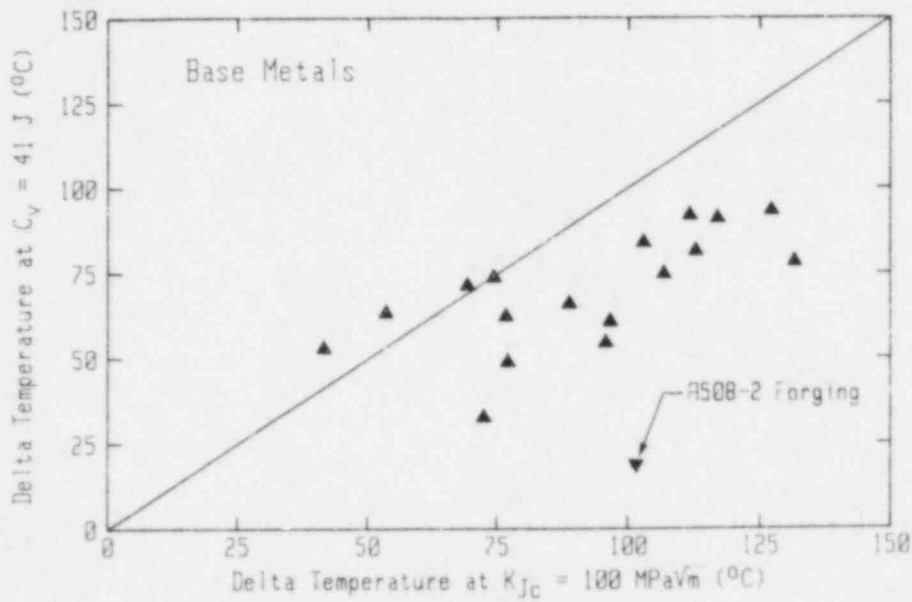


Fig. 1 Comparison of ΔT 's from C_v at 41 J and K_{Jc} at 100 MPa $\sqrt{\text{m}}$, for base metals. Only three data points exhibit conservative estimates of $\Delta T(K_{Jc})$ by $\Delta T(C_v)$, with the greatest nonconservative deviation from the A 508-2 forging.

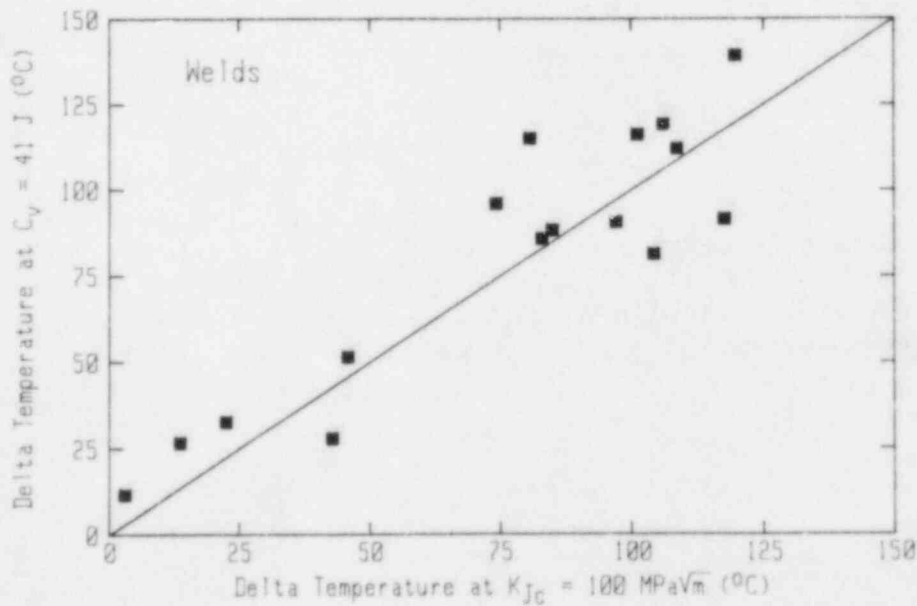


Fig. 2 Comparison of ΔT 's from C_v at 41 J and K_{Jc} at 100 MPa $\sqrt{\text{m}}$, for weld metals. As contrasted with Fig. 1, good agreement exists at all $\Delta T(K_{Jc})$ levels, with the tendency towards a conservative estimation of $\Delta T(K_{Jc})$ by $\Delta T(C_v)$.

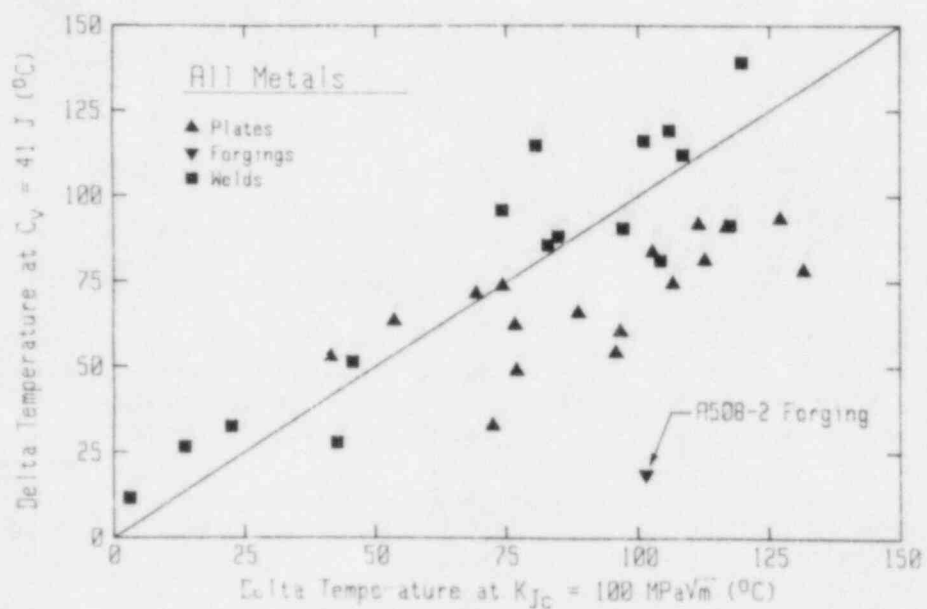


Fig. 3 Comparison of ΔT 's from C_v at 41 J and K_{Jc} at 100 MPa $\sqrt{\text{m}}$, for all of the data. Considerable scatter exists, especially at high $\Delta T(K_{Jc})$ levels, where the welds have good agreement with $\Delta T(C_v)$ and the base metals do not.

Table 2 Statistical Comparisons Between $\Delta T(C_v)$ and $\Delta T(K_{Jc})$ -- Eq. 18-20

C_v Level	K_{Jc} Level	Product Form	$\Delta T(K_{Jc}) = \Delta T(C_v)K_0 + K_1$			$\Delta T(K_{Jc}) = \Delta T(C_v) + K_2$			$\Delta T(K_{Jc}) = \Delta T(C_v)K_3$		
			K_0	K_1	$\pm 1\sigma$	K_2	$\pm 1\sigma$	1σ Range	K_3	$\pm 1\sigma$	$\pm 1\sigma$
(J)	(MPa \sqrt{m})			(°C)	(°C)	(°C)	(°C)	(°C)			(°C)
41	100	Base	1.039	19.3	18.6	22.0	18.6	+ 3.4:+40.6	1.303	0.260	19.1
		Weld	0.896	3.3	15.6	-5.1	16.1	-21.2:+11.0	0.929	0.171	15.7
		Both	0.835	21.2	21.4	8.9	22.0	-13.1:+30.9	1.081	0.280	22.8
	75	Base	1.106	12.6	20.6	19.9	20.7	- 0.8:+40.6	1.278	0.283	20.8
		Weld	0.908	1.9	15.3	-5.6	15.7	-21.3:+10.1	0.927	0.167	15.3
		Both	0.860	18.0	21.9	7.6	22.3	-14.7:+29.9	1.070	0.281	22.9
	150	Base	1.184	8.9	19.2	21.7	19.5	+ 2.2:+41.2	1.307	0.263	19.3
		Weld	0.987	-5.2	29.6	-6.3	29.6	-35.9:+23.3	0.933	0.324	29.6
		Both	0.929	13.5	28.2	8.2	28.3	-20.1:+36.5	1.085	0.352	28.7

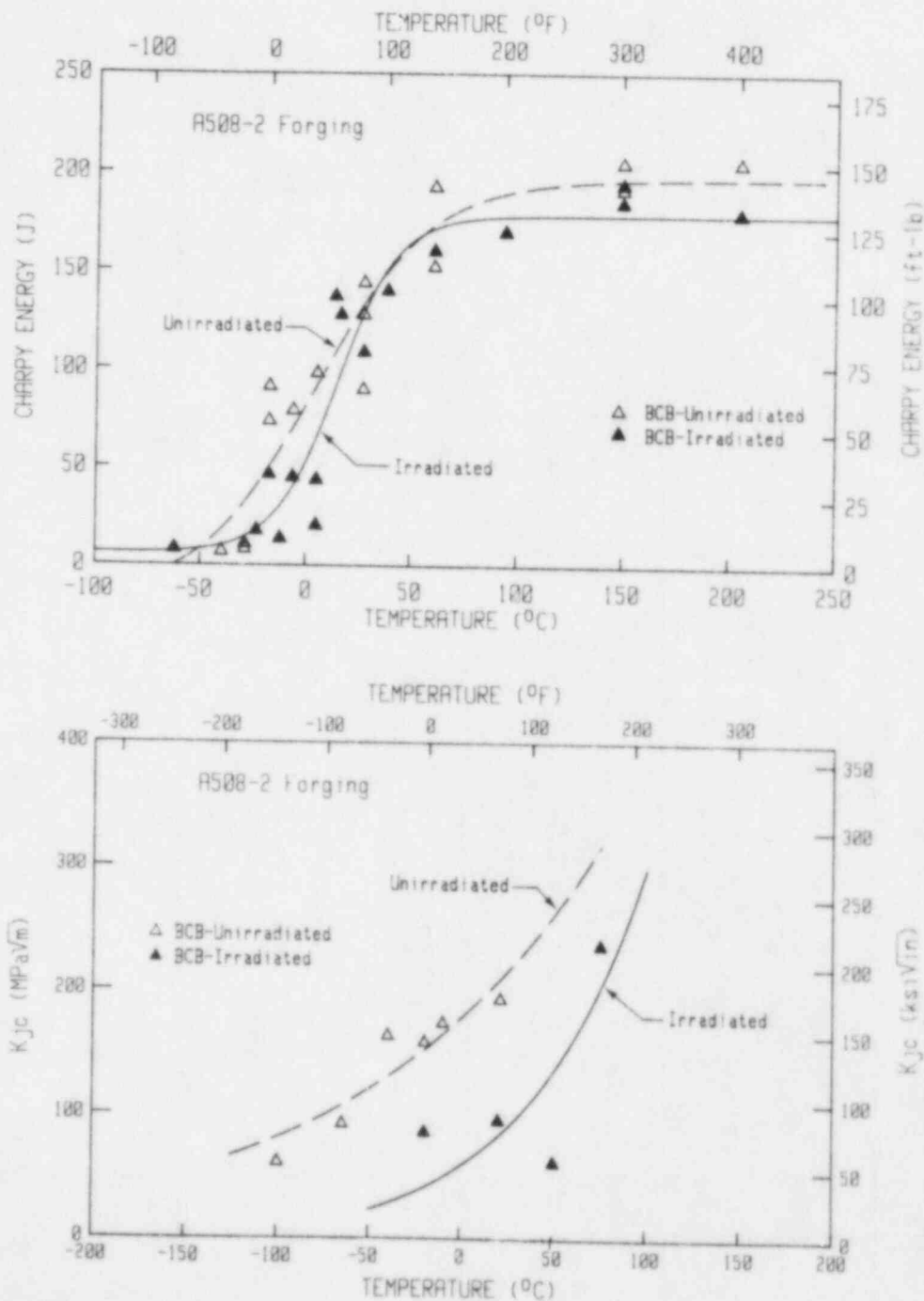


Fig. 4 Comparison of C_V and K_{JC} data for the A508-2 forging. While considerable variability is apparent for each data type, differences in irradiation effect are apparent: the C_V data show a small ΔT and the K_{JC} data have a much larger ΔT .

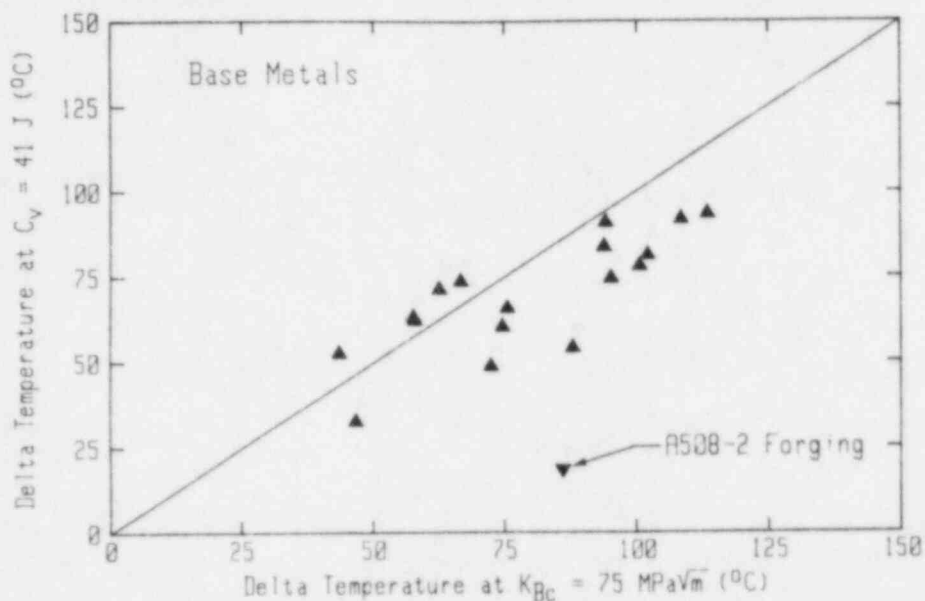


Fig. 5 Comparison of ΔT 's from C_v at 41 J and K_{Bc} at 75 MPa $\sqrt{\text{m}}$, for base metals. The situation here is similar to the K_{Jc} comparison in Fig. 1, with few $\Delta T(C_v)$ values exceeding the $\Delta T(K_{Bc})$ values. Again, the A 508-2 forging point far exceeds any reasonable scatter band.

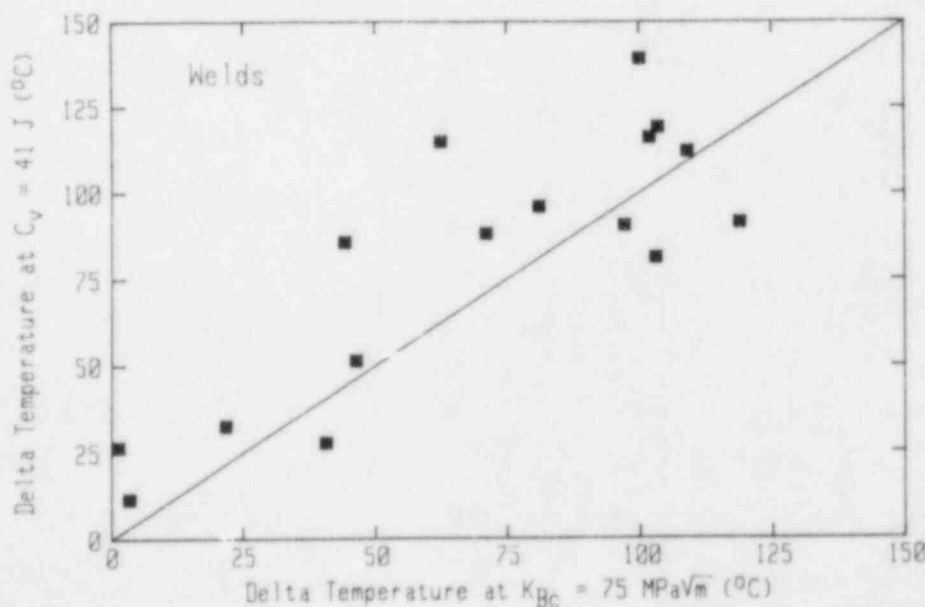


Fig. 6 Comparison of ΔT 's from C_v at 41 J and K_{Bc} at 75 MPa $\sqrt{\text{m}}$, for weld metals. As with K_{Jc} in Fig. 2, generally a conservative estimate of $\Delta T(K_{Bc})$ is made by $\Delta T(C_v)$, but the scatter here is much greater than for the K_{Jc} comparison.

Table 3 Statistical Comparisons Between $\Delta T(C_v)$ and $\Delta T(K_{\beta c})$

C_v Level	$K_{\beta c}$ Level	Product Form	$\Delta T(K_{\beta c}) = \Delta T(C_v)K_0 + K_1$			$\Delta T(K_{\beta c}) = \Delta T(C_v) + K_2$			$\Delta T(K_{\beta c}) = \Delta T(C_v)K_3$		
			K_0	K_1	$\pm 1\sigma$	K_2	$\pm 1\sigma$	1σ Range	K_3	$\pm 1\sigma$	$\pm 1\sigma$
(J)	(MPa \sqrt{m})			($^{\circ}C$)	($^{\circ}C$)	($^{\circ}C$)	($^{\circ}C$)	($^{\circ}C$)			($^{\circ}C$)
41	75	Base	1.028	8.2	13.3	10.2	13.3	- 3.1:+23.5	1.140	0.183	13.5
		Weld	0.839	1.7	21.1	-11.3	22.0	-33.3:+10.7	0.856	0.231	21.1
		Both	0.806	14.3	20.0	-0.2	20.8	-21.0:+20.6	0.972	0.254	20.7
41	100	Base	1.253	-26.6	21.2	-9.0	21.6	-30.6:+12.6	0.890	0.300	22.1
		Weld	0.785	-6.2	49.0	-23.5	49.7	-73.2:+26.2	0.722	0.536	49.1
		Both	0.821	-2.6	37.6	-16.0	38.0	-54.0:+22.0	0.790	0.462	37.6

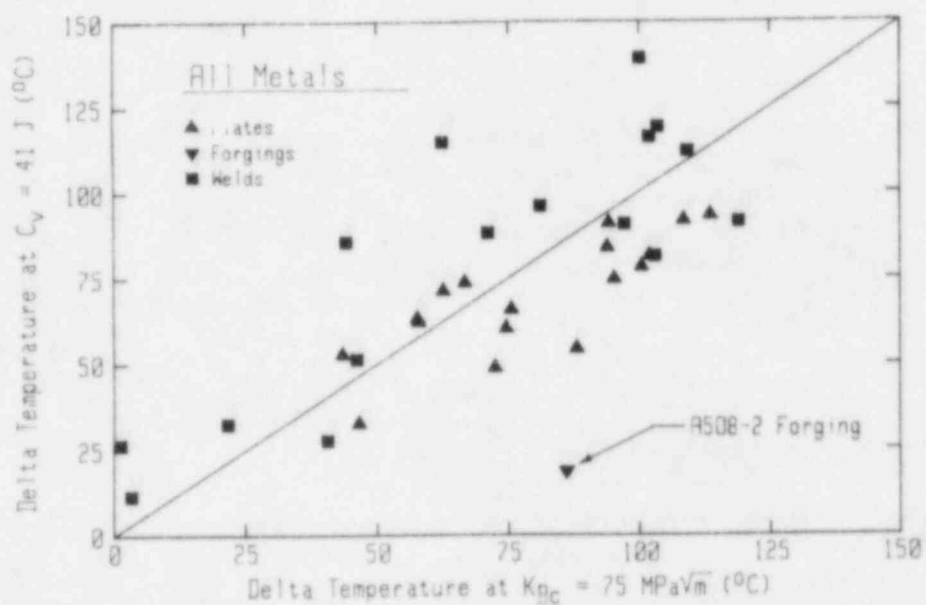


Fig. 7 Comparison of ΔT 's from C_v at 41 J and K_{IC} at 75 MPa $\sqrt{\text{m}}$, for all of the data. Considerable scatter is apparent.

At a $K_{\beta c}$ level of 100 MPa \sqrt{m} , the scatter increases significantly with 1- σ limits of $\pm 22^\circ\text{C}$ for base metals and $\pm 47^\circ\text{C}$ for welds (Table 3). In one case, $\Delta T(K_{\beta c} @ 100 \text{ MPa}\sqrt{m})$ is 150°C less than $\Delta T(K_{Jc} @ 100 \text{ MPa}\sqrt{m})$, with a $\Delta T(K_{\beta c})$ of -68°C at this level. This anomaly and in general the poor correspondence is at least partially attributable to an absence of $K_{\beta c}$ data above 80 MPa \sqrt{m} . This absence of data in combination with the very large reduction in unirradiated K level due to the β_{Ic} adjustment (and the much lower yield stress values for unirradiated material vs. irradiated material) lead to a question of the reliability of using $\Delta T(K_{\beta c})$ values extrapolated out to the 100 MPa \sqrt{m} level for these data; a recommendation here is to not include the latter in consideration of variances between $\Delta T(C_v)$ and $\Delta T(K)$.

4.3 K_{Jc} vs. $K_{\beta c}$

As mentioned above, the β_{Ic} adjustment has the effect of reducing high toughness, unirradiated K_{Jc} data much more than high toughness irradiated K_{Jc} data. Therefore, as a general rule, $\Delta T(K_{\beta c})$ will be less than $\Delta T(K_{Jc})$. In 73% of the cases, $\Delta T(K_{\beta c})$ is less than $\Delta T(K_{Jc})$, by as much as 39°C . In cases where $\Delta T(K_{\beta c})$ exceeds $\Delta T(K_{Jc})$, it does so by a maximum of 7°C . This correspondence is apparent in Fig. 8 for base metals and Fig. 9 for weld metals. From Table 4, on average the $\Delta T(K_{\beta c})$ for base metals is 12°C less than $\Delta T(K_{Jc})$, while for weld metals $\Delta T(K_{\beta c})$ is only 6°C less than $\Delta T(K_{Jc})$, on average.

4.4 Curve-Fit vs. Eyeball

Prior to this publication, all of the C_v (and most of the K_{Jc} and $K_{\beta c}$) data reported by current MEA personnel at MEA and earlier at the NRL had been analyzed using an eyeball or hand-fit method. This method does have advantages, such as the ability of an experienced user to synthesize a curve where insufficient data exist and "weighting" of data based upon historical perspectives. In general, however, the use of standardized computer routines for curve fitting guarantees a repeatable, unbiased fit, which is not user dependent. Since many of these C_v data (and other data not included here) originally were fit using a manual technique and form a unique data base used for assessing composition, fluence, and other effects on radiation sensitivity, comparison of the manual-fitting results with computerized results was considered germane to this study. These comparisons have been made for C_v data in terms of transition temperature (absolute) and ΔT at 41 J and 68 J. Additional comparisons were made for K_{Jc} and $K_{\beta c}$ data, with all of the results summarized in Table 5.

As is evident in Fig. 10 for all of the C_v temperatures at 41 J, excellent agreement exists at all levels, from low to high temperatures. In fact, the manual temperature overestimates the curve-fit temperature by less than 2°C on average, with base metals yielding an average overestimate less than 1°C and welds an average overestimate below 3°C (Table 5). The ΔT 's (Fig. 11) exhibit similar good agreement, with a 1- σ range of 6°C . Here, the weld ΔT 's yield a better average correspondence than the base metal ΔT 's.

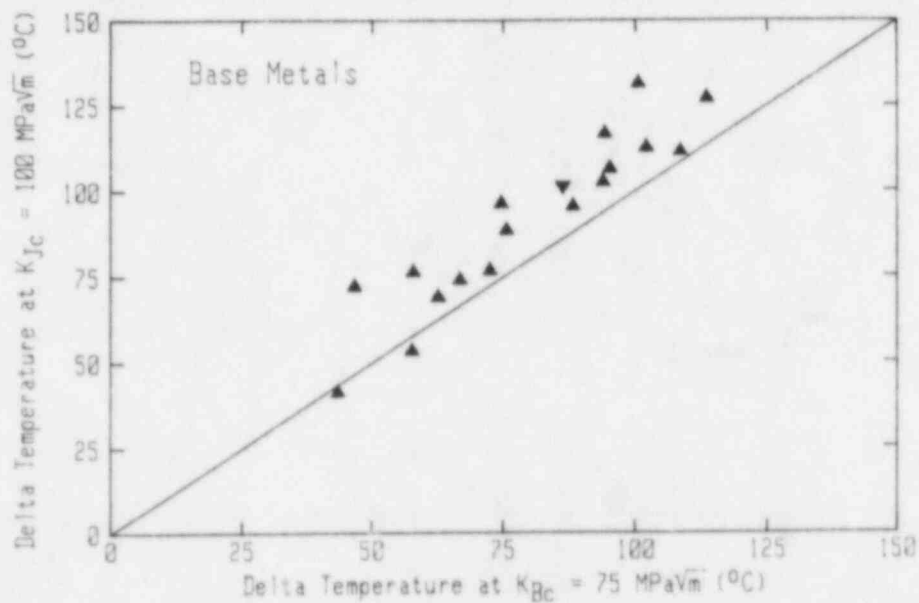


Fig. 8 Comparison of ΔT 's from K_{Jc} at $100 \text{ MPa}\sqrt{m}$ and K_{Bc} at $75 \text{ MPa}\sqrt{m}$, for base metals. Only in two cases does $\Delta T(K_{Bc})$ exceed $\Delta T(K_{Jc})$ at these levels.

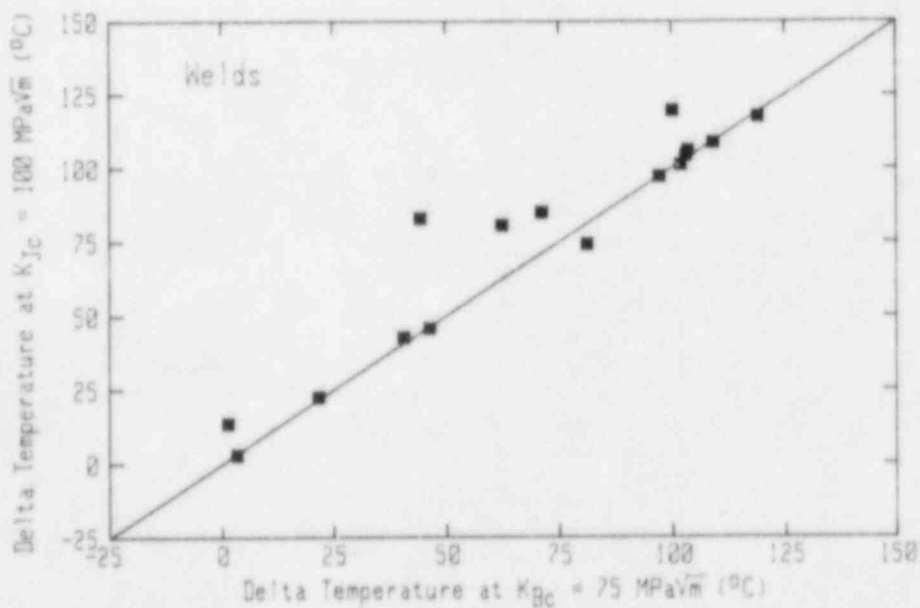


Fig. 9 Comparison of ΔT 's from K_{Jc} at $100 \text{ MPa}\sqrt{m}$ and K_{Bc} at $75 \text{ MPa}\sqrt{m}$, for weld metals. The correspondence here is much improved as compared to the base metal data.

Table 4 Statistical Comparisons Between $\Delta T(K_{Jc})$ and $\Delta T(K_{\beta c})$

K_{Jc} Level	$K_{\beta c}$ Level	Product Form	$\Delta T(K_{\beta c}) = \Delta T(K_{Jc})K_0 + K_1$			$\Delta T(K_{\beta c}) = \Delta T(K_{Jc}) + K_2$			$\Delta T(K_{\beta c}) = \Delta T(K_{Jc})K_3$		
			K_0	K_1	$\pm 1\sigma$	K_2	$\pm 1\sigma$	1σ Range	K_3	$\pm 1\sigma$	$\pm 1\sigma$
(J)	(MPa \sqrt{m})			(°C)	(°C)	(°C)	(°C)	(°C)			(°C)
100	75	Base	0.793	7.1	8.1	-11.9	9.6	-21.5:-2.3	0.865	0.085	8.3
		Weld	0.972	-4.1	11.5	-6.2	11.6	-17.8:+ 5.4	0.929	0.135	11.7
		Both	0.898	-0.6	10.3	-9.1	10.8	-19.9:+ 1.7	0.892	0.114	10.3

Table 5 Comparison of Manual-Fit and Computerized-Fit Results

Test Type- Index	Data Type	Product Form	Average Deviation	$\pm 1\sigma$
C_V -41J	T^a	Base	-0.6°C	$\pm 5.0^\circ\text{C}$
		Weld	-2.8	4.9
		Both	-1.6	5.0
	ΔT^b	Base	-1.4°C	5.5°C
		Weld	-0.1	6.0
		Both	-0.9	5.6
C_V -USE	Level ^c	Base	+0.4 J	2.9 J
		Weld	+2.2	3.4
		Both	+1.2	3.2
	Drop ^d	Base	+0.3 J	3.5 J
		Weld	+1.4	3.7
		Both	+0.8	3.5
K_{Jc} -100 MPa \sqrt{m}	T	Base	-0.4°C	7.4°C
		Weld	+0.7	6.2
		Both	+0.1	6.8
	ΔT	Base	+2.2°C	8.5°C
		Weld	-1.8	6.5
		Both	+0.4	7.8
$K_{\beta c}$ -75 MPa \sqrt{m}	T	Base	+0.9°C	3.6°C
		Weld	+0.0	5.7
		Both	+0.5	4.4
	ΔT	Base	+1.7°C	3.7°C
		Weld	-4.3	3.9
		Both	-0.5	4.7

^a Transition temperature

^b Transition temperature increase

^c Upper shelf level

^d Drop in upper shelf level

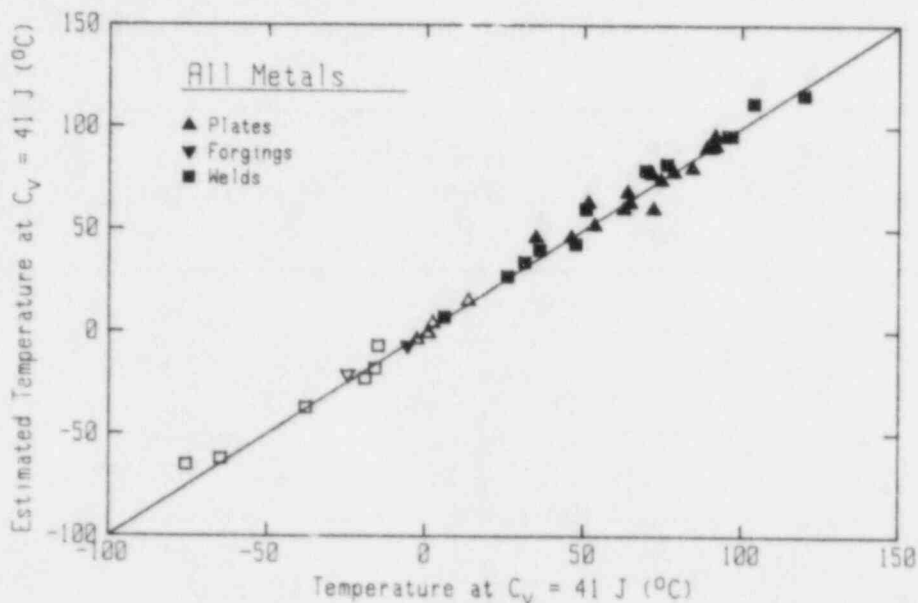


Fig. 10 Comparison of C_v temperatures at 41 J determined from manual fits to the data and computerized fits. The maximum deviation is 12°C for an irradiated A 533-B plate. Filled symbols are irradiated; open symbols are unirradiated. (The computerized-fit data are on the abscissa, with the manual-fit data on the ordinate.)

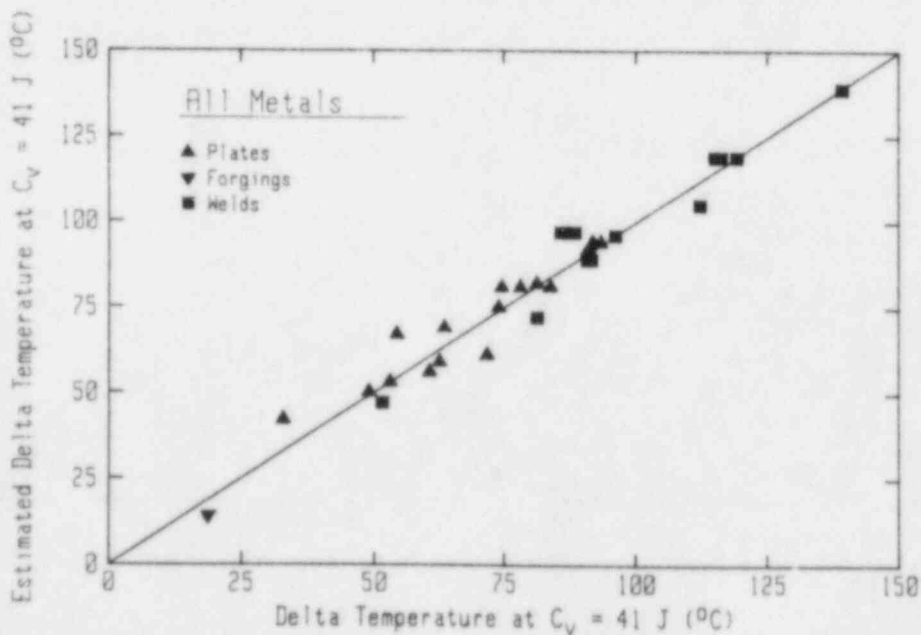


Fig. 11 Comparison of $\Delta T(C_v @ 41 \text{ J})$ determined from manual and computerized fits to the data. In this case, the maximum deviation is 11°C for a Linde 80 weld. (The computerized-fit data are on the abscissa, with the manual-fit data on the ordinate.)

For C_v upper shelf energy (Fig. 12), excellent agreement again results in comparing manual vs. curve-fit levels (1-J overestimate on average), with change in upper shelf level (Fig. 13) yielding a better average correspondence, but slightly greater variability. As with earlier data type comparisons, the greatest discrepancy is for the A 508-2 forging, with an underestimate of 16 J for the USE drop. That difference represents an equal 8-J increase for the unirradiated upper shelf and an 8-J decrease in the irradiated upper shelf, as determined from the curve-fit results.

For temperatures at K_{Jc} of 100 MPa \sqrt{m} , (Fig. 14) each product form has the manual result within 1°C of the curve-fit result, on average. For the ΔT 's, (Fig. 15), the manual result is again within 1°C of the curve-fit result, on average, but the variability is somewhat greater than for the absolute temperature comparisons.

For the $K_{\beta c}$ data at 75 MPa \sqrt{m} , both temperature (Fig. 16) and ΔT (Fig. 17) yield manual values within 1°C of the curve-fit values, on average. The standard deviations for the $K_{\beta c}$ comparisons are much less than the K_{Jc} comparisons, attributable to the smaller (and hence more controlled) number of data sets for which $K_{\beta c}$ had been manually curve fit.

4.5 Other Comparisons

While considerable interest is focused on the properties of so-called low upper shelf materials with USE levels below 68 J, use of a C_v index at 41 J forces consideration of the C_v curve at levels below the middle of the transition for heats with USE levels above 82 J. For such heats, it is of interest to compare temperature shifts at the 41-J level with shifts at higher energy levels. This comparison will give an indication of the relative curve shape between the unirradiated and irradiated conditions, with possibly a better indication of the average ΔT for such higher toughness materials. As an example of such a consideration, $\Delta T(C_v @ 68 \text{ J})$ is compared with $\Delta T(C_v @ 41 \text{ J})$. In Fig. 18, on average $\Delta T(C_v @ 68 \text{ J})$ is 5°C greater than $\Delta T(C_v @ 41 \text{ J})$, with a 1- σ range of 9°C (Table 6). This implies that the irradiated C_v curves have a tendency to "lay-over" or flatten-out in comparison to the unirradiated curves.

For the K_{Jc} data, alternative indices of 75 and 150 MPa \sqrt{m} have been considered here (Table 7). The $\Delta T(K_{Jc} @ 75 \text{ MPa}\sqrt{m})$ is 1°C lower than the $\Delta T(K_{Jc} @ 100 \text{ MPa}\sqrt{m})$, on average, with a 1- σ range of 11°C (Fig. 19). $\Delta T(K_{Jc} @ 150 \text{ MPa}\sqrt{m})$ is on average 1°C lower than the $\Delta T(K_{Jc} @ 100 \text{ MPa}\sqrt{m})$, with a 1- σ range of 18°C (Fig. 20). The variability of the latter comparison here is much greater than that for the former comparison, as the 1- σ ranges indicate. Nevertheless, the lack of variability in average values imply that the K_{Jc} curve does not tend to change shape with radiation.

Unlike the K_{Jc} and C_v data comparisons which show only minor changes in ΔT by changing the index point, the $\Delta T(K_{\beta c} @ 100 \text{ MPa}\sqrt{m})$ is considerably different from that at 75 MPa \sqrt{m} , on average (Table 8). As illustrated in Fig. 21, considerable variability is apparent, with

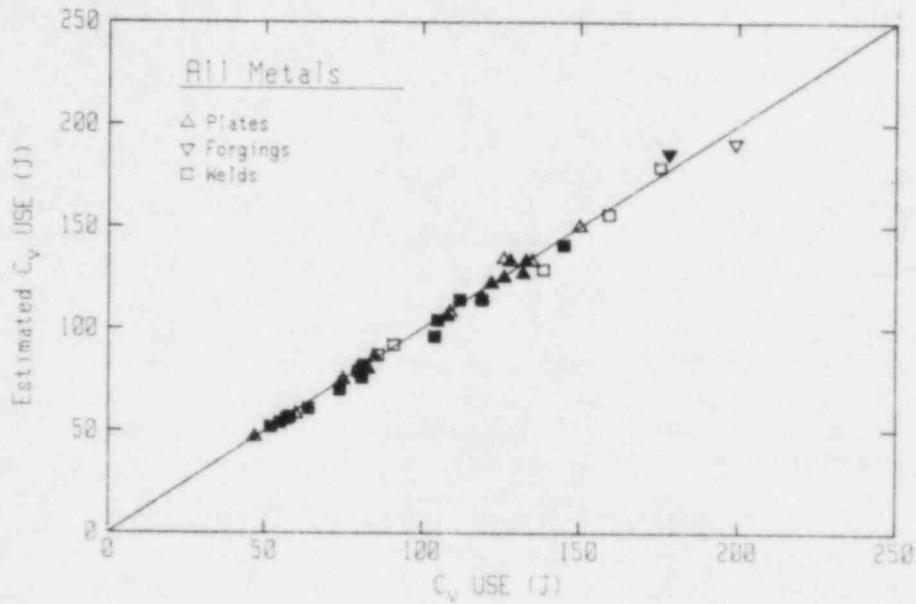


Fig. 12 Comparison of C_v upper shelf level determined from manual and computerized fits to the data. Good agreement is seen at all upper shelf levels. Filled symbols are irradiated; open symbols are unirradiated. (The computerized-fit data are on the abscissa, with the manual-fit data on the ordinate.)

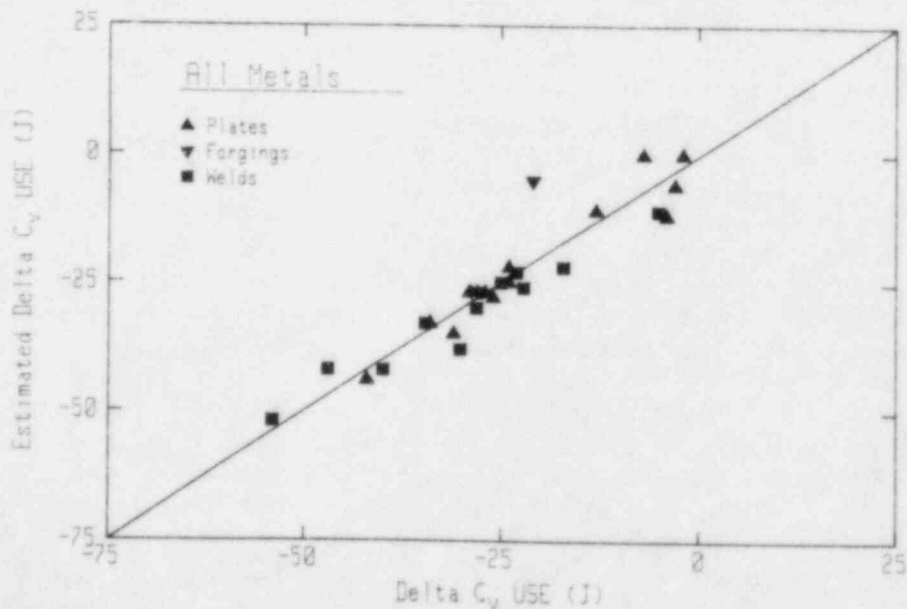


Fig. 13 Comparison of C_v upper shelf drop determined from manual and computerized fits to the data. On average, the manual fit is 1 J less than the computerized fit, with the maximum deviation from the A 508-2 forging, a 16-J discrepancy. (The computerized-fit data are on the abscissa, with the manual-fit data on the ordinate.)

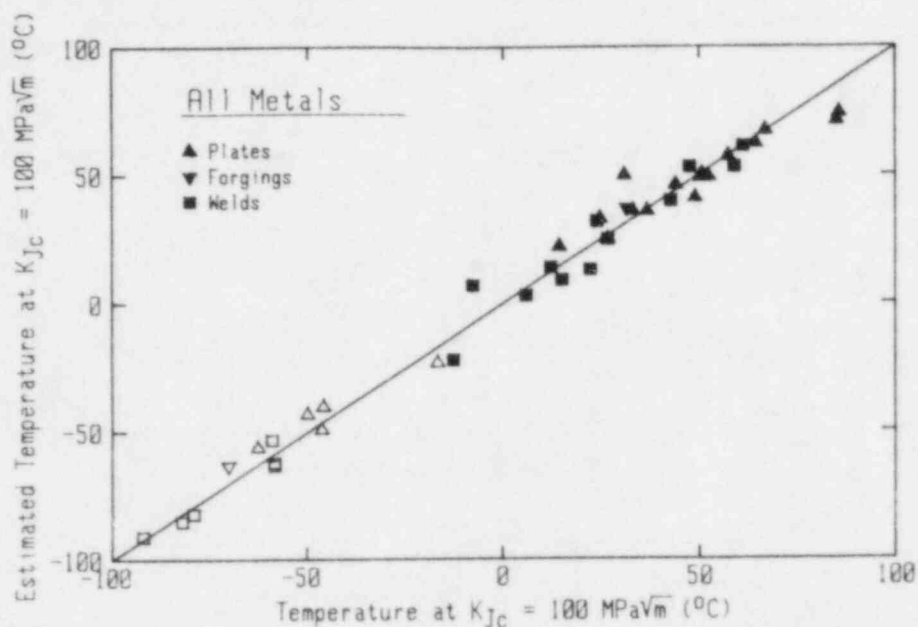


Fig. 14 Comparison of K_{Jc} temperature at 100 MPa \sqrt{m} from manual and computerized fits to the data. Good agreement is seen at all temperatures, with a maximum deviation of 20°C for irradiated A 533-B plate. Filled symbols are irradiated; open symbols are unirradiated. (The computerized-fit data are on the abscissa, with the manual-fit data on the ordinate.)

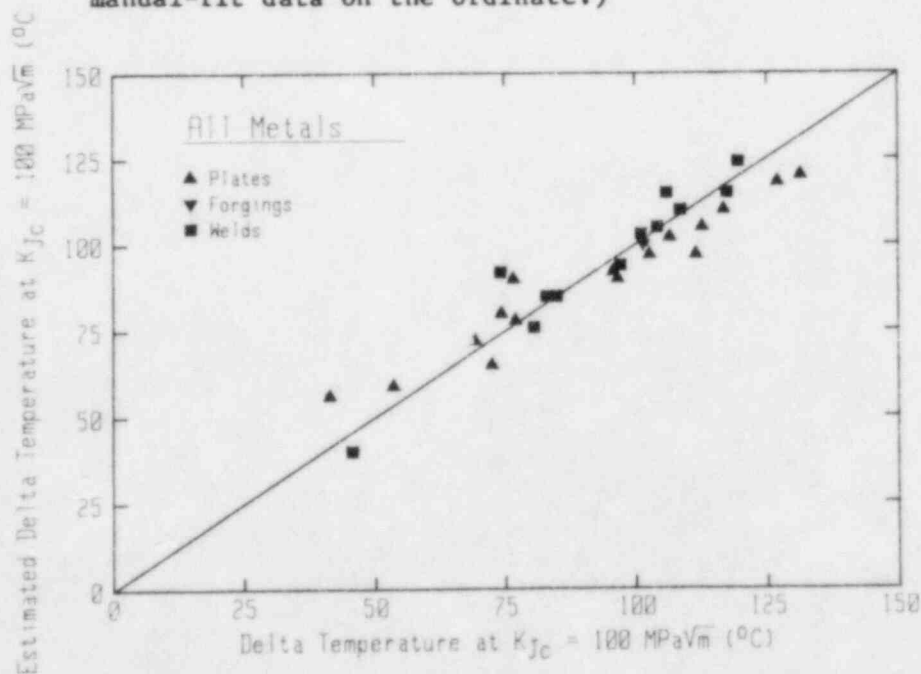


Fig. 15 Comparison of $\Delta T(K_{Jc} @ 100 \text{ MPa}\sqrt{m})$ determined from manual and computerized fits to the data. Good agreement is observed, on average, with a maximum deviation of 18°C for a Linde 0091 flux weld. (The computerized-fit data are on the abscissa, with the manual-fit data on the ordinate.)

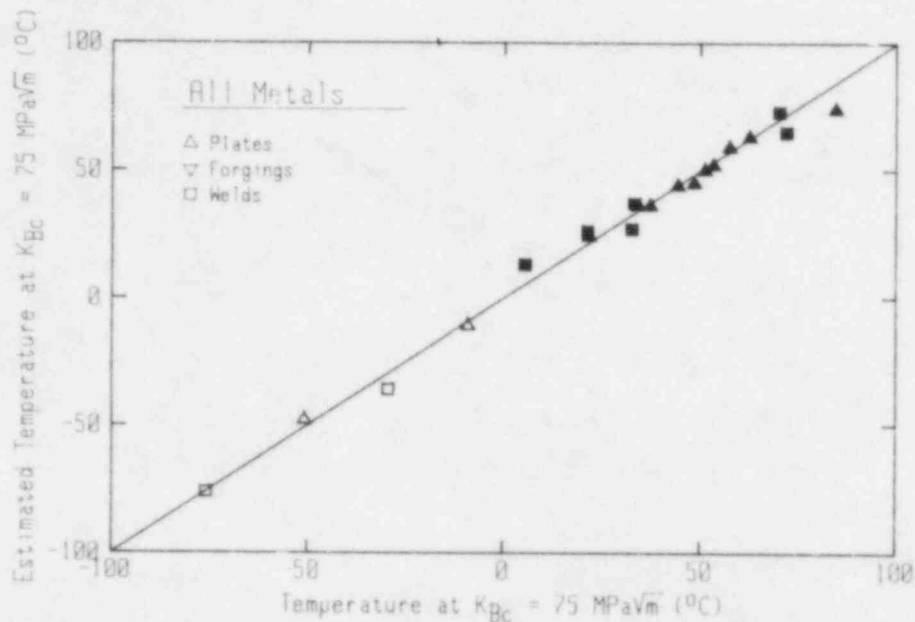


Fig. 16 Comparison of K_{Bc} temperature at $75 \text{ MPa}\sqrt{\text{m}}$ determined from manual and computerized fits to the data. The largest deviation is 10°C for an irradiated A 533-B plate. Filled symbols are irradiated; open symbols are unirradiated. (The computerized-fit data are on the abscissa, with the manual-fit data on the ordinate.)

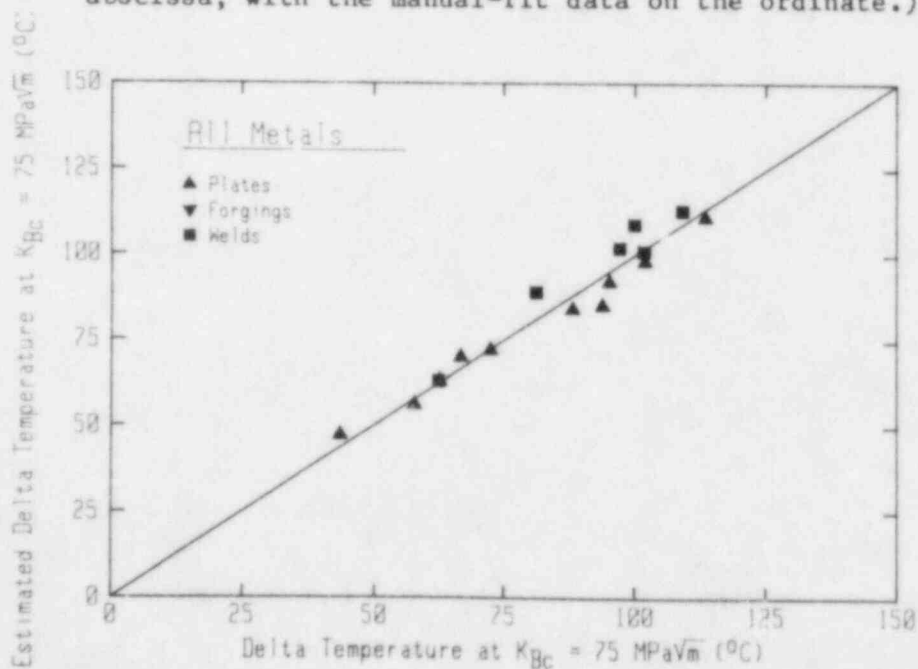


Fig. 17 Comparison of $\Delta T(K_{Bc} @ 75 \text{ MPa}\sqrt{\text{m}})$ determined from manual and computerized fits to the data. An A 533-B plate and a Linde 80 flux weld both have 9°C differences. (The computerized-fit data are on the abscissa, with the manual-fit data on the ordinate.)

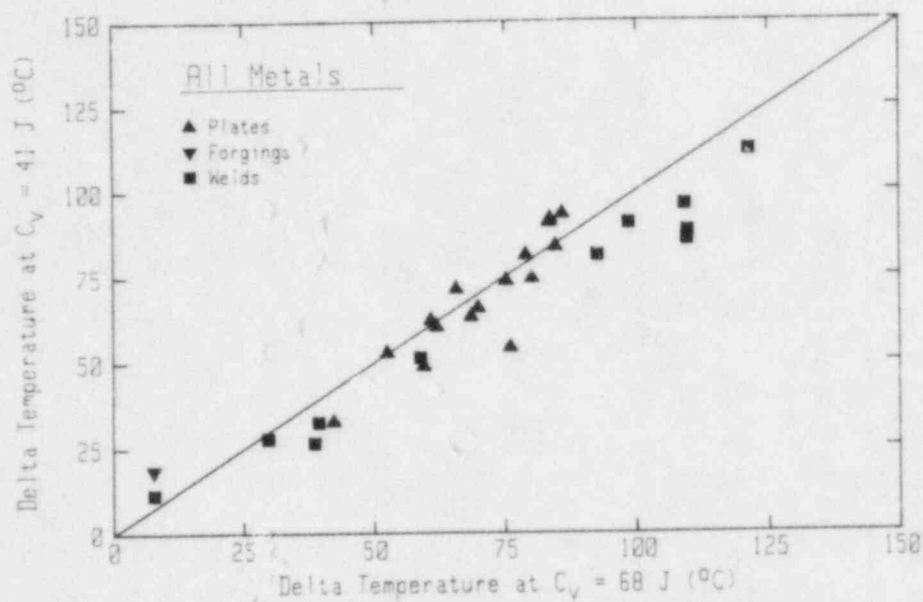


Fig. 13 Comparison of $\Delta T(C_v)$ as determined at 41 J and 68 J. On average, $\Delta T(C_v @ 68 \text{ J})$ is 5°C higher than $\Delta T(C_v @ 41 \text{ J})$.

Table 6 Statistical Comparisons Between ΔT 's at C_v Indices of 41 J and 68 J

Product Form	$\Delta T(C_v @ 68 J) = \Delta T(C_v @ 41 J)K_0 + K_1$			$\Delta T(C_v @ 68 J) = \Delta T(C_v @ 41 J) + K_2$			$\Delta T(C_v @ 68 J) = \Delta T(C_v @ 41 J)K_3$		
	K_0	K_1	$\pm 1\sigma$	K_2	$\pm 1\sigma$	1σ Range	K_3	$\pm 1\sigma$	$\pm 1\sigma$
		(°C)	(°C)	(°C)	(°C)	(°C)			(°C)
Base	0.670	24.5	5.5	1.8	7.9	- 6.1:+ 9.7	1.006	0.110	8.1
Weld	1.139	1.2	6.1	10.2	7.8	+ 2.4:+18.0	1.155	0.082	6.2
Both	0.998	5.3	8.8	5.2	8.8	- 3.6:+14.0	1.068	0.123	9.0

Table 7 Statistical Comparisons Between $\Delta T(K_{Jc} \text{ @ } 100 \text{ MPa}\sqrt{m})$ with Alternate Indices of 75 and 150 $\text{MPa}\sqrt{m}$

K_{Jc} Level ($\text{MPa}\sqrt{m}$)	Product	$\Delta T(K_{Jc}) = \Delta T(K_{Jc} \text{ @ } 100)K_0 + K_1$			$\Delta T(K_{Jc}) = \Delta T(K_{Jc} \text{ @ } 100) + K_2$			$\Delta T(K_{Jc}) = \Delta T(K_{Jc} \text{ @ } 100)K_3$		
		K_0	K_1	$\pm 1\sigma$	K_2	$\pm 1\sigma$	$1\sigma \text{ Range}$	K_3	$\pm 1\sigma$	$\pm 1\sigma$
			($^{\circ}\text{C}$)	($^{\circ}\text{C}$)	($^{\circ}\text{C}$)	($^{\circ}\text{C}$)	($^{\circ}\text{C}$)			($^{\circ}\text{C}$)
75	Base	1.014	-3.3	10.1	-2.1	10.1	-12.2:+ 8.0	0.980	0.104	10.2
	Weld	0.963	2.3	11.3	-0.5	11.4	-11.9:+10.9	0.988	0.131	11.3
	Both	0.974	0.9	10.6	-1.3	10.7	-12.0:+ 9.4	0.983	0.116	10.6
150	Base	0.914	7.6	14.9	-0.3	15.0	-15.3:+14.7	0.992	0.154	15.0
	Weld	1.143	-11.9	21.0	-1.2	21.7	-22.9:+20.5	1.015	0.251	21.7
	Both	1.068	-6.4	18.2	-0.7	18.3	-19.0:+17.6	1.001	0.201	18.3

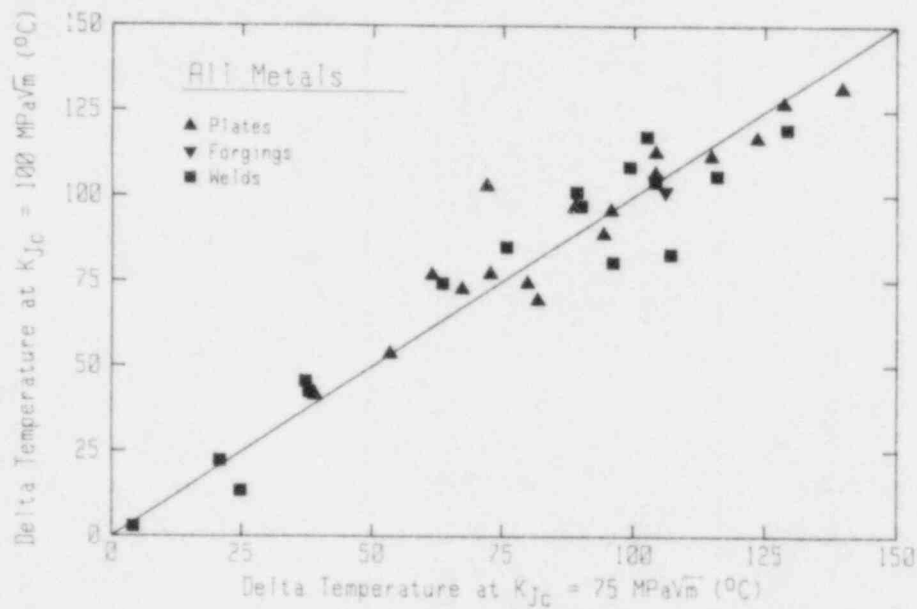


Fig. 19 Comparison of $\Delta T(K_{Jc})$ determined at $75 \text{ MPa}\sqrt{\text{m}}$ and $100 \text{ MPa}\sqrt{\text{m}}$. A high degree of scatter is apparent, but on average these two levels give ΔT 's about 1°C apart.

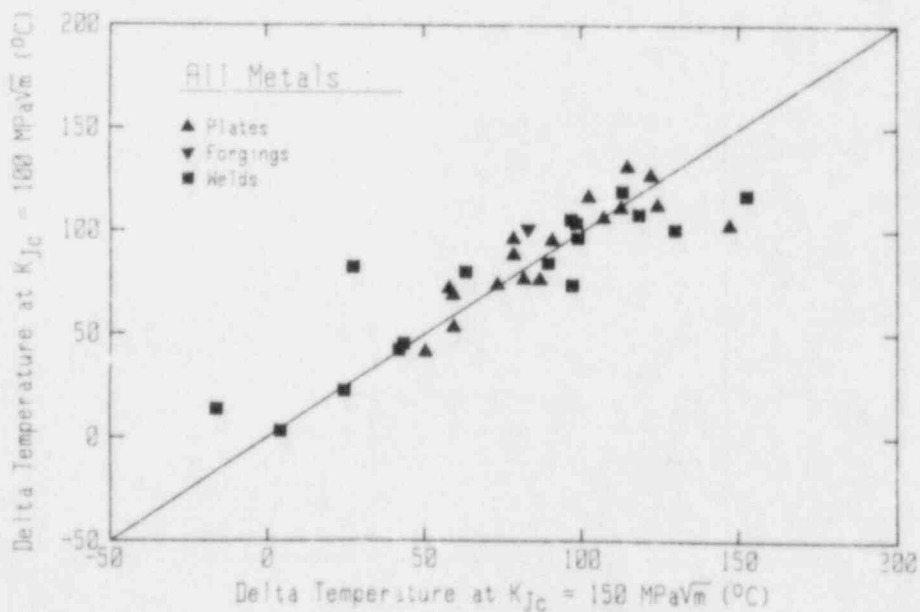


Fig. 20 Comparison of $\Delta T(K_{Jc})$ at $100 \text{ MPa}\sqrt{\text{m}}$ and $150 \text{ MPa}\sqrt{\text{m}}$. Here, the variability is greater than for the $75 \text{ MPa}\sqrt{\text{m}}$ comparison (Fig. 19), but on average the differences are still below 1°C .

Table 8 Statistical Comparisons Between $\Delta T(K_{\beta c})$ at Indices of 75 and 100 MPa \sqrt{m}

Product Form	$\Delta T(K_{\beta c} @ 100) = \Delta T(K_{\beta c} @ 75)K_0 + K_1$			$\Delta T(K_{\beta c} @ 100) = \Delta T(K_{\beta c} @ 75) + K_2$			$\Delta T(K_{\beta c} @ 100) = \Delta T(K_{\beta c} @ 75)K_3$		
	K_0	K_1	$\pm 1\sigma$	K_2	$\pm 1\sigma$	1σ Range	K_3	$\pm 1\sigma$	$\pm 1\sigma$
		(°C)	(°C)	(°C)	(°C)	(°C)			(°C)
Base	1.047	-22.9	19.2	-19.2	19.2	-38.4:+ 0.0	0.778	0.237	20.1
Weld	1.244	-29.1	31.6	-12.2	33.0	-45.2:+20.8	0.919	0.428	34.7
Both	1.170	-28.4	26.1	-15.8	26.6	-42.4:+10.8	0.843	0.346	28.3

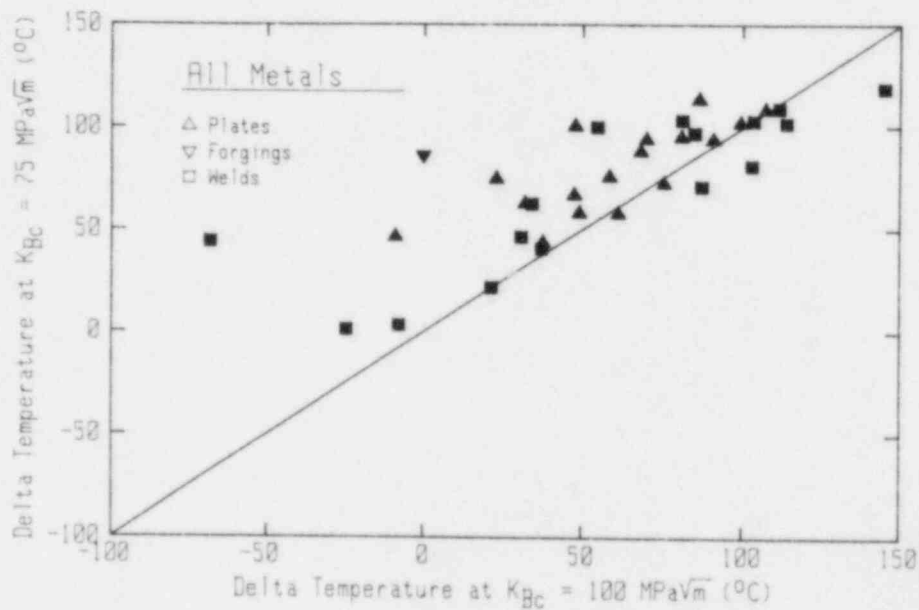


Fig. 21 Comparison of $\Delta T(K_{Bc})$ at $75 \text{ MPa}\sqrt{\text{m}}$ and $100 \text{ MPa}\sqrt{\text{m}}$. The ΔT 's at $100 \text{ MPa}\sqrt{\text{m}}$ tend to be much below ΔT 's at $75 \text{ MPa}\sqrt{\text{m}}$, at least partially attributable to extrapolation of the curves beyond the available data.

an average decrease of 16°C using ΔT at 100 MPa \sqrt{m} , with 1 σ of 27°C. The cause of this extreme variability is the extrapolation of the K_{Ic} curve fits beyond the available data to 100 MPa \sqrt{m} , while little data extends above 80 MPa \sqrt{m} .

5. COMPARISON OF CHARPY-V SHIFTS WITH CORRELATIONS

Many differing and independent efforts have sought to develop procedures for predicting transition temperature shifts induced by 288°C irradiation (Refs. 9 to 19). These procedures typically take into account product form (either weld or base metal), atomic or weight percentage of key elements such as copper, nickel, phosphorus, silicon, molybdenum, manganese and carbon, and most importantly, the neutron fluence for the pertinent material. Some of these procedures are based upon surveillance or experimental (test reactor) irradiation data, with no distinction made in some cases. In addition, mean values are sought by some of these procedures, and upper bound values are determined in other cases.

This section compares these data (C_v , K_{Ic} and K_{Ic}) with predictions of ΔT from the various correlations, to assess the applicability of the correlation to the data (or the data to the correlation). First, a description of each of the correlations is given, along with the assumptions and limitations of the equations.

5.1 Guthrie Trend Curves - 1983 (Ref. 9)

Guthrie of the Hanford Engineering Development Laboratory (HEDL) used 177 PWR surveillance data points (126 from plates and 51 from welds) to develop separate trend curves based on product form, and nickel and copper content. The mean trend curves are:

$$\text{Welds: } \Delta T = [624\text{Cu} - 333.1 \sqrt{\text{CuNi}} + 251.2\text{Ni}] \phi^{(0.28185 - 0.0409 \ln \phi)} \quad (21)$$

$$\text{Plates: } \Delta T = [-38.39 + 555.6\text{Cu} + 480.1\text{Cu} \tanh(0.353\text{Ni}/\text{Cu})] \phi^{(0.2661 - 0.0449 \ln \phi)} \quad (22)$$

with ϕ = fluence (ϕt)/ 10^{19} n/cm² ($E > 1$ MeV)
 Cu = weight % of copper
 Ni = weight % of nickel
 ΔT = °F

Standard deviations from the data used were 28°F for welds and 17°F for plates.

5.2 Odette/Perrin Correlations - 1984 (Ref. 10)

These correlations were developed using the Electric Power Research Institute's Irradiated Pressure Vessel Steel Data Base (Ref. 20), composed of data from power reactor surveillance only. Fluence, copper and nickel content, and product form are the primary variables in these mean correlations, which take the form of:

$$\text{Plates: } \Delta T = 216 \text{ Cu} [1 + 0.33 (\text{erf}[\frac{0.77\text{Ni}-\text{Cu}}{\text{Cu}}] + 1)] \phi^{0.28} \quad (23)$$

$$\begin{aligned} \text{Welds: } \Delta T = 200 \text{ Cu} [1 + 1.38 (\text{erf}[\frac{0.3\text{Ni}-\text{Cu}}{\text{Cu}}] + 1)] \\ [1 - \exp(-\frac{\phi}{0.11})]^{1.36} \phi^{0.18} \end{aligned} \quad (24)$$

with ϕ = fluence (ϕt)/ 10^{19} n/cm² ($E > 1$ MeV)
 Cu = weight % of copper
 Ni = weight % of nickel
 erf = an error function tabulated in Ref. 10
 ΔT = °C

For upper bound shift estimates, recommendations are to add a 24°C uncertainty to the nominal calculations above, based upon twice the mean residual error for the data base used.

Limits of applicability of these correlations are:

Fluence	:	0.2 to 6 • 10 ¹⁹ n/cm ²
Flux	:	< 5 • 10 ¹¹ n/cm ² /sec
Composition:		
Plate	:	Ni < 0.8, Cu < 0.25
Weld	:	Ni < 0.8, Cu < 0.38
		Ni < 1.2, 0.2 < Cu < 0.25
Irradiation Temperature:		275°C to 310°C

5.3 Metal Properties Council - 1983 (Ref. 11)

MPC Subcommittee 6 on Nuclear Materials used surveillance and experimental irradiation data collected prior to November 1977 in their analyses. Fluence and copper content were the primary variables, with the mean shift equation given by:

$$\Delta T = (a_1 + b_1 \text{ Cu}) (\phi)^{k_1} \quad (25)$$

with ϕ = fluence (ϕt)/ 10^{19} n/cm² ($E > 1$ MeV)
 Cu = weight % of copper
 ΔT = °F

Tabulated values of a_1 , b_1 , and k_1 are given in Table 9 based upon product form and data type (surveillance or experimental). A modified equation gives upper bound estimates:

$$\Delta T = (a_2 + b_2 \text{ Cu}) \phi^{k_2} + c \phi^{k_3} \quad (26)$$

with Table 10 listing values for these constants based upon data type only. (A lower limit of 0.05% Cu is placed on Eq. 26.)

These equations are limited to:

Fluence : 10^{16} to 10^{20} n/cm² (E > 1 MeV)
Irradiation Temperature: 277°C to 310°C

5.4 ASTM E 900 - 1983 (Ref. 12)

The ASTM guide for predicting transition temperature shifts is based upon the MPC report. Specifically,

$$\Delta T = (4 + 5/0 \text{ Cu}) \phi^{0.31} \quad (27)$$

with ϕ = fluence (ϕt)/ 10^{19} n/cm² (E > 1 MeV)
Cu = weight % of copper
 ΔT = °F

With this mean curve, copper values below 0.05% should use 0.05%, and values above 0.4% should use 0.4%. For upper bound estimates, predicted values of 90°F and above should be supplemented with 67°F (based on 2 σ), while predicted values below 90°F should be multiplied by 1.75 (based on an inspection of residuals) for the upper bound.

5.5 Varsik - 1983 (Ref. 13)

Varsik used available surveillance data, in this case over 200 data points. Primary variables used are fluence, and nickel, copper, silicon and phosphorus content. The mean expression developed was of the form:

$$\Delta T = [A + B \text{ Cu} + C \text{ Ni} + D \text{ Si}] \phi^k \quad (28)$$

with ϕ = fluence (ϕt)/ 10^{19} n/cm² (E > 1 MeV)
Cu = weight % of copper
Ni = weight % of nickel
Si = weight % of silicon
 ΔT = °F

Tabulated values of A, B, C, D and k are given in Table 11, depending on product form, nickel content and fluence.

Table 9 Constants for MPC Mean ΔT Equation (Ref. 11)

Data Type	Product Form	$\Delta T = (a_1 + b_1 Cu) (\phi)^{k_1}$		
		a_1	b_1	k_1
Experimental Only	Weld ^a	-2.3 ^c	602.1	0.327
	A302-B, A508 ^a	-29.12	603.6	0.428
	A533-B ^a	17.71	466.6	0.320
	All ^b	5.20	519.4	0.332
Experimental and Surveillance	Weld ^c	-7.23	637.5	0.330
	A533-B, A302-B, A508 ^c	15.25	432.0	0.332
	All ^d	3.58	539.9	0.314

Table 10 Constants for MPC Upper Bound ΔT Equation (Ref. 11)

Data Type	Product Form	$\Delta T = (a_2 + b_2 Cu) \phi^{k_2} + c \phi^{k_3}$				
		a_2	b_2	k_2	c	k_3
Experimental Only	All ^e	5.20	519.4	0.332	45.63	0.220
Experimental and Surveillance	All ^f	3.58	539.9	0.314	41.82	0.207

- a = Experimental, welds and plates separately, mean curve
 b = Experimental, all data, mean curve
 c = Surv. and exp., welds and plates separately, mean curve
 d = Surv. and exp., all data, mean curve
 e = Experimental, upper bound
 f = Surveillance and experimental, upper bound

Table 11 Constants for Varsik ΔT Equation

Product	Nickel (wt%)	Fluence ^a	A	B	C	D	k	1 σ (°F)
A 302-B	< 0.3	All	-299.98	27.47	5188.57	-2330.69	0.44	19.8
A 533								
A 302-B	> 0.3	< 1	-10.28	818.99	-----	-----	0.38	21.4
A 508-2								
A 533								
A 302-B	> 0.3	> 1	4.38	817.47	-----	-----	-----	20.5
A 508-2								
Welds	All	All	-6.20	320.93	166.34	-----	0.29	39.2

^a Units of 10^{19} n/cm², $E > 1$ MeV

5.6 Varsik and Byrne - 1979 (Ref. 14)

The Varsik-Byrne correlations were derived using both surveillance and experimental data, with the irradiation temperature limited to $288^\circ\text{C} \pm 20^\circ\text{C}$, and fluence below $5 \cdot 10^{19}$ n/cm² ($E > 1$ MeV). These mean correlations, separated by product form, involve calculation of a chemistry ratio, a normalized ΔT , then finally the actual ΔT . These mean correlations are:

$$\text{CR} = \left[\frac{3\text{Ni} + 2\text{Si} + \text{C} + (\text{Mn} - 0.5)}{1 + \text{Mo}} \right] \text{Cu} \quad (29)$$

$$\text{Welds: } \Delta T_N = 377.9 \log_{10}(\text{CR}) + 331.9 \quad (30)$$

$$\text{Plates: } \Delta T_N = 515.9 \log_{10}(\text{CR}) + 343.0 \quad (31)$$

$$\Delta T = \Delta T_N (\phi/3)^{0.43} \quad (32)$$

with ϕ = fluence (ϕt)/ 10^{19} n/cm² ($E > 1$ MeV)
 Cu = atomic % of copper
 Ni = atomic % of nickel
 Si = atomic % of silicon
 C = atomic % of carbon
 Mn = atomic % of manganese
 Mo = atomic % of molybdenum
 ΔT = °F

The primary caution given with these correlations is in extrapolating ΔT_N (the normalized shift at a fluence of $3 \cdot 10^{19}$ n/cm², $E > 1$ MeV) to higher fluences.

In compiling the data for Ref. 13, Varsik also recomputed the weld metal correlation given in Eqs. 29, 30 and 32. The revised weld correlation is (Ref. 13):

$$CR = \left[\frac{3.293 Ni - 0.417 Si - 0.587 C + 0.826 (Mn - 0.05)}{0.5 - 0.615 Mo} \right] Cu \quad (33)$$

$$\Delta T = (135.058 \log_{10}(CR) + 168.474) \phi^{0.298} \quad (34)$$

with ϕ = fluence (ϕt)/ 10^{19} n/cm² ($E > 1$ MeV)
 Cu = atomic % of copper
 Ni = atomic % of nickel
 Si = atomic % of silicon
 C = atomic % of carbon
 Mn = atomic % of manganese
 Mo = atomic % of molybdenum
 ΔT = °F

5.7 Heller and Lowe - 1984 (Ref. 15)

The Heller and Lowe correlation is based on surveillance data from Linde 80 flux submerged-arc welds only. Their correlation is given by:

$$\Delta T = -4.66 + (200 \phi)^{0.326} [-18.17 + 61.88 Ni + 49.12 Cu] \quad (35)$$

with ϕ = fluence (ϕt)/ 10^{19} n/cm² ($E > 1$ MeV)
 Cu = weight % of copper
 Ni = weight % of nickel
 ΔT = °F

A 1- σ level of 28°F was found using the input data.

5.8 Berggren and Stallman - 1983 (Ref. 16)

Reference 16 is not a true correlation, but is a summary of fitting seven submerged arc weld data sets to the model:

$$\Delta T = [30.7 - 0.218 (T_1 - 299) + 89 (Cu - 0.30)] \phi^{0.5} \quad (36)$$

with T_1 = the irradiation temperature (°C)
 Cu = weight percent of copper
 ϕ = fluence/ 10^{18} n/cm² ($E > 1$ MeV)
 ΔT = °C

This formulation is included here for information only.

5.9 Regulatory Guide 1.99 Rev. 1 - 1977 (Ref. 17)

Regulatory Guide 1.99 gives procedures for estimating the adjustment of the reference temperature due to neutron radiation. The equation given is

$$\Delta T = [40 + 1000 (C_u - 0.080) + 5000 (P - 0.008)] \phi^{0.5} \quad (37)$$

with C_u = weight percent of copper
 P = weight percent of phosphorus
 ϕ = fluence (ϕt)/ 10^{19} n/cm² ($E > 1$ MeV)
 ΔT = °F

If C_u is below 0.08%, then 0.08% should be used, and if P is below 0.008%, then 0.008 should be used. The fluence should be lower than $6 \cdot 10^{19}$ n/cm² ($E > 1$ MeV), and ΔT should be not less than 50°F. An upper limit of ΔT is defined as:

for fluence below $0.6 \cdot 10^{19}$ n/cm² ($E > 1$ MeV): $\Delta T < 330 \phi^{0.5}$
 for fluences from 0.6 to $6 \cdot 10^{19}$ n/cm² ($E > 1$ MeV): $\Delta T < 282 \phi^{0.1955}$

The Regulatory Guide is different from the other prediction methods previously mentioned, in that conservative (upper bound) estimates are desired, and not mean values.

5.10 Draft Revision 2 to Regulatory Guide 1.99 - 1985 (Ref. 18)

The draft of Revision 2 of the Regulatory Guide is based upon several factors, including the previously described works by Guthrie and Odette. The mean value of ΔT here is

$$\Delta T = (CF) \phi (0.28 - 0.10 \log \phi) \quad (38)$$

with ϕ = fluence/ 10^{19} n/cm² ($E > 1$ MeV)
 CF = a tabulated chemistry factor, based on nickel and copper content, with separate weld and plate tabulations
 ΔT = °F

Upper bound estimates of the shift are found by adding 56°F to weld ΔT 's and 34°F to base metal ΔT 's.

5.11 NRC Screening Criteria - 1982 (Ref. 19)

As a part of the NRC staff evaluation of pressurized thermal shock (PTS), a Guthrie mean curve was recommended for use:

$$\Delta T = [-10 + 470 C_u + 350 C_{Ni}] \phi^{0.27} \quad (39)$$

with Cu = weight percent of copper
 Ni = weight percent of nickel
 Φ = fluence/ 10^{19} n/cm² (E > 1 MeV)
 ΔT = °F

Upper bound values are then found by adding 48°F to the calculated mean value, where this represents a 2 σ bound based on the input data.

5.12 C_v Comparisons

Statistical comparisons of $\Delta T(C_v @ 41 \text{ J})$ with predictions based on the correlations are listed in Table 12. (Any correlation prediction yielding a negative ΔT was set to a zero shift.) Average deviation of the predicted ΔT and the measured $\Delta T(C_v @ 41 \text{ J})$ and $\pm 1\text{-}\sigma$ standard deviations are listed in this table. In addition, the number of data points overpredicted and underpredicted by the correlation are listed. In this table, a positive number indicates an underestimate of the actual $\Delta T(C_v @ 41 \text{ J})$, with a negative number indicating an overestimate (conservative estimate) of the actual $\Delta T(C_v @ 41 \text{ J})$. Plots comparing the measured and predicted ΔT values are given in Appendix A.

With each correlation, the ΔT for weld metal is conservatively estimated on average by the correlations, with the closest (average) predictions from the MPC mean curve derived from all experimental data. For the base metals, most of the correlations give accurate-to-slightly-nonconservative average estimates of $\Delta T(C_v @ 41 \text{ J})$, with all of the correlations having an average underestimate of less than 10°C. The closest prediction in terms of the average, absolute deviation is the MPC mean curve for all experimental data with the Varsik-Byrne correlation yielding the smallest, average deviation from the conservative correlations. In general, the ΔT 's for base metal are well predicted by the correlations.

5.13 K_{Jc} Comparisons

The $\Delta T(K_{Jc} @ 100 \text{ MPa}\sqrt{\text{m}})$ comparisons with the correlation predictions are listed in Table 13, with comparison plots given in Appendix B. The major difference between this table and Table 12 is that A 508-2 forging data have not been included here, due to the large discrepancies between the $\Delta T(K_{Jc})$ and $\Delta T(C_v)$ for this heat noted earlier in section 4.1

As with $\Delta T(C_v)$, on average the weld metal ΔT 's were conservatively estimated by each correlation. The MPC mean curve from all experimental data provided the best match, on average. For base metals, several of the correlations overestimate the $\Delta T(K_{Jc})$ on average, but most of the correlations result in a large underestimate, on average. The closest correlation on average is the MPC upper bound curve based on surveillance and experimental data, with the MPC upper bound curve from experimental data giving the next best match.

Table 12 Comparison of Measured $\Delta T(C_v @ 41J)$ with Correlation Predictions

	Base Metals			Weld Metals			All Data		
	Avg.	(1 σ)	Over/ Under	Avg.	(1 σ)	Over/ Under	Avg.	(1 σ)	Over/ Under
	(°C)	(°C)		(°C)	(°C)		(°C)	(°C)	
Guthrie (Ref. 9)	+6.3	(12.7)	5/13	-33.9	(23.7)	16/0	-12.6	(27.4)	21/13
Odette/Perrin (Ref. 10)	+4.7	(10.7)	5/13	-22.5	(20.2)	14/2	-8.1	(20.8)	19/15
MPC (Ref. 11)									
1 ^a	+1.6	(14.7)	5/13	-25.1	(31.8)	12/4	-11.0	(27.5)	17/17
2 ^b	+0.8	(17.1)	8/10	-15.3	(25.5)	11/5	-6.8	(22.6)	19/15
3 ^c	+3.3	(15.1)	7/11	-28.5	(34.9)	11/5	-11.7	(30.5)	18/16
4 ^d	+1.0	(17.3)	8/10	-17.3	(26.3)	11/5	-7.6	(23.5)	19/15
5 ^e	-31.1	(17.8)	18/0	-42.5	(26.8)	16/0	-36.4	(22.8)	34/0
6 ^f	-27.8	(17.7)	18/0	-42.1	(27.2)	16/0	-34.5	(23.5)	34/0
ASTM E 900 (Ref. 12)	+0.9	(17.2)	8/10	-17.4	(26.1)	11/5	-7.7	(23.4)	19/15
Varsik (Ref. 13)	-5.4	(21.1)	11/7	-29.6	(23.0)	14/2	-16.8	(24.9)	25/9
Varsik/Byrne (Ref. 14)	-5.5	(18.4)	10/8	-33.4	(36.4)	12/4	-18.6	(31.3)	22/12
Rev. Varsik/Byrne (Ref. 13)	----	----	----	-20.8	(19.7)	13/3	----	----	----
Heller/Lowe (Ref. 15)	----	----	----	-22.1	(22.9)	6/2	----	----	----
Berggren/Stallman (Ref. 16)	-40.9	(27.0)	18/0	-40.6	(36.4)	14/2	-40.8	(31.3)	32/2
RG 1.99 Rev. 1 (Ref. 17)	-51.4	(45.5)	17/1	-46.4	(26.6)	16/0	-49.1	(37.3)	33/1
RG 1.99 Rev. 2 (Ref. 18)	+4.8	(11.9)	5/13	-29.0	(20.5)	16/0	-11.1	(23.6)	21/13
NRC Screening Criteria (Ref. 19)	+8.3	(12.6)	5/13	-32.4	(38.1)	11/5	-10.8	(34.2)	16/18

a = Experimental, welds and plates separately, mean curve

b = Experimental, all data, mean curve

c = Surv. and exp., welds and plates separately, mean curve

d = Surv. and exp., all data, mean curve

e = Experimental, upper bound

f = Surveillance and experimental, upper bound

Table 13 Comparison of Measured $\Delta T(K_{JC})$ @ 100 MPa \sqrt{m} with Correlation Predictions of $\Delta T(C_v)$ @ 41J

	Base Metals			Weld Metals			All Data		
	Avg.	(1 σ)	Over/ Under	Avg.	(1 σ)	Over/ Under	Avg.	(1 σ)	Over/ Under
	(°C)	(°C)		(°C)	(°C)		(°C)	(°C)	
Guthrie (Ref. 9)	+33.6	(24.9)	2/15	-39.0	(30.4)	15/1	-1.7	(45.8)	17/16
Odette/Perrin (Ref. 10)	+31.8	(21.6)	2/15	-27.6	(24.5)	14/2	+3.0	(37.7)	16/17
MPC (Ref. 11)									
1 ^a	+28.6	(24.8)	2/15	-30.2	(36.5)	12/4	+0.1	(42.7)	14/19
2 ^b	+27.7	(21.5)	1/16	-20.4	(30.7)	12/4	+4.4	(35.6)	13/20
3 ^c	+30.3	(19.7)	0/17	-33.6	(39.5)	12/4	-0.7	(44.5)	12/21
4 ^d	+27.9	(21.7)	0/17	-22.4	(31.2)	12/4	+3.5	(36.6)	12/21
5 ^e	-6.0	(23.0)	11/6	-47.6	(32.6)	16/0	-26.2	(34.7)	27/6
6 ^f	-2.6	(23.0)	10/7	-47.2	(32.7)	16/0	-24.2	(35.7)	26/7
ASTM E 900 (Ref. 12)	+27.9	(21.6)	1/16	-22.5	(31.0)	12/4	+3.4	(36.6)	13/20
Varsik (Ref. 13)	+21.1	(25.3)	3/14	-34.7	(30.1)	15/1	-5.9	(39.4)	18/15
Varsik/Byrne (Ref. 14)	+21.0	(27.2)	4/13	-38.4	(44.3)	13/3	-7.8	(46.9)	17/16
Rev. Varsik/Byrne (Ref. 13)	----	----	----	-25.9	(26.6)	13/3	----	----	----
Heller/Lowe (Ref. 15)	----	----	----	-31.8	(31.0)	7/1	----	----	----
Berggren/Stallman (Ref. 16)	-16.5	(30.7)	13/4	-45.7	(43.4)	13/3	-30.7	(39.7)	26/7
RG 1.99 Rev. 1 (Ref. 17)	-27.6	(45.4)	13/4	-51.5	(31.2)	16/0	-39.2	(40.4)	29/4
RG 1.99 Rev. 2 (Ref. 18)	+31.9	(22.5)	2/15	-34.0	(26.3)	15/1	-0.1	(41.2)	17/16
NRC Screening Criteria (Ref. 19)	+35.7	(21.3)	1/16	-37.5	(42.1)	12/4	+0.2	(49.4)	13/20

- a = Experimental, welds and plates separately, mean curve
 b = Experimental, all data, mean curve
 c = Surv. and exp., welds and plates separately, mean curve
 d = Surv. and exp., all data, mean curve
 e = Experimental, upper bound
 f = Surveillance and experimental, upper bound

5.14 $K_{\beta c}$ Comparisons

The $\Delta T(K_{\beta c} @ 75 \text{ MPa}\sqrt{\text{m}})$ comparisons with the correlation predictions are given in Table 14. As with the $\Delta T(K_{Jc} @ 100 \text{ MPa}\sqrt{\text{m}})$ comparisons, the A508-2 forging data were not used in this table. The results also are comparable to the $\Delta T(K_{Jc})$ comparisons, as base metals are underestimated on average and welds are overestimated on average, by the mean equations. In this case, the Varsik-Byrne correlation gives the most accurate average estimate of the ΔT for base metal, with the MPC mean curve from experimental data yielding the best match with the weld data.

6. DISCUSSION

One aspect made apparent by the preceding sections is that plates and welds exhibit different trends for relating fracture toughness and notch ductility assessments of irradiation-induced transition temperature shifts (increases). This observation is supported in Tables 2 and 3 (for K_{Jc} and $K_{\beta c}$, respectively), where $\Delta T(C_v)$ for plates underestimates $\Delta T(K_{Jc})$ and $\Delta T(K_{\beta c})$ on average, while $\Delta T(C_v)$ for welds overestimates $\Delta T(K_{Jc})$ and $\Delta T(K_{\beta c})$ on average. (The $\Delta T(K_{\beta c})$ plate data at $100 \text{ MPa}\sqrt{\text{m}}$ are ignored in this context, since this $K_{\beta c}$ level exceeds the available data in all cases.) Comparison of Figs. 1 and 2 and Fig. 5 and 6 show that $\Delta T(C_v)$ for welds gives a consistent overestimate of $\Delta T(K_{Jc})$ and $\Delta T(K_{\beta c})$ at all ΔT levels. However, $\Delta T(C_v)$ for plates tends to underestimate large $\Delta T(K_{Jc})$ and $\Delta T(K_{\beta c})$ shifts, while giving accurate estimates at a ΔT of 75°C and lower only. This indicates that high base metal embrittlement conditions (as determined from K_{Jc} or $K_{\beta c}$) are not reflected by the base metal notch ductility trends at the same flux and fluence conditions.

Further differences in plate and weld behavior are apparent when comparing correlation (model) predictions of $\Delta T(C_v @ 41 \text{ J})$ with measured values. For base metals from Table 12, the average correlations give accurate estimates of $\Delta T(C_v @ 41 \text{ J})$, even though many of the correlations are based upon surveillance conditions while the data in this report are from test reactor irradiations with much higher fluxes. This good agreement would indicate "flux independence" for notch ductility determinations from plates.

With the large differences observed between $\Delta T(K_{Jc})$ or $\Delta T(K_{\beta c})$ and $\Delta T(C_v)$ from the correlation predictions for plates (Tables 12 and 13), one interpretation is a "real" difference between static (K) and dynamic (C_v) assessments of ΔT , or possibly a flux dependence of static fracture toughness. The flux dependence of static fracture toughness would result in greater embrittlement at higher flux for plates, as compared to dynamic (C_v) assessments of embrittlement.

For weld metals, the average correlations overestimate $\Delta T(C_v)$, $\Delta T(K_{Jc})$ and $\Delta T(K_{\beta c})$ at all measured toughness energy levels (Tables 11 to 13). This overestimate tends to become greatest at high embrittlement (ΔT) levels. One interpretation of these findings is a flux

Table 14 Comparison of Measured $\Delta T(K_{BC})$ @ 75 MPa/ \sqrt{m} with Correlation Predictions of $\Delta T(C_v)$ @ 41 J)

	Base Metals			Weld Metals			All Data		
	Avg.	(1 σ)	Over/ Under	Avg.	(1 σ)	Over/ Under	Avg.	(1 σ)	Over/ Under
	(°C)	(°C)		(°C)	(°C)		(°C)	(°C)	
Guthrie (Ref. 9)	+20.8	(21.4)	2/15	-45.2	(30.0)	15/1	-11.2	(42.1)	17/16
Odette/Perrin (Ref. 10)	+19.1	(17.5)	2/15	-33.7	(24.6)	14/2	-6.5	(34.0)	16/17
MPC (Ref. 11)									
1 ^a	+15.8	(21.1)	3/14	-36.4	(34.5)	15/1	-9.5	(38.5)	18/15
2 ^b	+15.0	(17.2)	1/16	-26.6	(28.6)	12/4	-5.2	(31.3)	13/20
3 ^c	+17.6	(15.1)	1/16	-39.8	(37.5)	14/2	-10.2	(40.2)	15/18
4 ^d	+15.2	(17.4)	1/16	-28.6	(29.1)	13/3	-6.0	(32.3)	14/19
5 ^e	-18.8	(17.5)	16/1	-53.7	(30.6)	16/0	-35.7	(30.1)	32/1
6 ^f	-15.4	(17.7)	16/1	-53.3	(30.7)	16/0	-33.8	(31.1)	32/1
ASTM E 900 (Ref. 12)	+15.1	(17.4)	1/16	-28.7	(28.9)	13/3	-6.1	(32.2)	14/19
Varsik (Ref. 13)	+8.4	(21.9)	5/12	-40.8	(29.8)	15/1	-15.5	(35.8)	20/13
Varsik/Byrne (Ref. 14)	+8.3	(23.5)	6/11	-44.6	(45.1)	13/3	-17.4	(44.2)	19/14
Rev. Varsik/Byrne (Ref. 13)	-----	-----	-----	-32.1	(27.3)	13/3	-----	-----	-----
Heller/Lowe (Ref. 15)	-----	-----	-----	-42.9	(32.3)	7/1	-----	-----	-----
Berggren/Stallman (Ref. 16)	-29.2	(26.3)	16/1	-51.9	(41.7)	15/1	-40.2	(35.9)	31/2
RG 1.99 Rev. 1 (Ref. 17)	-40.4	(41.6)	16/1	-57.6	(30.1)	16/0	-48.7	(37.0)	32/1
RG 1.99 Rev. 2 (Ref. 18)	+19.2	(18.6)	3/14	-40.2	(28.5)	15/1	-9.6	(38.2)	18/15
NRC Screening Criteria (Ref. 19)	+23.0	(17.1)	0/17	-43.7	(39.9)	14/2	-9.4	(45.1)	14/19

a = Experimental, welds and plates separately, mean curve

b = Experimental, all data, mean curve

c = Surv. and exp., welds and plates separately, mean curve

d = Surv. and exp., all data, mean curve

e = Experimental, upper bound

f = Surveillance and experimental, upper bound

dependence, characterized by reduced weld metal embrittlement at high flux levels, from the test reactor data in this report. This postulated flux dependence is reflected in both notch ductility and fracture toughness (K_{Jc} and K_{Jc}) assessments of irradiation-induced embrittlement of weld metals. The suggested flux dependence is itself dependent on the assumption that the correlations used here give accurate estimates of weld metal embrittlement trends.

These trends of possible flux dependence are consistent with observations of Odette/Perrin (Ref. 10). Further data on flux effects will be available in the near future (Ref. 22).

7. SUMMARY AND CONCLUSIONS

For RPV safety assessments, knowledge of the fracture toughness (K_{Ic}) of the RPV materials is required. Since surveillance irradiations of sufficiently-large fracture toughness specimens for valid K_{Ic} measurements are not possible, estimates of the irradiated K_{Ic} properties are required. These approximations are made by using pre-irradiation properties (RT_{NDT}) and the transition temperature shift from Charpy-V specimens [$\Delta T(C_v)$] to index the ASME K_{Ic} and K_{IR} curves. To assess the appropriateness of using $\Delta T(C_v)$ to estimate $\Delta T(K_{Ic})$, comparisons of notch ductility (C_v) and fracture toughness (K_{Jc} and K_{Jc}) assessments of transition temperature shifts for RPV base metals and welds were made. This study provides the first assessment of the suitability of $\Delta T(C_v)$ for estimating $\Delta T(K_{Ic})$. Although these fracture toughness data are not valid according to ASTM E399, the data collected here (K_{Jc}) have been adjusted (K_{Jc}) to what is thought to be an accurate approximation to K_{Ic} values. However, this adjustment may over-correct high toughness values, leading to a real K_{Ic} curve which may lie somewhere between the K_{Jc} and K_{Jc} curves. Better insight to this will result from the HSST Fifth Irradiation Series (Ref. 21), where large CT specimens (up to 4T-CT) will be tested in an irradiated condition to provide valid K_{Ic} data at high toughness levels.

Also, comparisons between computerized and manual fits to the C_v and K curves were made, with predictions based on various shift correlations compared to measured C_v and K transition curve shifts.

Future work in this study will examine dependence of these observations on chemical composition, with additional data added to the study as more testing is completed.

Initial conclusions from this study are:

- (1) Transition temperature shifts (ΔT 's) measured by fracture toughness methods (K_{Jc} at 100 MPa \sqrt{m}) are only slightly greater than ΔT 's from notch ductility (C_v at 41 J) tests, on average by 9°C.
- (2) A product form effect influences the $\Delta T(K_{Jc})$ vs. $\Delta T(C_v)$ relationship, whereby $\Delta T(K_{Jc})$ for welds is overestimated by 5°C on average by C_v results and $\Delta T(K_{Jc})$ for plates is underestimated by 22°C on average by C_v results.

- (3) Adjusting the fracture toughness (K_{Jc}) data for lack of constraint (K_{Bc} values) results in an average match of $\Delta T(K_{Bc} @ 75 \text{ MPa}\sqrt{\text{m}})$ and $\Delta T(C_v @ 41 \text{ J})$ within 1°C . In this case, weld $\Delta T(C_v)$ values overestimate $\Delta T(K_{Bc})$ values by an average of 11°C , with plate $\Delta T(C_v)$ values underpredicting $\Delta T(K_{Bc})$ values by 10°C on average.
- (4) Comparison of ΔT values at various indices along the C_v , K_{Jc} and K_{Bc} curves give some basis for assessing irradiation effect on curve shape. In general, the C_v curves tend to flatten-out or lay-over, the K_{Jc} curve has no change in curve shape, and the irradiated K_{Bc} curve tends to be steeper than the unirradiated curve.
- (5) Manual and computerized fits to C_v and K data yield temperatures and ΔT 's at transition temperature indices within 5°C of one another, on average, for the data base examined. C_v upper shelf energy level and drop values from the manual fits are within 2 J of the computerized fit values, on average.
- (6) The correlation methods for predicting $\Delta T(C_v)$ tend to overestimate measured $\Delta T(C_v)$ values for weld metals, with base metal $\Delta T(C_v)$ values slightly underestimated by the correlation methods, on average.
- (7) The $\Delta T(C_v)$ correlation predictions show a large overestimate of $\Delta T(K_{Jc})$ and $\Delta T(K_{Bc})$ for welds; however, the $\Delta T(C_v)$ correlations underestimate $\Delta T(K_{Jc})$ and $\Delta T(K_{Bc})$ for plate, on average.
- (8) While the A 508-2 forging $\Delta T(C_v)$ is predicted reasonably well by the correlations, $\Delta T(K_{Jc})$ and $\Delta T(K_{Bc})$ for the forging are much larger than the $\Delta T(C_v)$ or any of the correlation predictions. This behavior is atypical of the other heats in the data base, and may indicate a problem limited in magnitude to forgings, or just this single forging. Consideration of this will be made in future work.
- (9) These results may indicate a flux dependence, whereby weld metals exhibit significantly lower embrittlement with higher flux, while plates exhibit slightly higher embrittlement at higher fluxes. This effect may be magnified for fracture toughness vs. notch ductility leading to the product form dependence observed here. This possibly will be studied closer in future work.

The above conclusions must be tempered by the understanding that many of the fracture toughness curves were composed of six or fewer data points. In general, irradiations of fracture toughness specimens result in too few specimens of too small a thickness to provide for complete and unambiguous definition of the fracture toughness behavior with temperature. Several bench-mark irradiations of many small thickness specimens of several compositions and product forms would be an excellent supplement to the HSST Fifth Irradiation Series mentioned previously.

REFERENCES

1. J. R. Hawthorne, et al., "Evaluation and Prediction of Neutron Embrittlement in Reactor Pressure Vessel Materials," EPRI NP-2782, Electric Power Research Institute, Dec. 1982.
2. J. R. Hawthorne, B. H. Menke and A. L. Hiser, "Notch Ductility and Fracture Toughness Degradation of A 302-B and A 533-B Reference Plates from PSF Simulated Surveillance and Through-Wall Irradiation Capsules," USNRC Report NUREG/CR-3295 Vol. 1, MEA-2017, May 1983.
3. B. H. Menke, et al., "Effects of Neutron Irradiation on Fracture Toughness of A 533 Grade B Class 1 Plate and Four Submerged-Arc Welds," presented at the ASTM 12th Irradiation Effects Symposium, June 12-22, 1984 (in press).
4. J. R. Hawthorne, "Evaluation of Reembrittlement Rate Following Annealing and Related Investigations of RPV Steels," Proceedings of the 11th Water Reactor Safety Research Information Meeting, USNRC Proceedings NUREG/CP-0048, Vol. 4, Jan. 1984, pp. 361-375.
5. S. T. Rolfe and S. R. Novak, "Slow-Bend K_{IC} Testing of Medium-Strength High-Toughness Steels," Review of Developments in Plane Strain Fracture Toughness Testing, ASTM STP 463, American Society for Testing and Materials, Phila., PA, 1970, pp. 124-159.
6. R. H. Sailors and H. T. Corten, "Relationship Between Material Fracture Toughness Using Fracture Mechanics and Transition Temperature Tests," Fracture Toughness, ASTM STP 514, American Society for Testing and Materials, Phila., PA, 1972, pp. 164-191.
7. J. G. Merkle, "An Examination of the Size Effects and Data Scatter Observed in Small Specimen Cleavage Fracture Toughness Testing," USNRC NUREG/CR-3672, ORNL/TM-9088, Oak Ridge National Laboratory, April 1984.
8. G. R. Irwin, "Fracture Mode Transition for a Crack Traversing a Plate," J. of Basic Eng., ASME, 82(2), 1960, pp. 417-425.
9. G. L. Guthrie, "LWR Pressure Vessel Surveillance Dosimetry Improvement Program, Quarterly Progress Report for the Period April-June 1982," USNRC Report NUREG/CR-2805, Vol. 2, HEDL-TME-82-19, Hanford Engineering Development Laboratory, Jan. 1983, pp. HEDL-3-4.
10. J. F. Perrin, R. A. Wullaert, G. R. Odette and P. M. Lombrozo, "Physically Based Regression Correlations of Embrittlement Data From Reactor Pressure Vessel Surveillance Programs," EPRI NP-3319, Electric Power Research Institute, Jan. 1984.

11. Metal Properties Council Subcommittee 6 on Nuclear Materials, "Prediction of the Shift in the Brittle-Ductile Transition Temperature of Light-Water Reactor (LWR) Pressure Vessel Materials," Journal of Testing and Evaluation, Vol. 11(4), July 1983, pp. 237-260.
12. ASTM Committee E 900-83, "Standard Guide For Predicting Neutron Radiation Damage to Reactor Vessel Materials," Volume 12.02, pp. 703-706, April 1983.
13. J. D. Varsik, S. M. Schloss and J. J. Koziol, "Evaluation of Irradiation Response of Reactor Pressure Vessel Materials," EPRI NP-2720, Electric Power Research Institute, Nov. 1982.
14. J. D. Varsik and S. T. Byrne, "An Empirical Evaluation of the Irradiation Sensitivity of Reactor Pressure Vessel Materials," Effects of Radiation on Structural Materials, Effects of Radiation on Structural Materials, ASTM STP 683, J. A. Sprague and D. Kramer, eds., American Society for Testing and Materials, Phila, PA, 1979, pp. 252-266.
15. A. S. Heller and A. L. Lowe, Jr., "Correlations for Predicting the Effects of Neutron Radiation on Linde 80 Submerged-Arc Welds," BAW-1803, Babcock & Wilcox Co., Jan. 1984.
16. R. G. Berggren and F. W. Stallmann, "Statistical Analysis of Pressure Vessel Steel Embrittlement Data," from the ANS Special Session on Correlations and Implications of Neutron Irradiation Embrittlement of Pressure Vessel Steels, Detroit, MI, June 12-16, 1983, Trans. Am. Nucl. Soc., Vol. 44, 1983, p. 225.
17. Regulatory Guide 1.99, Effects of Residual Elements on Predicted Radiation Damage to Reactor Vessel Materials, Rev. 1, USNRC, Washington, D.C., April 1977.
18. Draft of Revision 2 to Regulatory Guide 1.99, "Radiation Damage to Reactor Vessel Materials," USNRC, Washington, D.C., Working Paper G, August 14, 1985.
19. W. Dircks, NRC Staff Evaluation of Pressurized Thermal Shock, NRC-SECY-82-465, Nov., 1982.
20. W. Oldfield, P. McConnel, W. Server, and F. Oldfield, "Irradiated Pressure Vessel Steel Data Base," EPRI NP2428, Electric Power Research Institute, 1982.
21. "Heavy-Section Steel Technology Program: Five-Year Plan, FY 1983-1987," USNRC Report NUREG/CR-3595, ORNL/TM-9008, Oak Ridge National Laboratory.
22. "Structural Integrity of Light Water Reactor Pressure Boundary Components: Four-Year Plan 1984-1988," USNRC Report NUREG/CR-3788, MEA-2047, Sept. 1984.

APPENDIX A

Comparison Plots of Measured
and Predicted $\Delta T(C_v @ 41 J)$

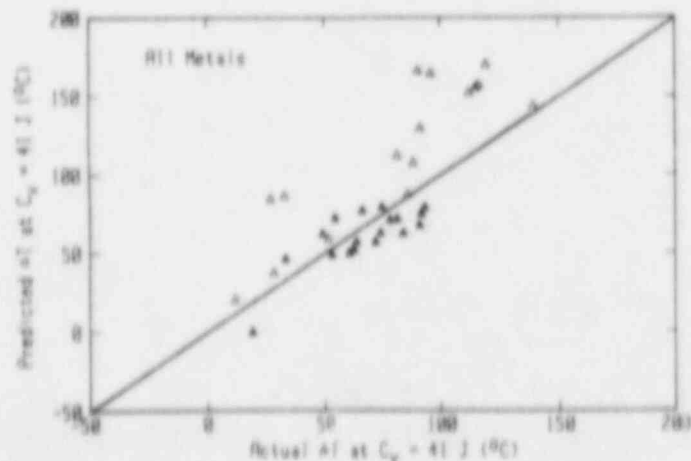
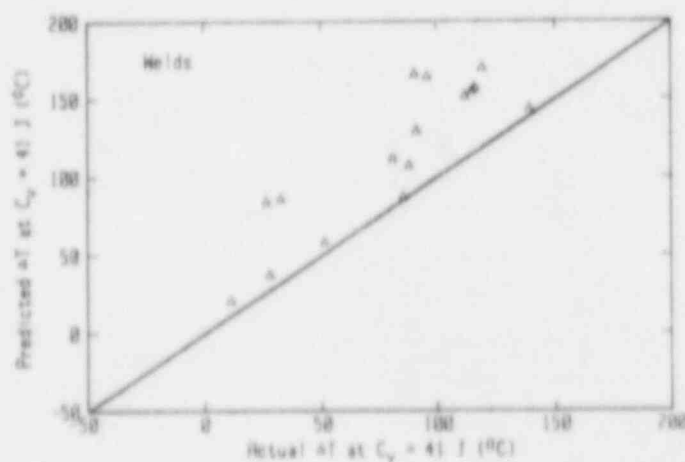
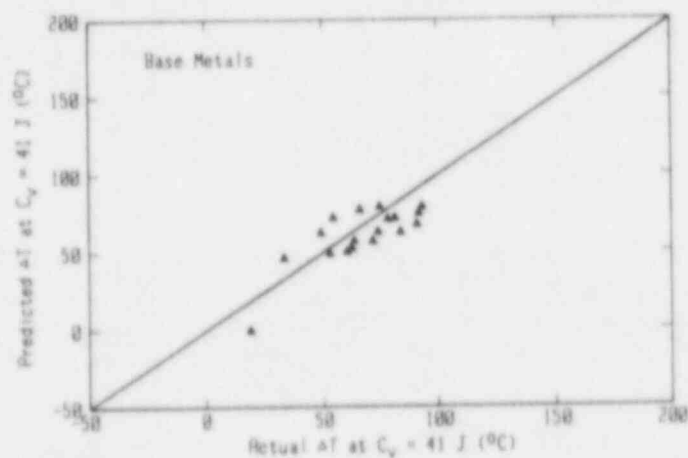


Fig. A-1 Comparison of $\Delta T(C_V @ 41 \text{ J})$ from the experimental data with values predicted using Guthrie (Ref. 9). In this figure and others in the appendix, filled symbols are for base metals and open symbols are for welds.

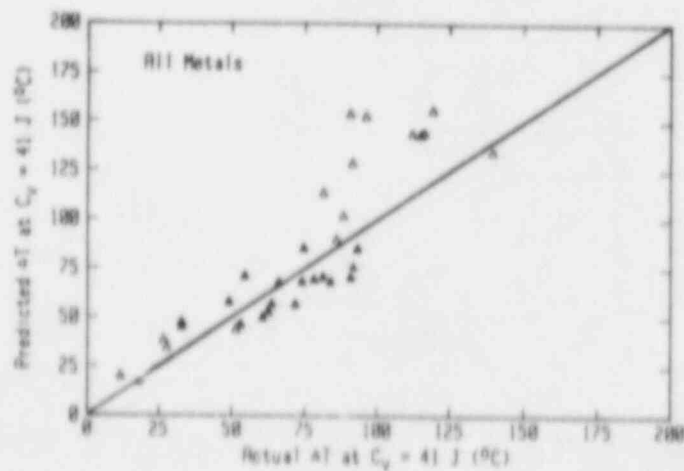
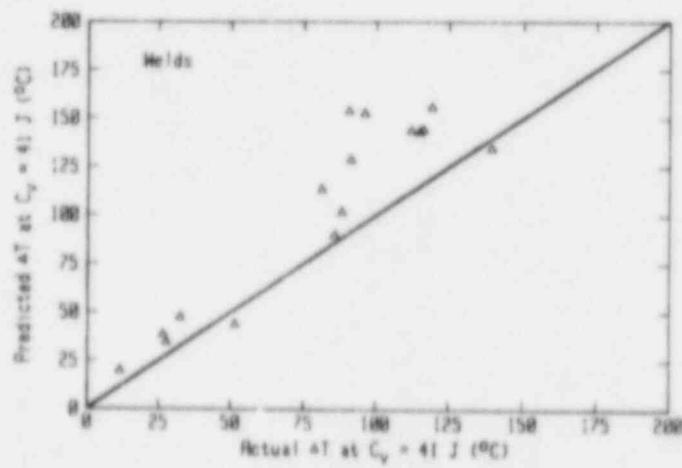
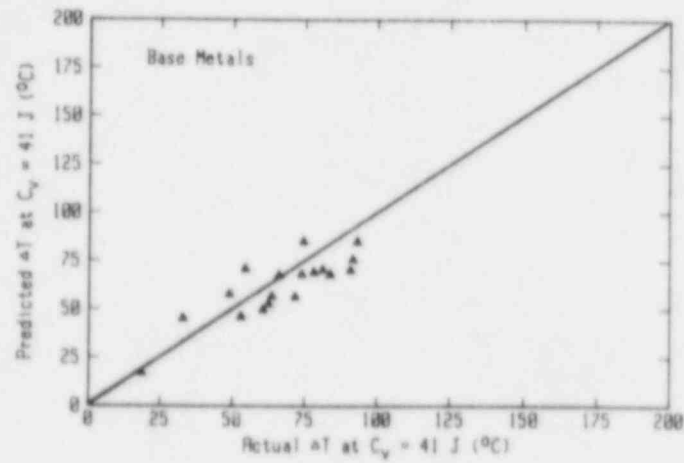


Fig. A-2 Comparison of $\Delta T(C_v @ 41 \text{ J})$ from the experimental data with values predicted using Odette/Perrin (Ref. 10).

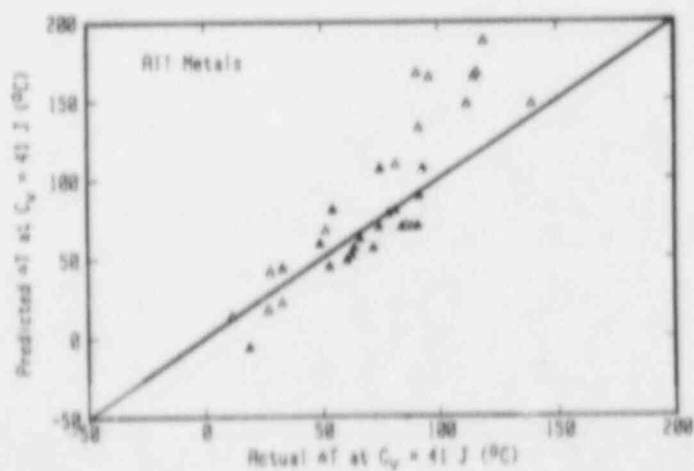
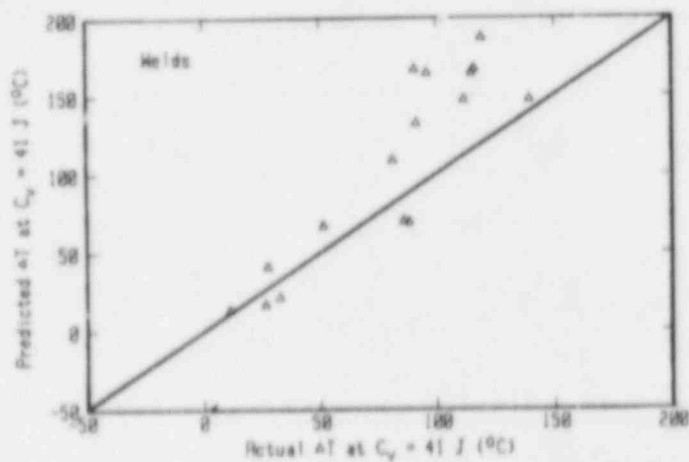
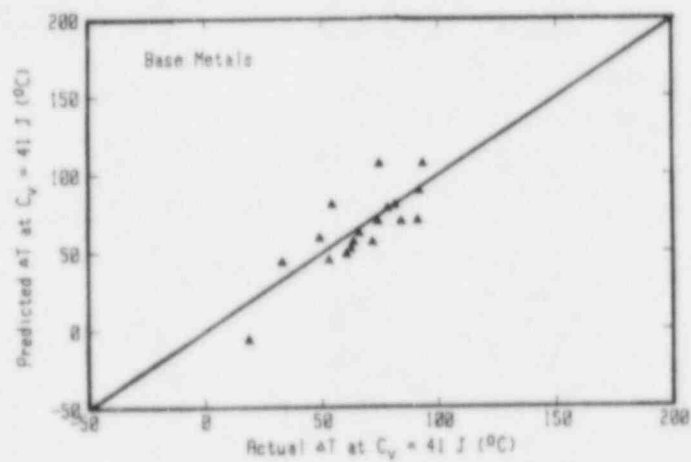


Fig. A-3 Comparison of $\Delta T(C_v @ 41 \text{ J})$ from the experimental data with values predicted using MPC set 1 (Ref. 11).

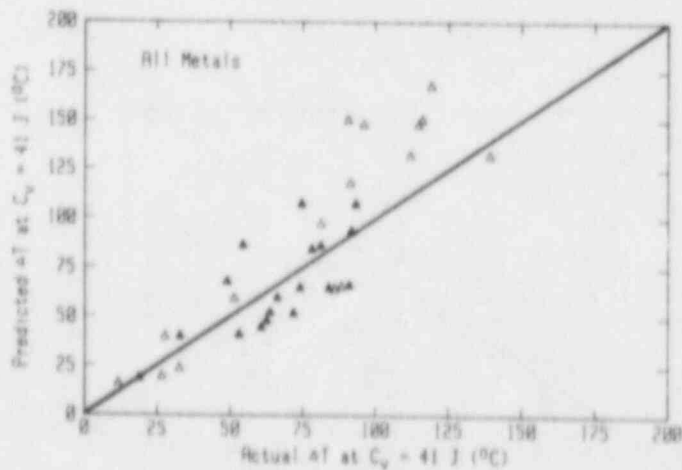
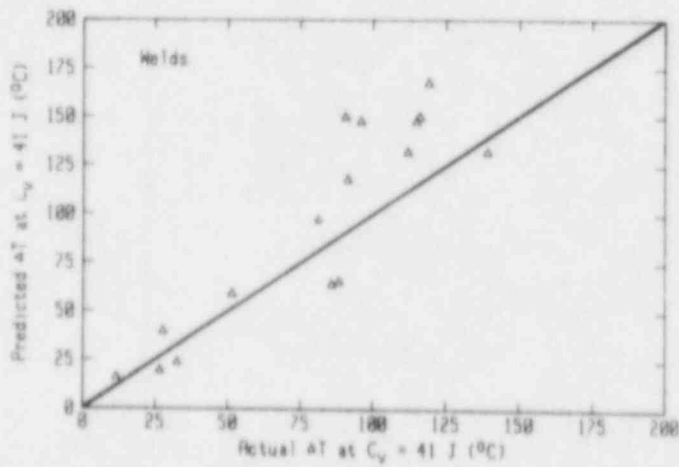
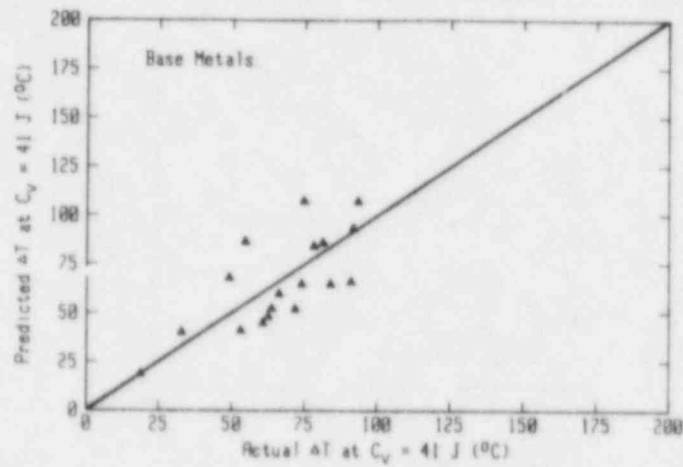


Fig. A-4 Comparison of $\Delta T(C_V @ 41 \text{ J})$ from the experimental data with values predicted using MPC set 2 (Ref. 11).

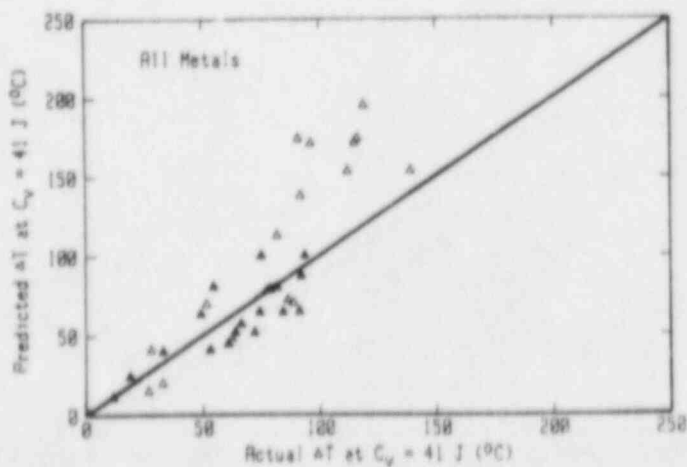
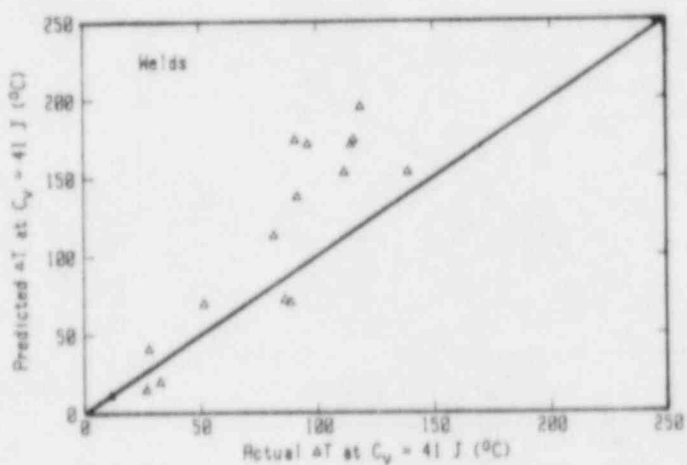
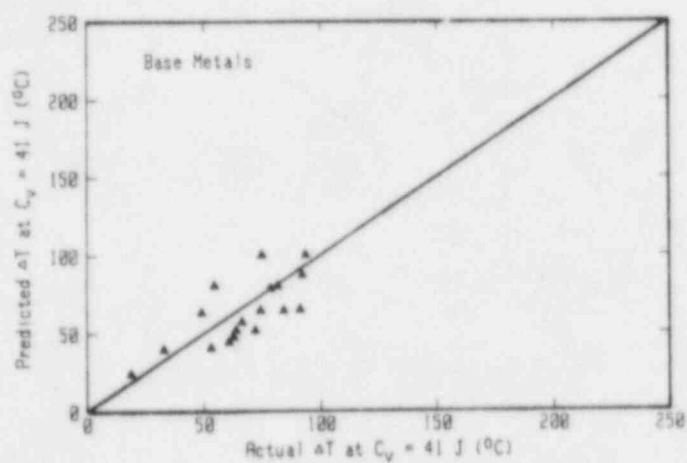


Fig. A-5 Comparison of $\Delta T(C_v @ 41 \text{ J})$ from the experimental data with values predicted using MPC set 3 (Ref. 11).

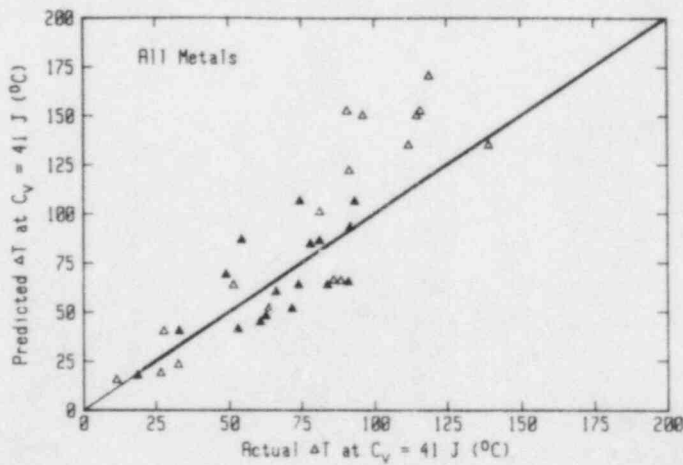
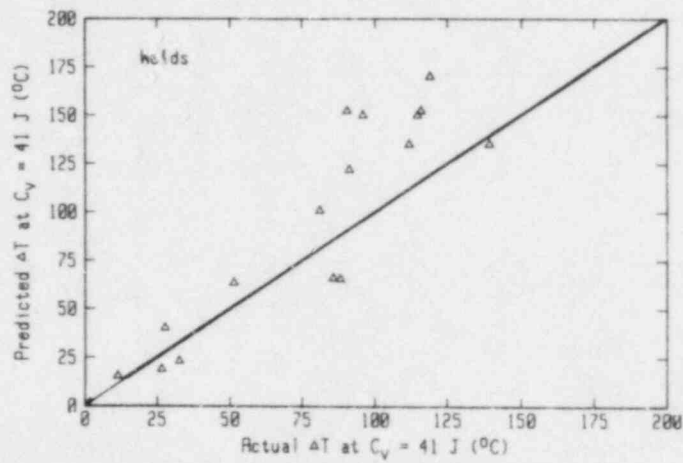
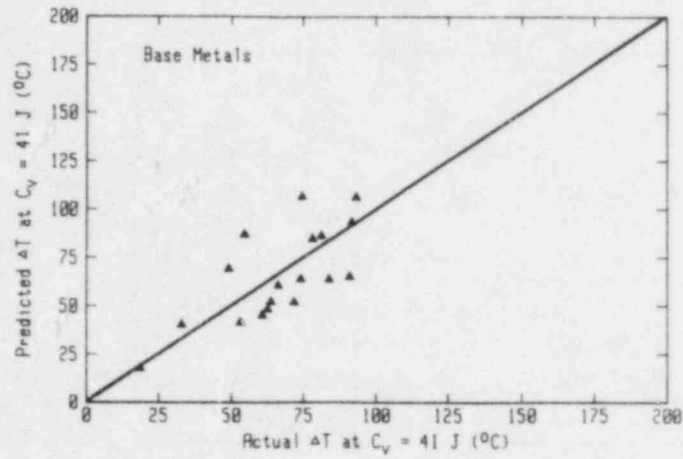


Fig. A-6 Comparison of $\Delta T(C_V @ 41 \text{ J})$ from the experimental data with values predicted using MPC set 4 (Ref. 11).

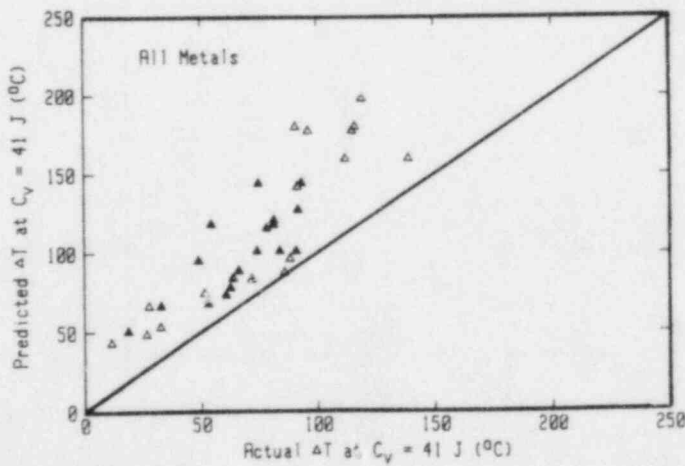
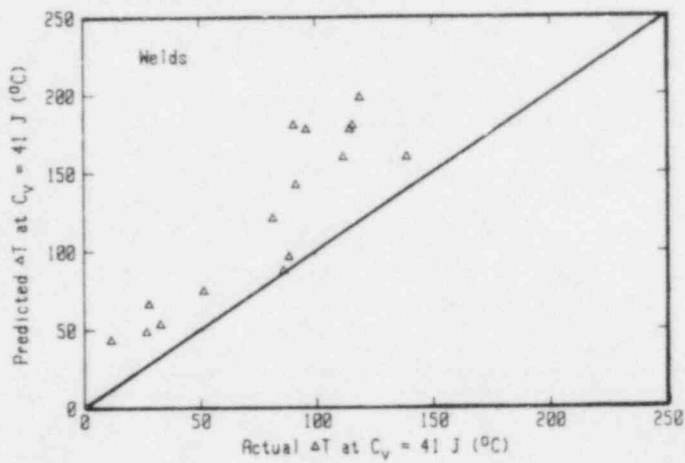
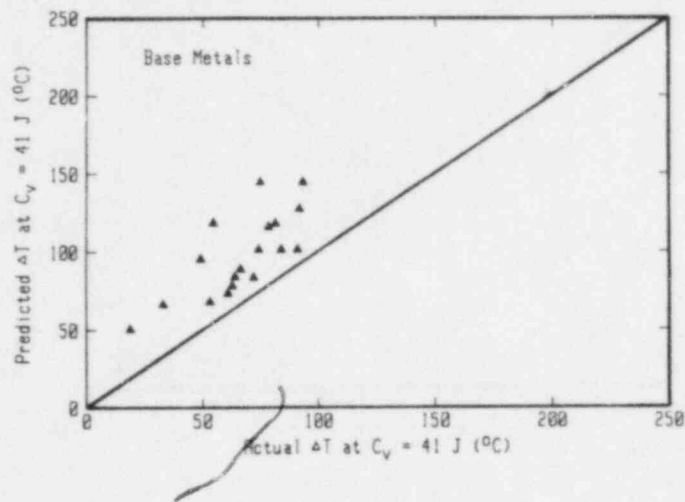


Fig. A-7 Comparison of $\Delta T(C_v @ 41 \text{ J})$ from the experimental data with values predicted using MPC set 5 (Ref. 11).

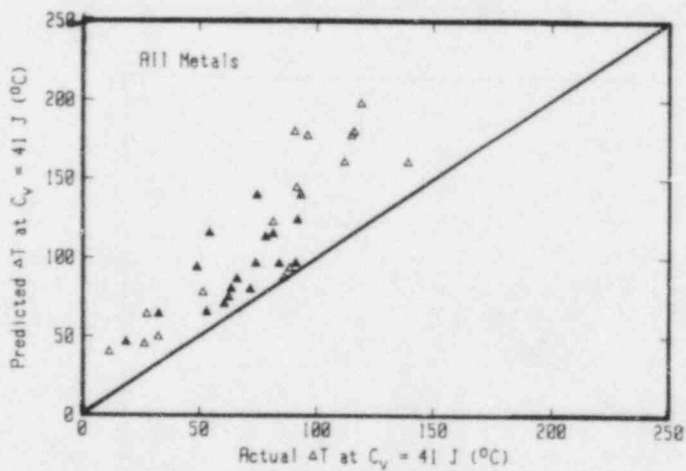
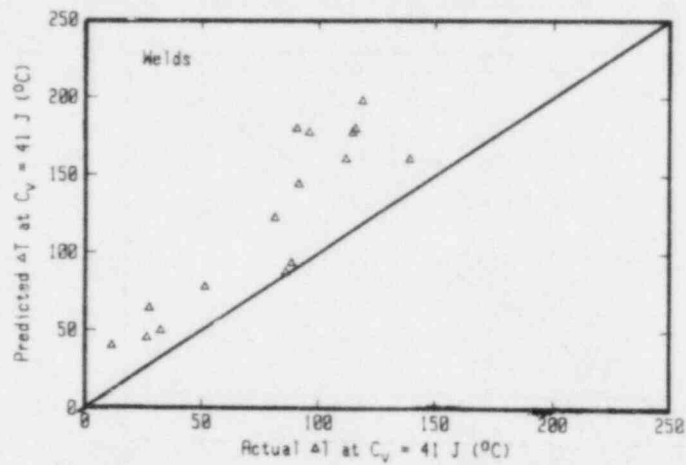
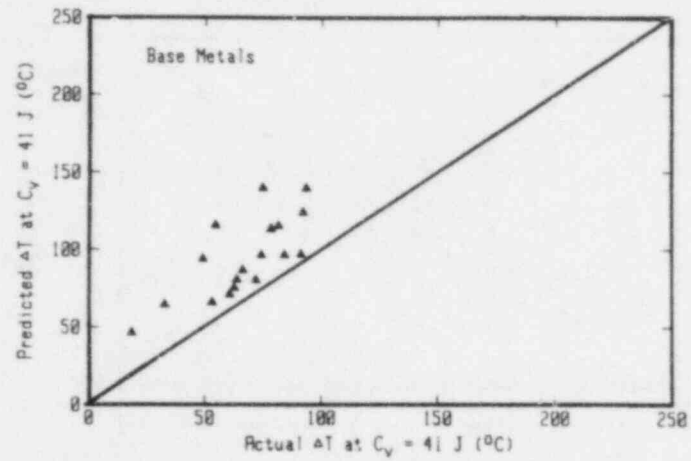


Fig. A-8 Comparison of $\Delta T(C_v @ 41 \text{ J})$ from the experimental data with values predicted using MPC set 6 (Ref. 11).

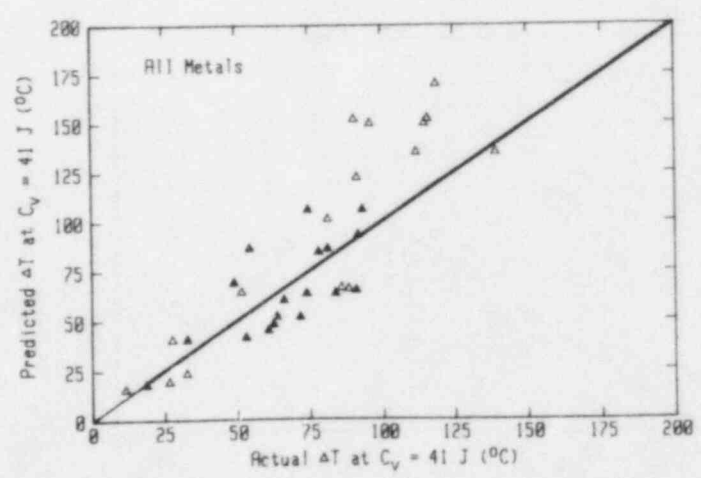
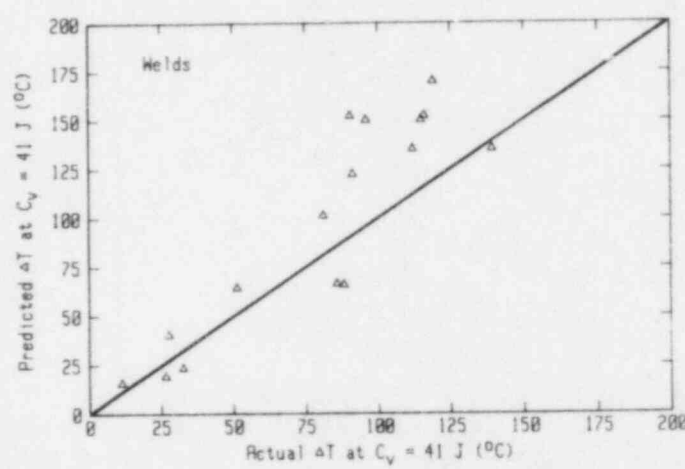
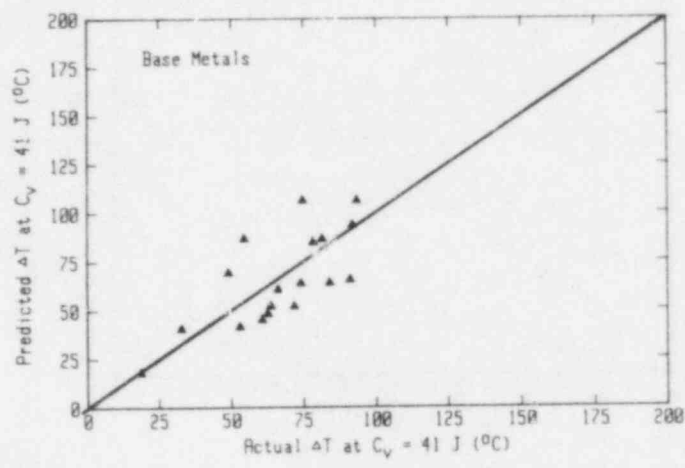


Fig. A-9 Comparison of $\Delta T(C_v @ 41 \text{ J})$ from the experimental data with values predicted using ASTM E 900 (Ref. 12).

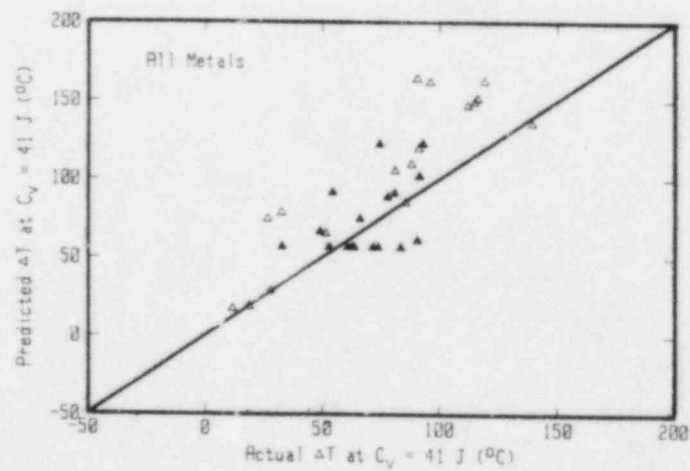
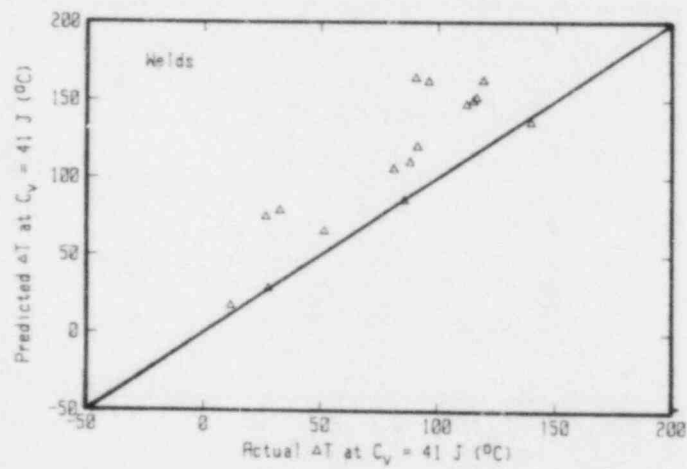
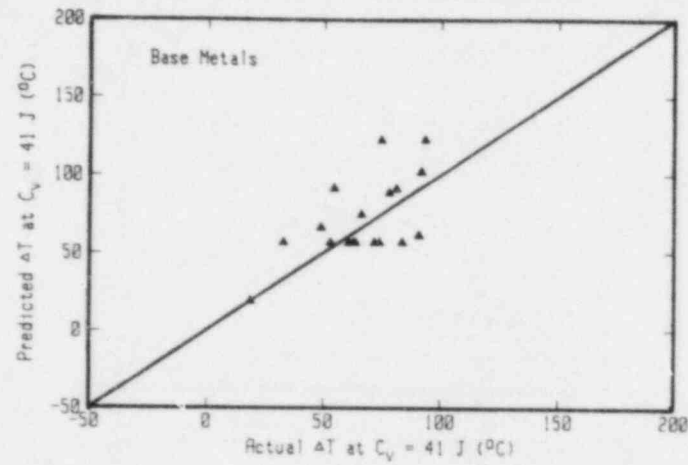


Fig. A-10 Comparison of $\Delta T(C_v @ 41 \text{ J})$ from the experimental data with values predicted using Varsik (Ref. 13).

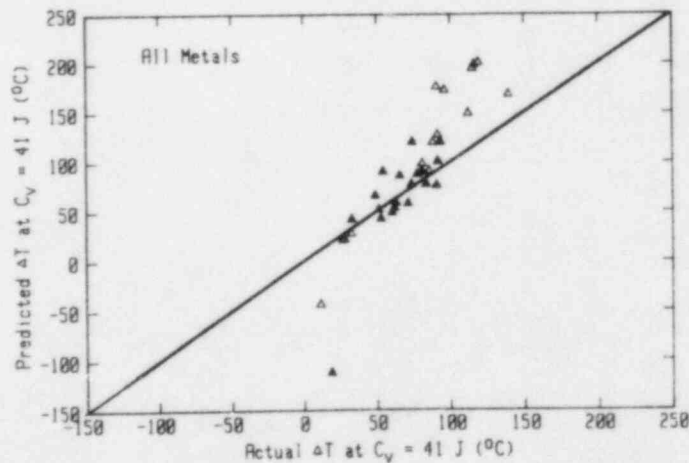
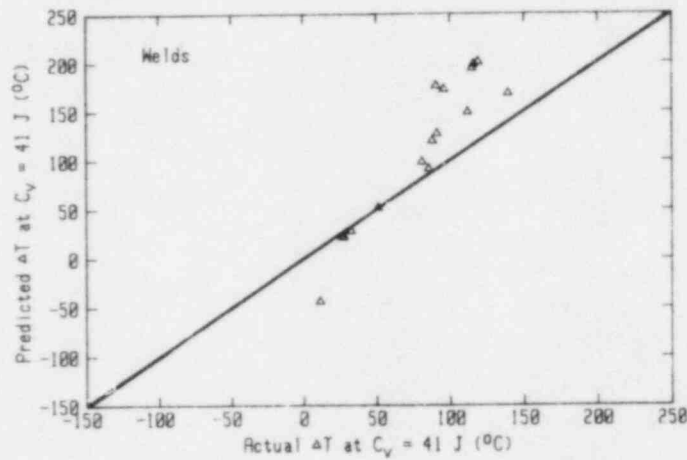
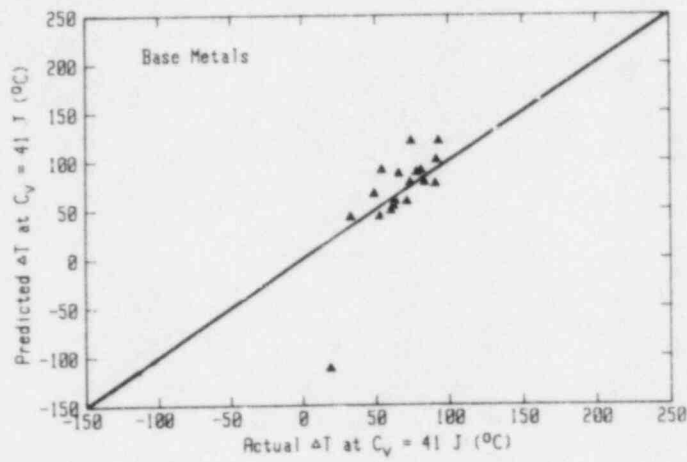


Fig. A-11 Comparison of $\Delta T(C_V @ 41 \text{ J})$ from the experimental data with values predicted using Varsik/Byrne (Ref. 14).

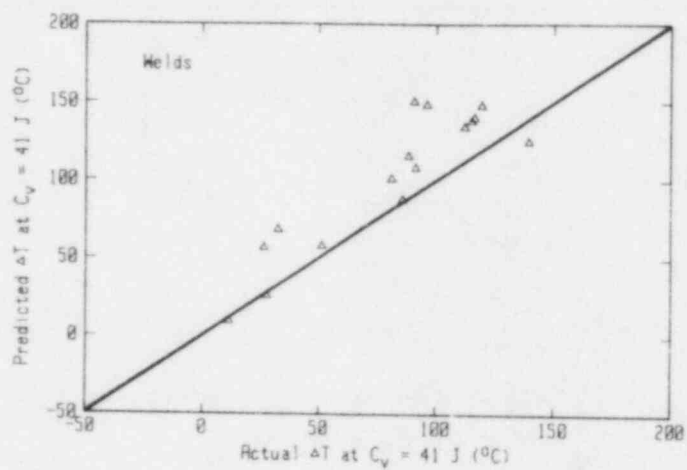


Fig. A-12 Comparison of $\Delta T(C_v @ 41 \text{ J})$ from the experimental data with values predicted using revised Varsik/Byrne (Ref. 13).

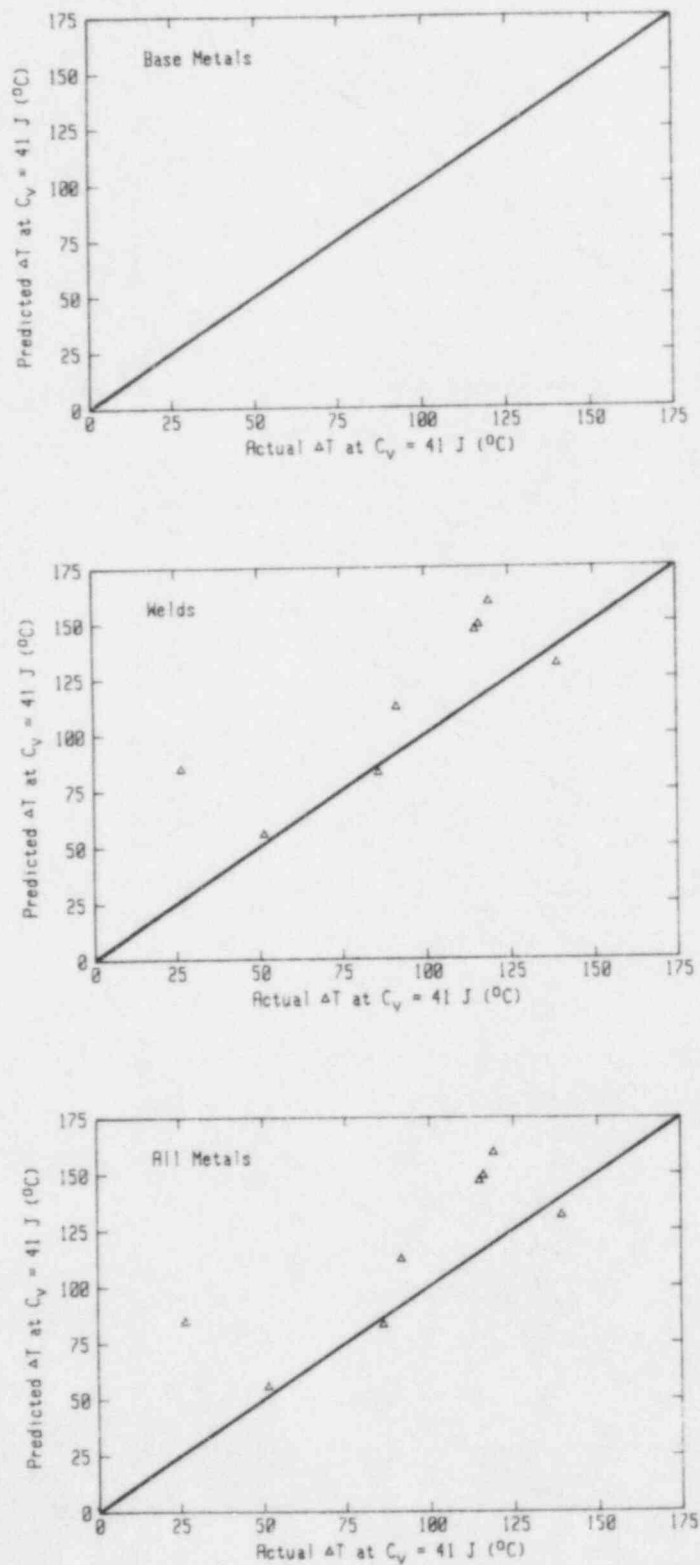


Fig. A-13 Comparison of $\Delta T(C_v @ 41 \text{ J})$ from the experimental data with values predicted using Heller/Lowe (Ref. 15). This correlation is applicable to Linde 80 welds only.

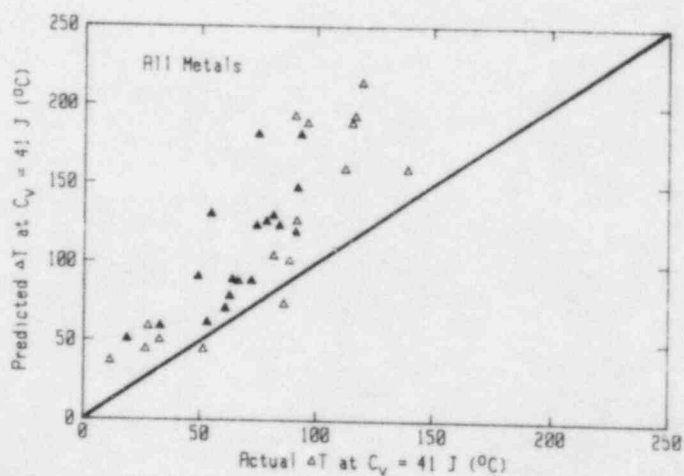
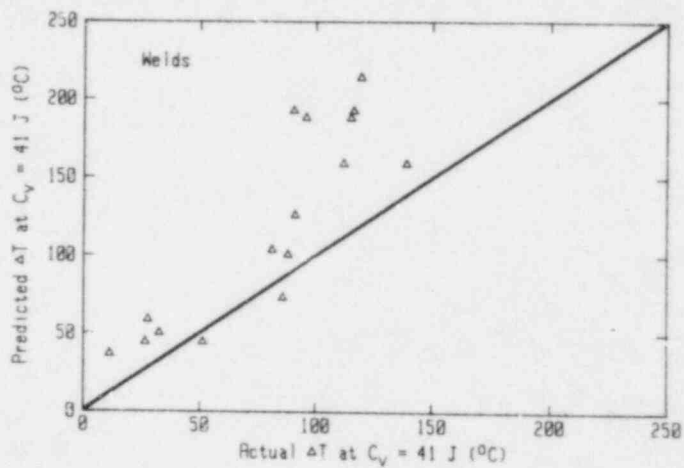
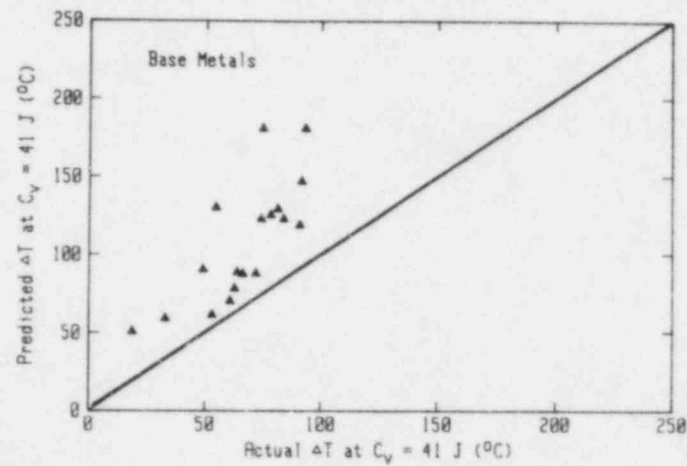


Fig. A-14 Comparison of $\Delta T(C_V @ 41 \text{ J})$ from the experimental data with values predicted using Berggren/Stallman (Ref. 16).

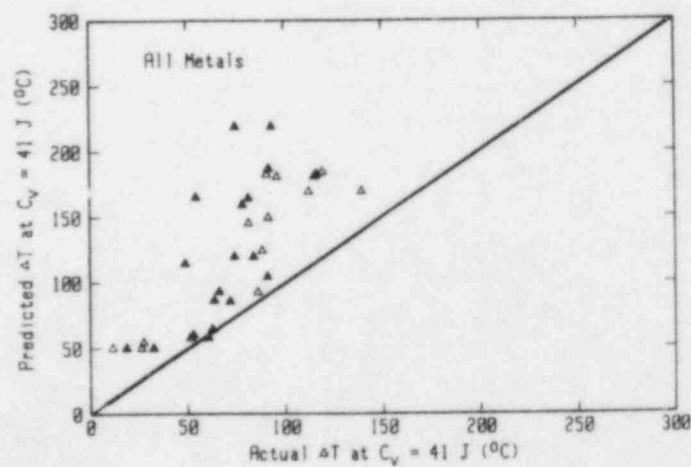
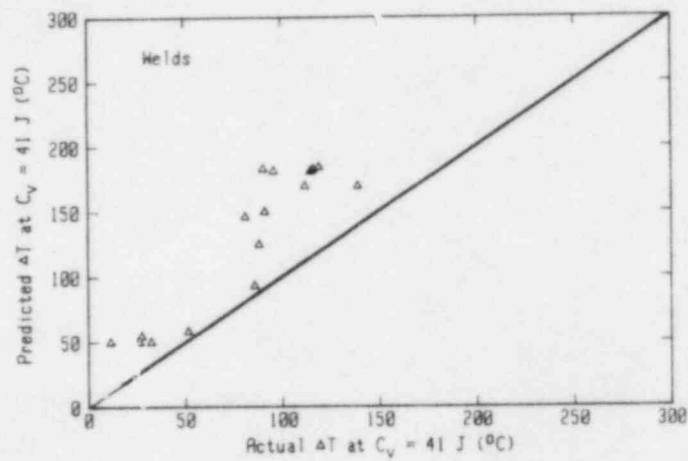
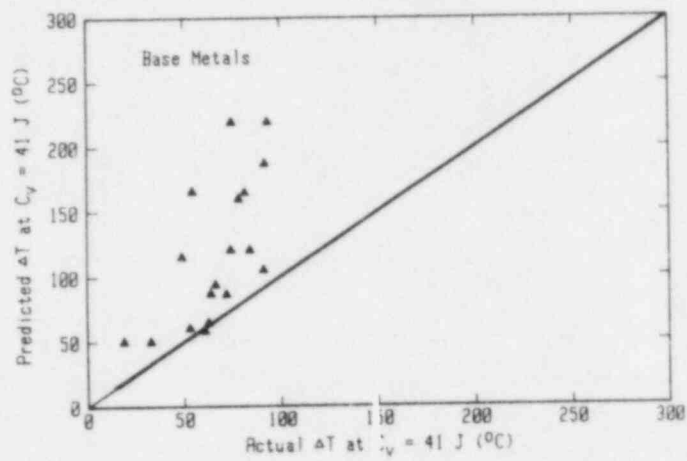


Fig. A-15 Comparison of $\Delta T(C_v @ 41 \text{ J})$ from the experimental data with values predicted using Regulatory Guide 1.99, Rev. 1 (Ref. 17).

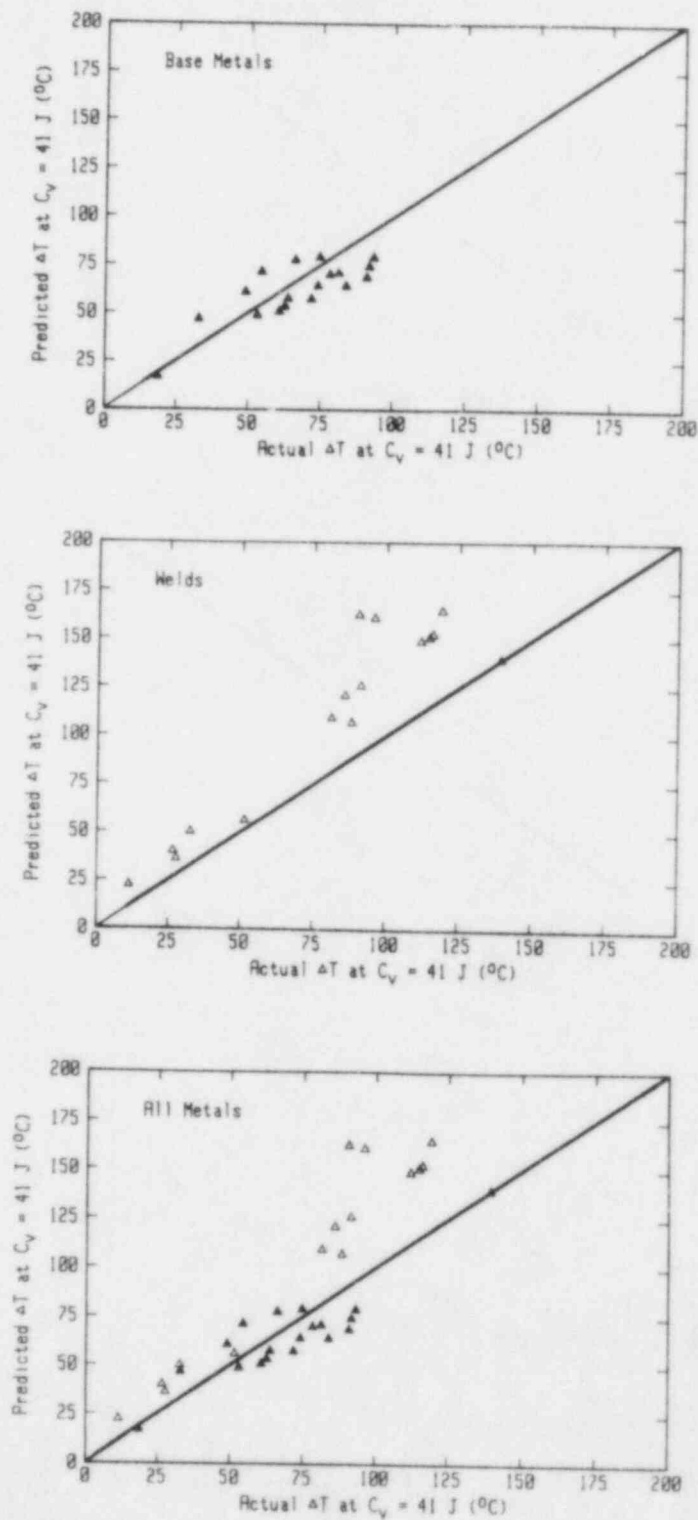


Fig. A-16 Comparison of $\Delta T(C_v @ 41 \text{ J})$ from the experimental data with values predicted using draft of Revision 2 to Regulatory Guide 1.99 (Ref. 18).

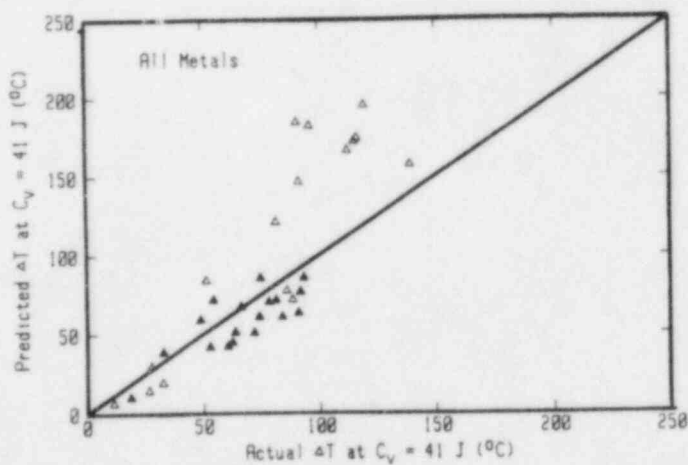
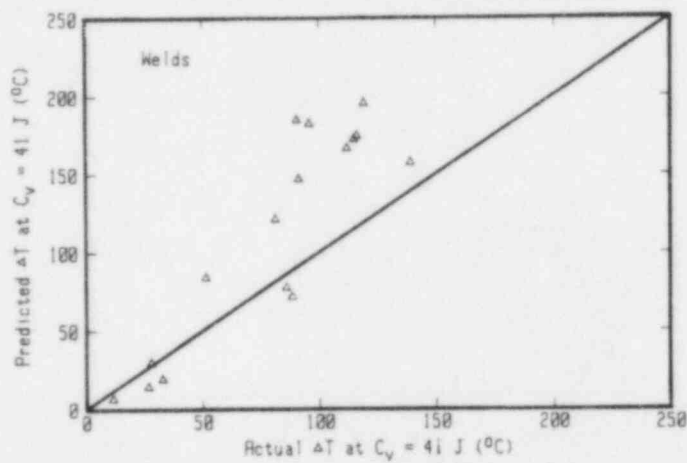
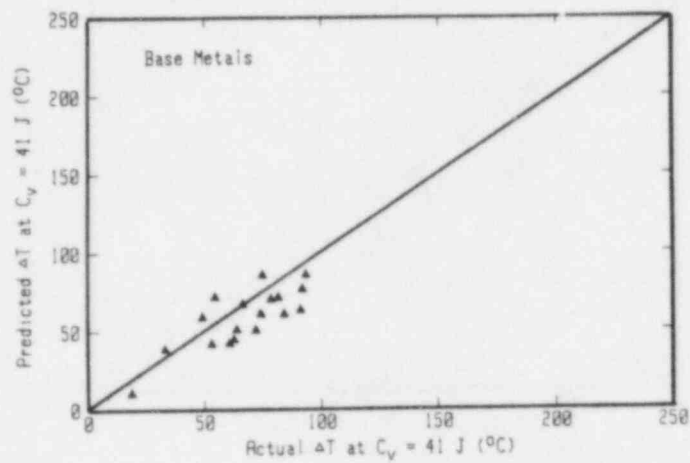


Fig. A-17 Comparison of $\Delta T(C_V @ 41 \text{ J})$ from the experimental data with values predicted using NRC Screening Criteria (Ref. 19).

APPENDIX B

Comparison Plots of Measured $\Delta T(K_{Jc} @ 100 \text{ MPa}\sqrt{\text{m}})$
and Predicted $\Delta T(C_v @ 41 \text{ J})$

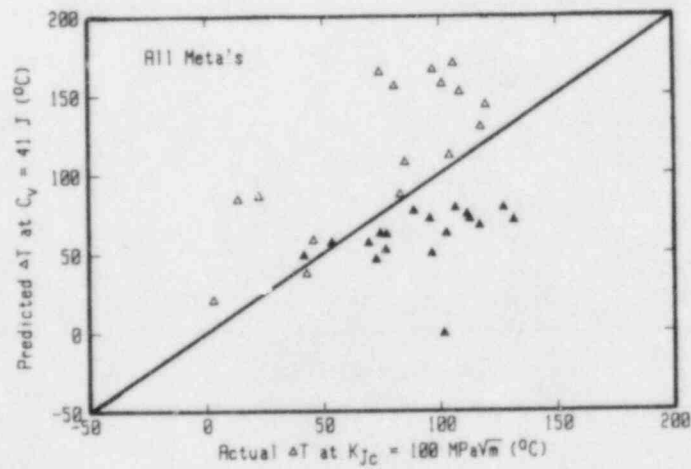
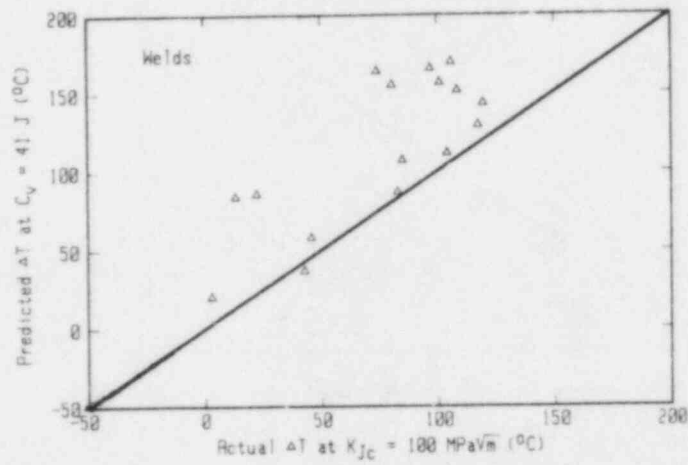
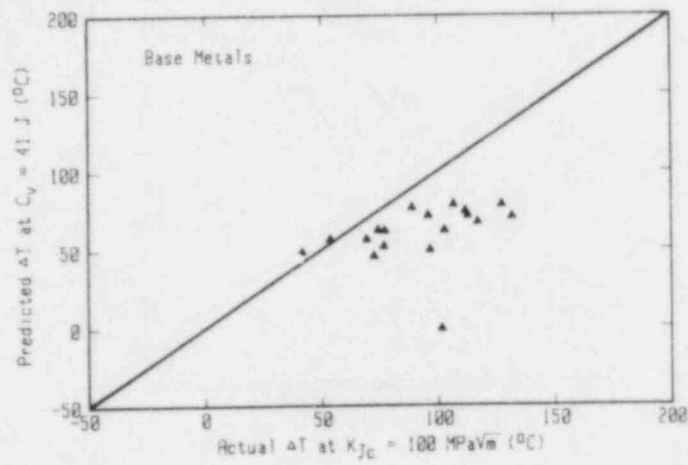


Fig. B-1 Comparison of $\Delta T(K_{JC} @ 100 \text{ MPa}\sqrt{\text{m}})$ from the experimental data with values of $\Delta T(C_V @ 41 \text{ J})$ predicted using Guthrie (Ref. 9).

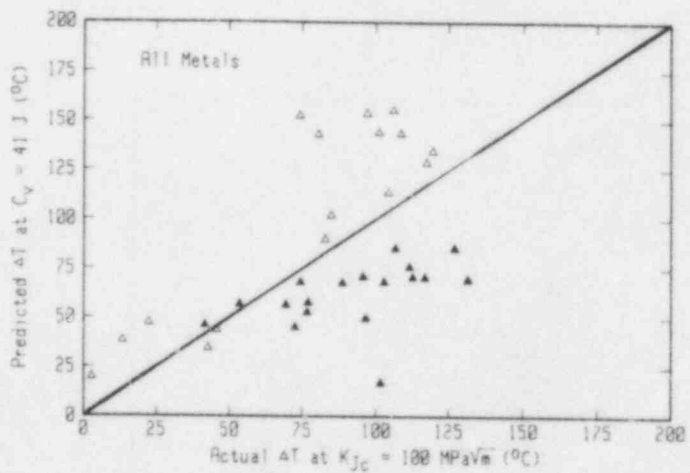
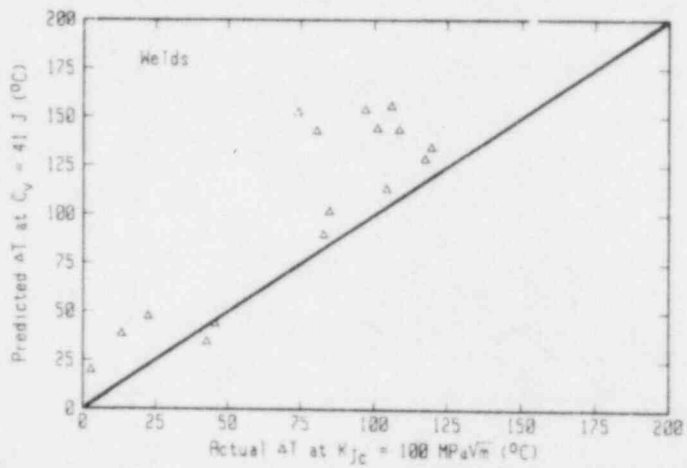
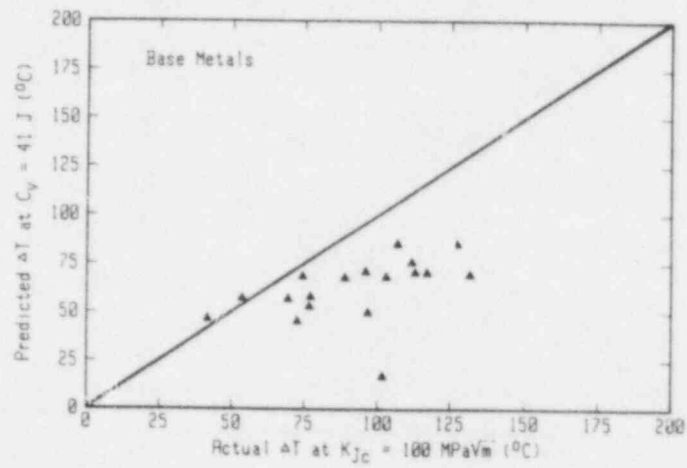


Fig. B-2 Comparison of $\Delta T(K_{Jc} @ 100 \text{ MPa}\sqrt{\text{m}})$ from the experimental data with values of $\Delta T(C_v @ 41 \text{ J})$ predicted using Odette/Perrin (Ref. 10).

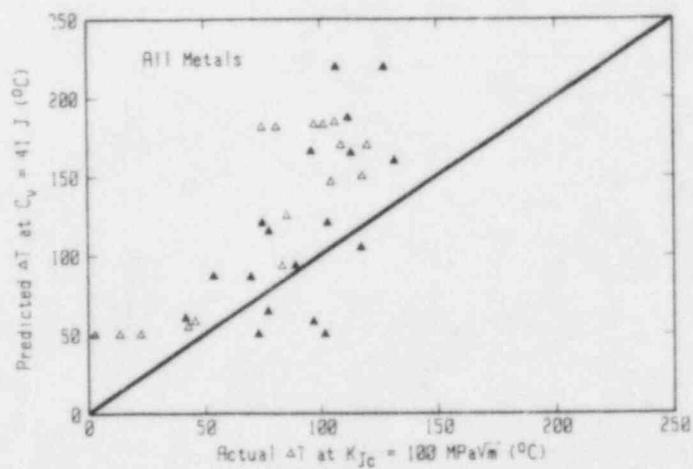
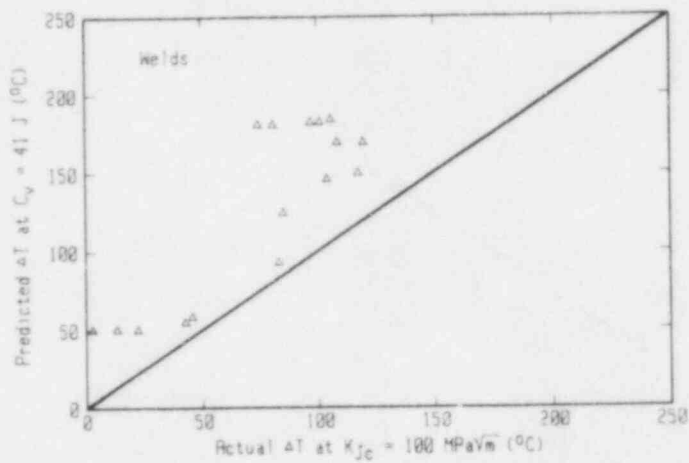
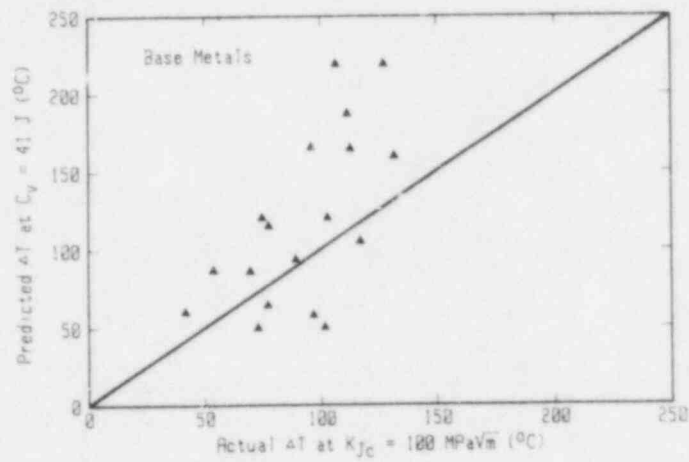


Fig. B-3 Comparison of $\Delta T(K_{Jc} @ 100 \text{ MPa}\sqrt{\text{m}})$ from the experimental data with values of $\Delta T(C_v @ 41 \text{ J})$ predicted using MPC set 1 (Ref. 11).

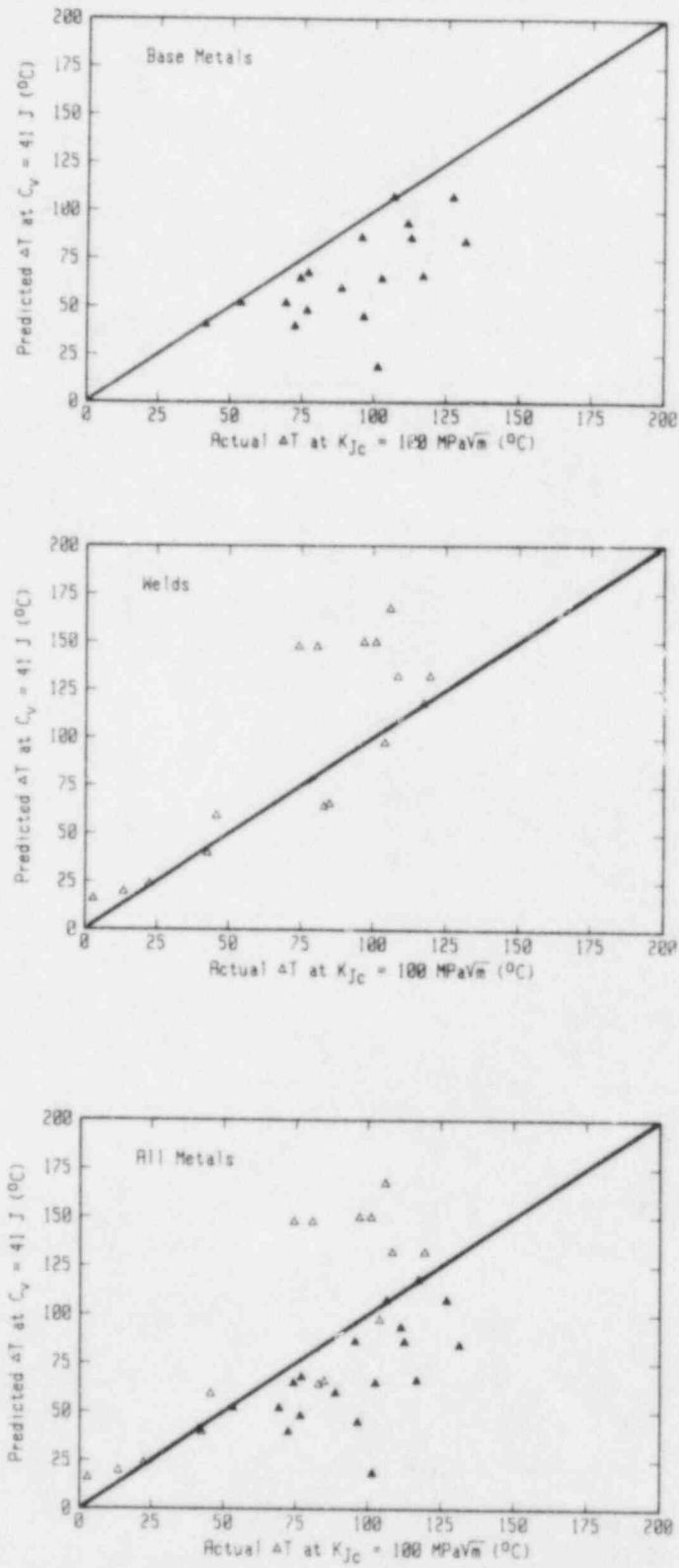


Fig. B-4 Comparison of $\Delta T(K_{IC} @ 100 \text{ MPa}\sqrt{\text{m}})$ from the experimental data with values of $\Delta T(C_V @ 41 \text{ J})$ predicted using MPC set 2 (Ref. 11).

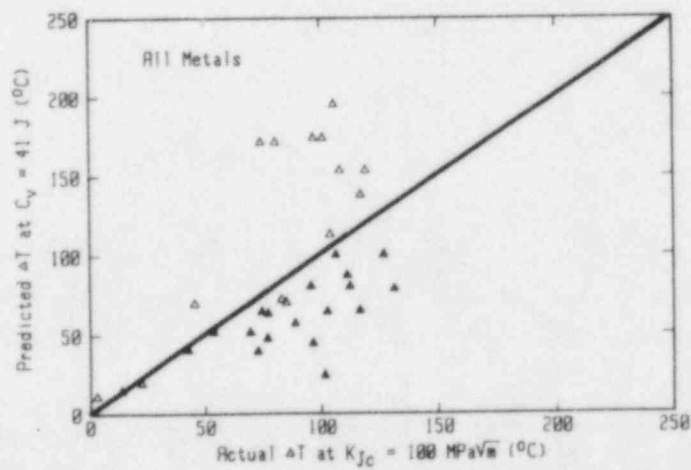
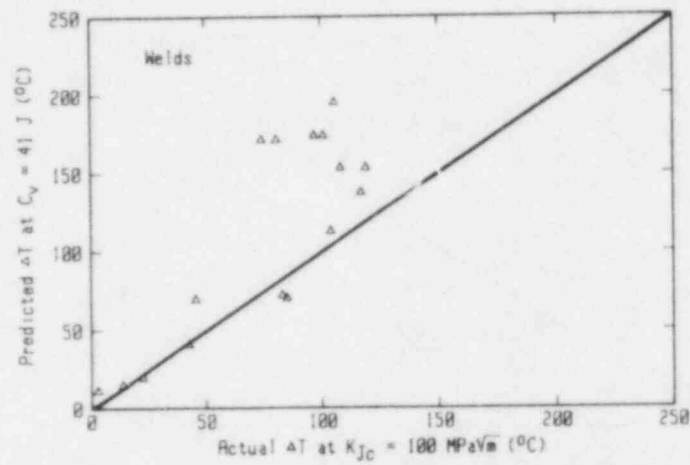
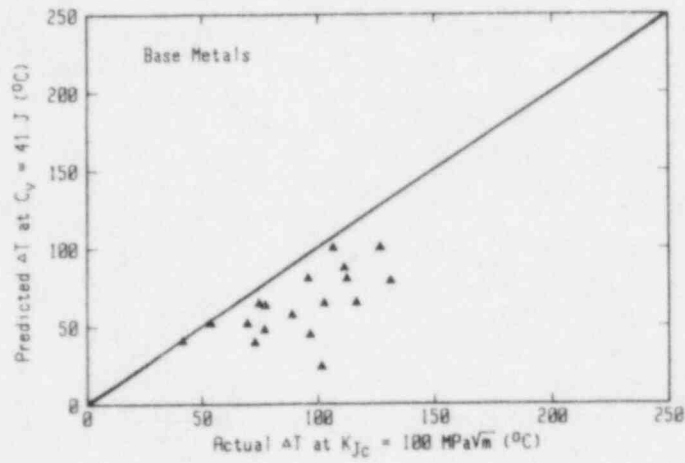


Fig. B-5 Comparison of $\Delta T(K_{JC} @ 100 \text{ MPa}\sqrt{\text{m}})$ from the experimental data with values of $\Delta T(C_V @ 41 \text{ J})$ predicted using MPC set 3 (Ref. 11).

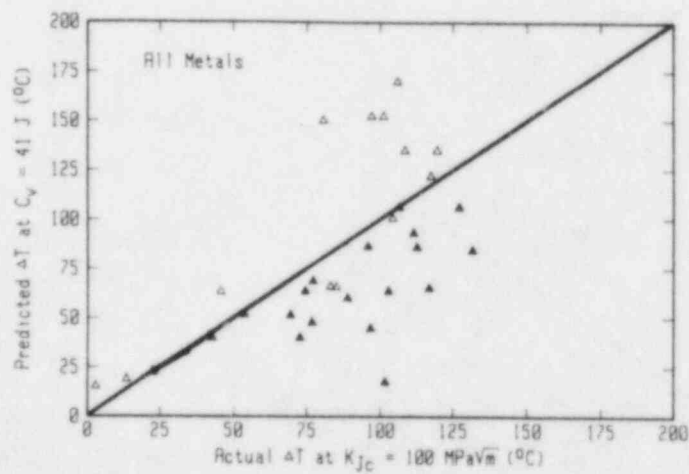
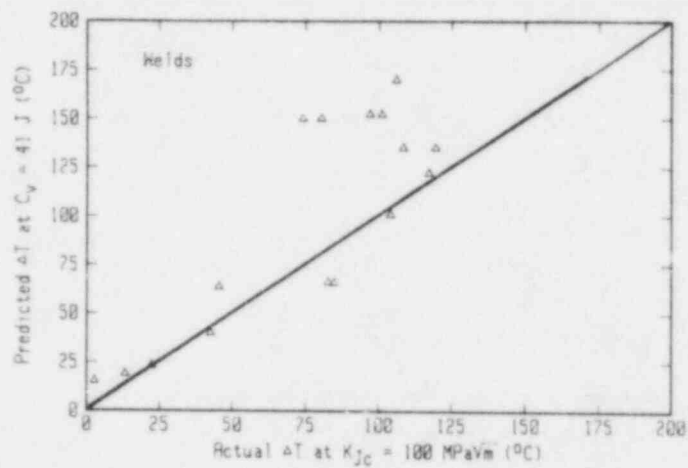
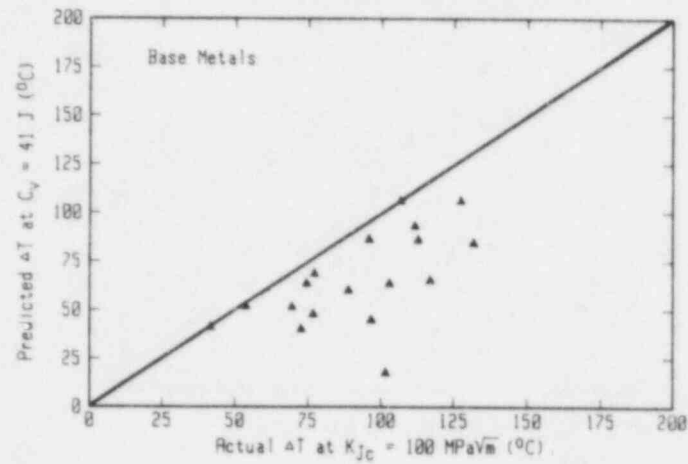


Fig. B-6 Comparison of $\Delta T(K_{Jc} @ 100 \text{ MPa}\sqrt{\text{m}})$ from the experimental data with values of $\Delta T(C_v @ 41 \text{ J})$ predicted using MPC set 4 (Ref. 11).

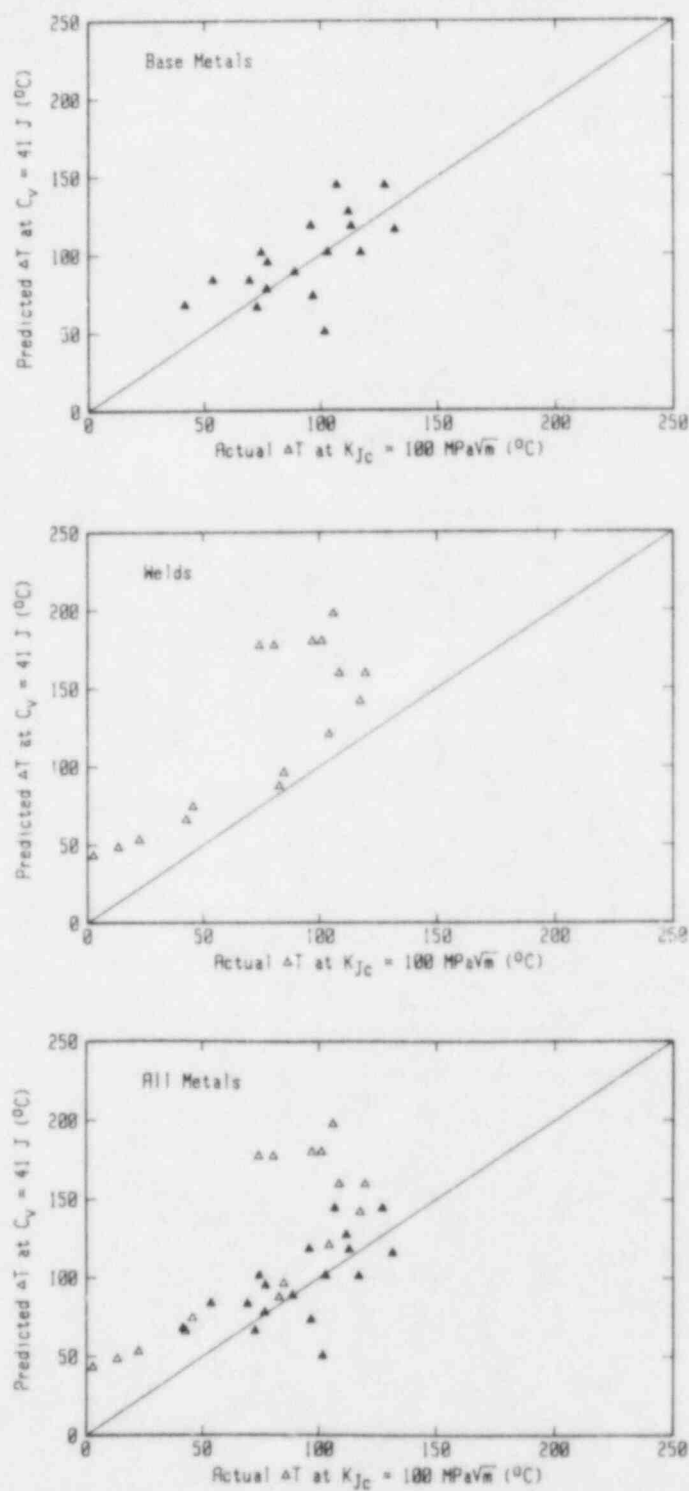


Fig. B-7 Comparison of $\Delta T(K_{JC} @ 100 \text{ MPa}\sqrt{\text{m}})$ from the experimental data with values of $\Delta T(C_v @ 41 \text{ J})$ predicted using MPC set 5 (Ref. 11).

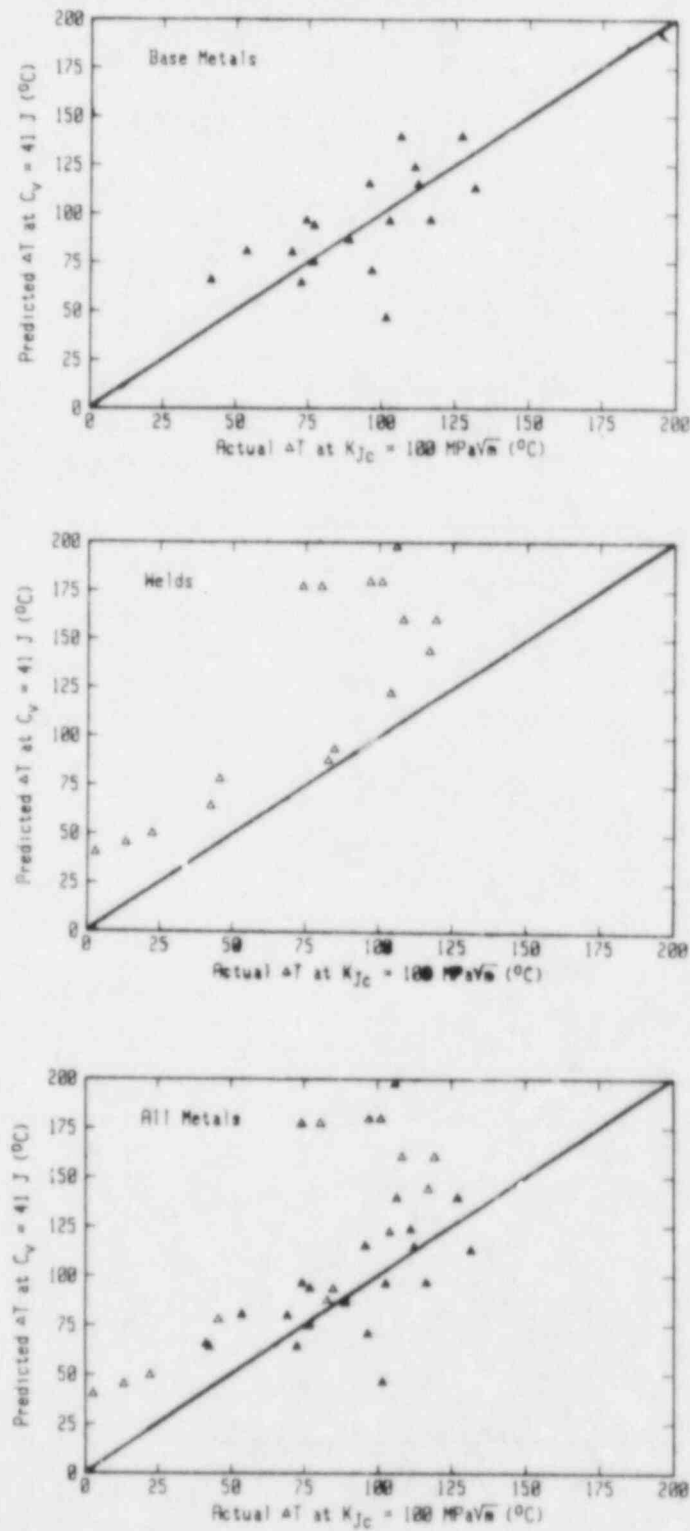


Fig. B-8 Comparison of $\Delta T(K_{JC} @ 100 \text{ MPa}\sqrt{\text{m}})$ from the experimental data with values of $\Delta T(C_v @ 41 \text{ J})$ predicted using MPC set 6 (Ref. 11).

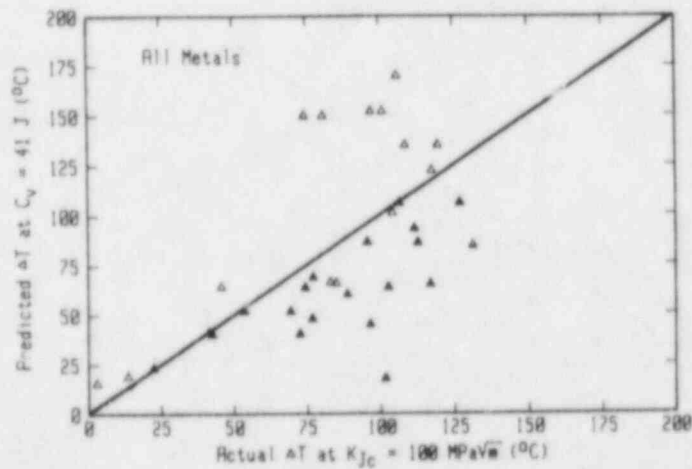
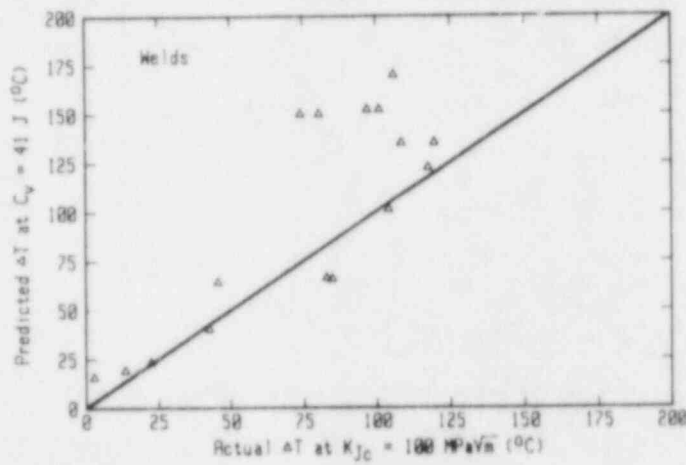
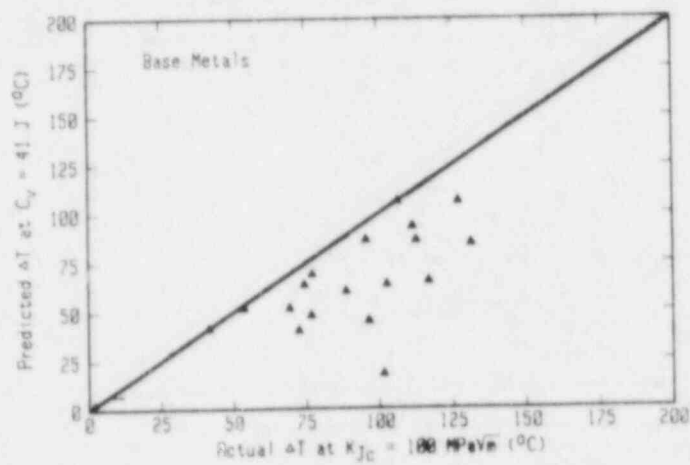


Fig. B-9 Comparison of $\Delta T(K_{JC} @ 100 \text{ MPa}\sqrt{\text{m}})$ from the experimental data with values of $\Delta T(C_V @ 41 \text{ J})$ predicted using ASTM E 900 (Ref. 12).

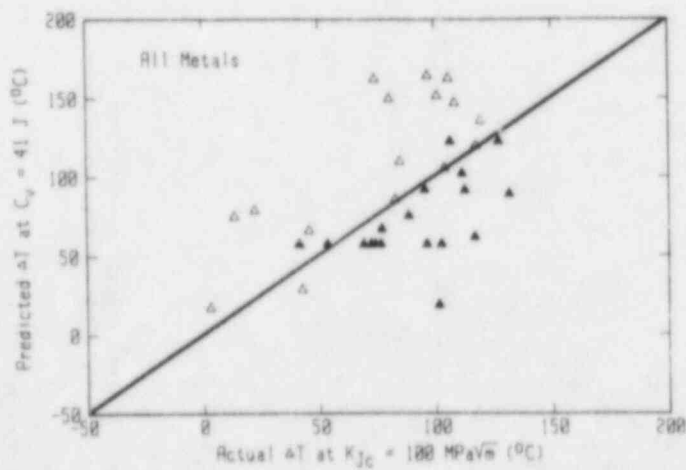
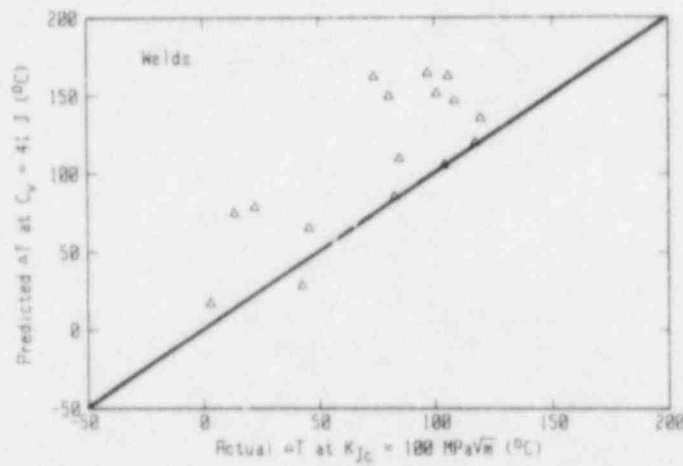
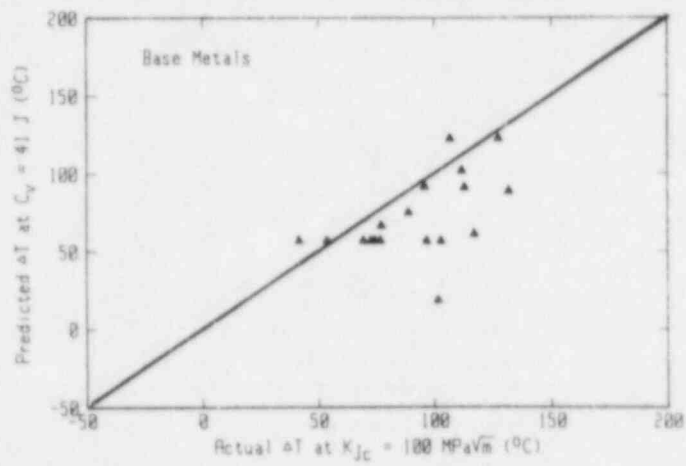


Fig. B-10 Comparison of $\Delta T(K_{Jc} @ 100 \text{ MPa}\sqrt{\text{m}})$ from the experimental data with values of $\Delta T(C_v @ 41 \text{ J})$ predicted using Varsik (Ref. 13).

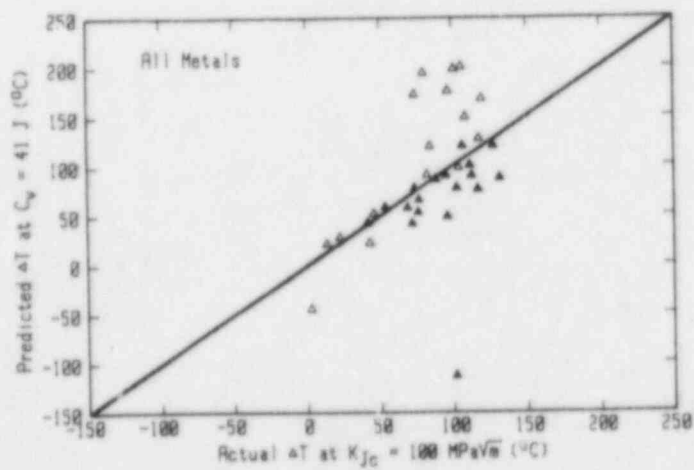
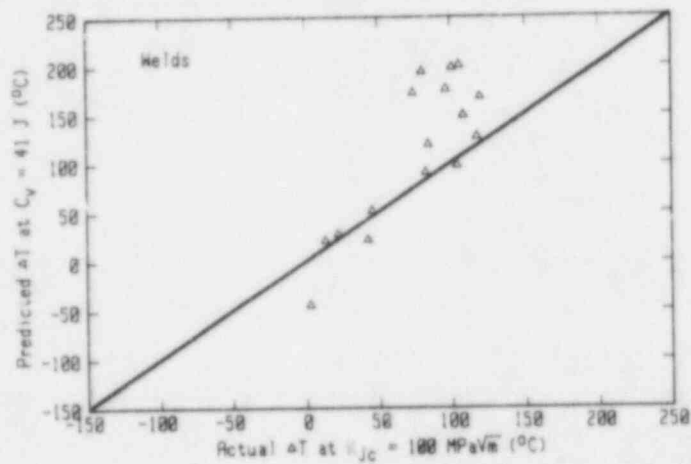
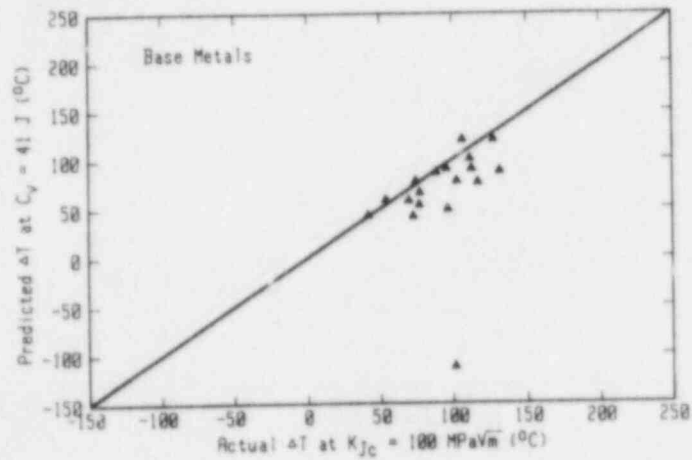


Fig. B-11 Comparison of $\Delta T(K_{Jc} @ 100 \text{ MPa}\sqrt{\text{m}})$ from the experimental data with values of $\Delta T(C_v @ 41 \text{ J})$ predicted using Varsik/Byrne (Ref. 14).

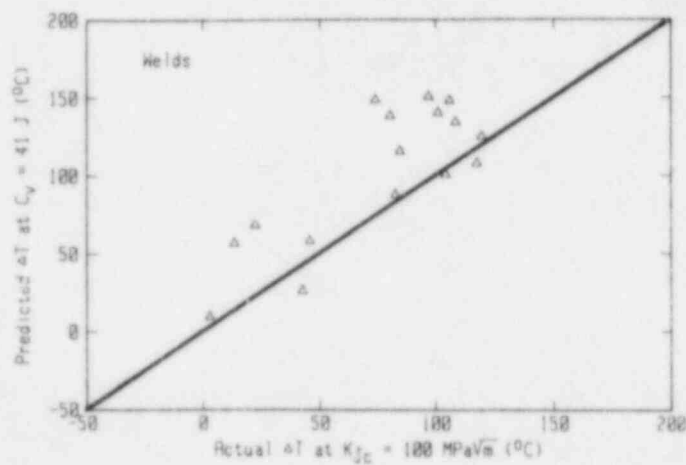


Fig. B-12 Comparison of $\Delta T(K_{Jc} @ 100 \text{ MPa}\sqrt{\text{m}})$ from the experimental data with values of $\Delta T(C_y @ 41 \text{ J})$ predicted using revised Varsik/Byrne (Ref. 13).

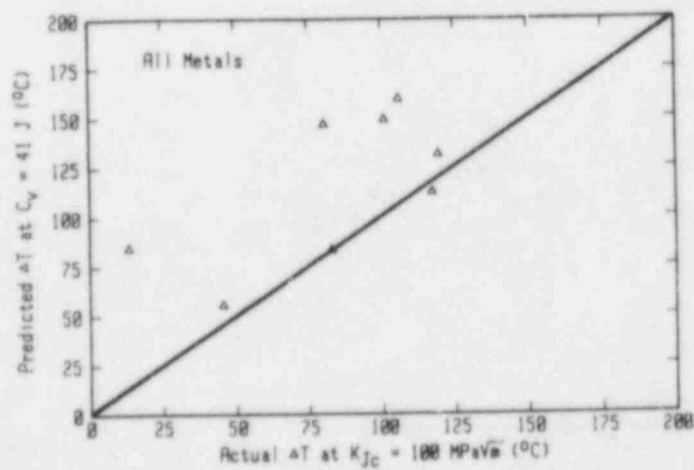
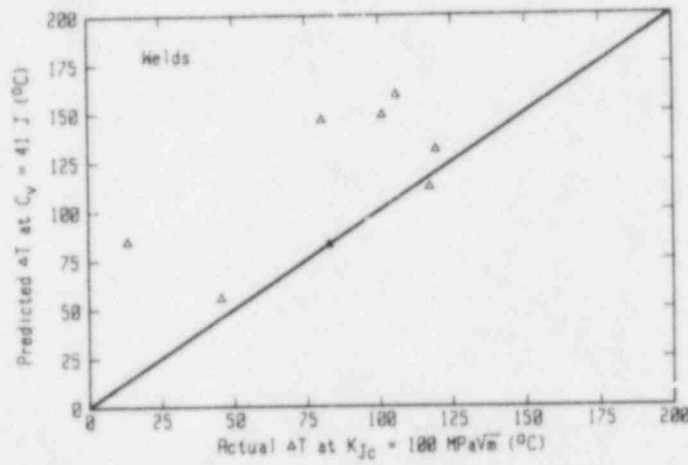
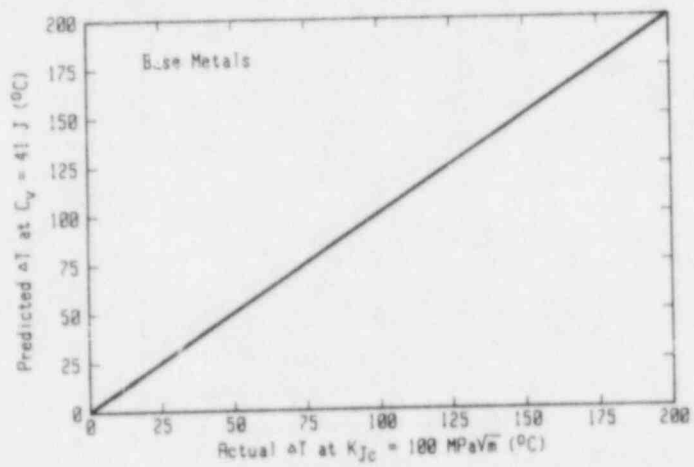


Fig. B-13 Comparison of $\Delta T(K_{Jc} @ 100 \text{ MPa}\sqrt{m})$ from the experimental data with values of $\Delta T(C_v @ 41 \text{ J})$ predicted using Heller/Lowe (Ref. 15). This correlation is applicable to Linde 80 welds only.

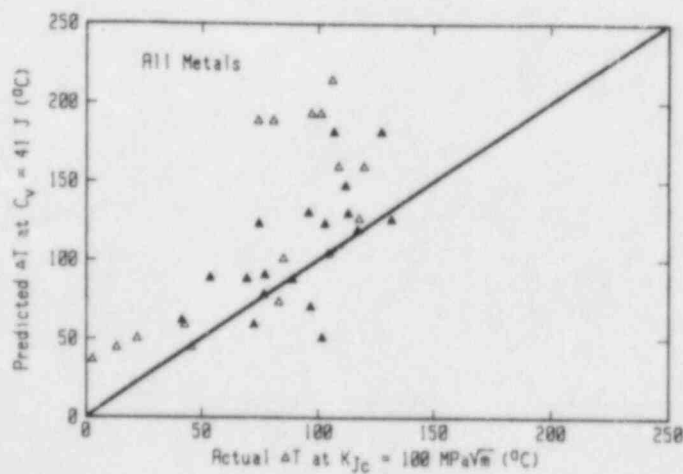
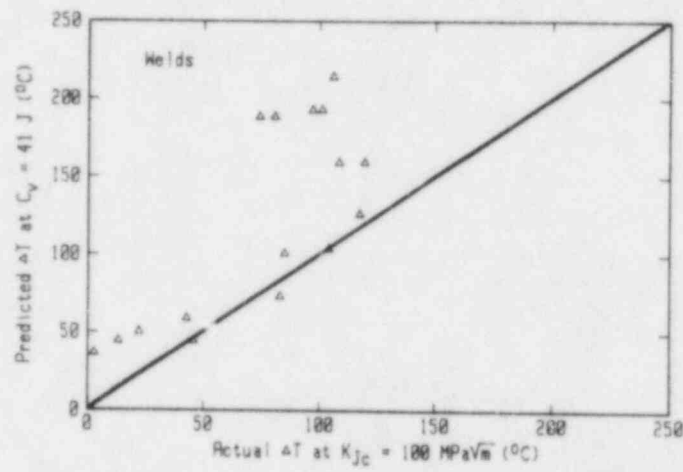
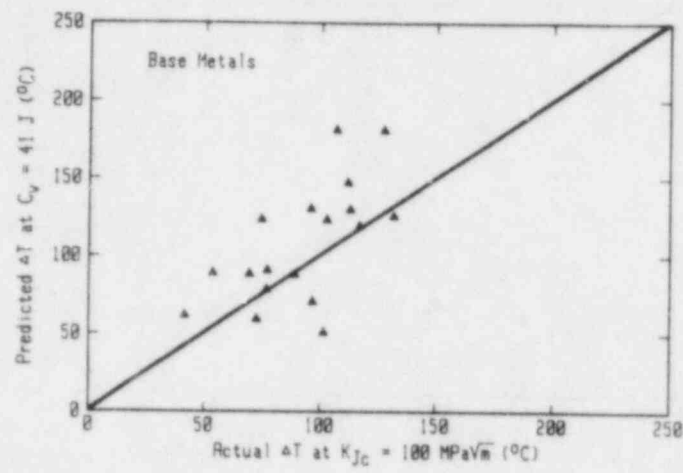


Fig. B-14 Comparison of $\Delta T(K_{Jc} @ 100 \text{ MPa}\sqrt{\text{m}})$ from the experimental data with values of $\Delta T(C_v @ 41 \text{ J})$ predicted using Berggren/Stallman (Ref. 16).

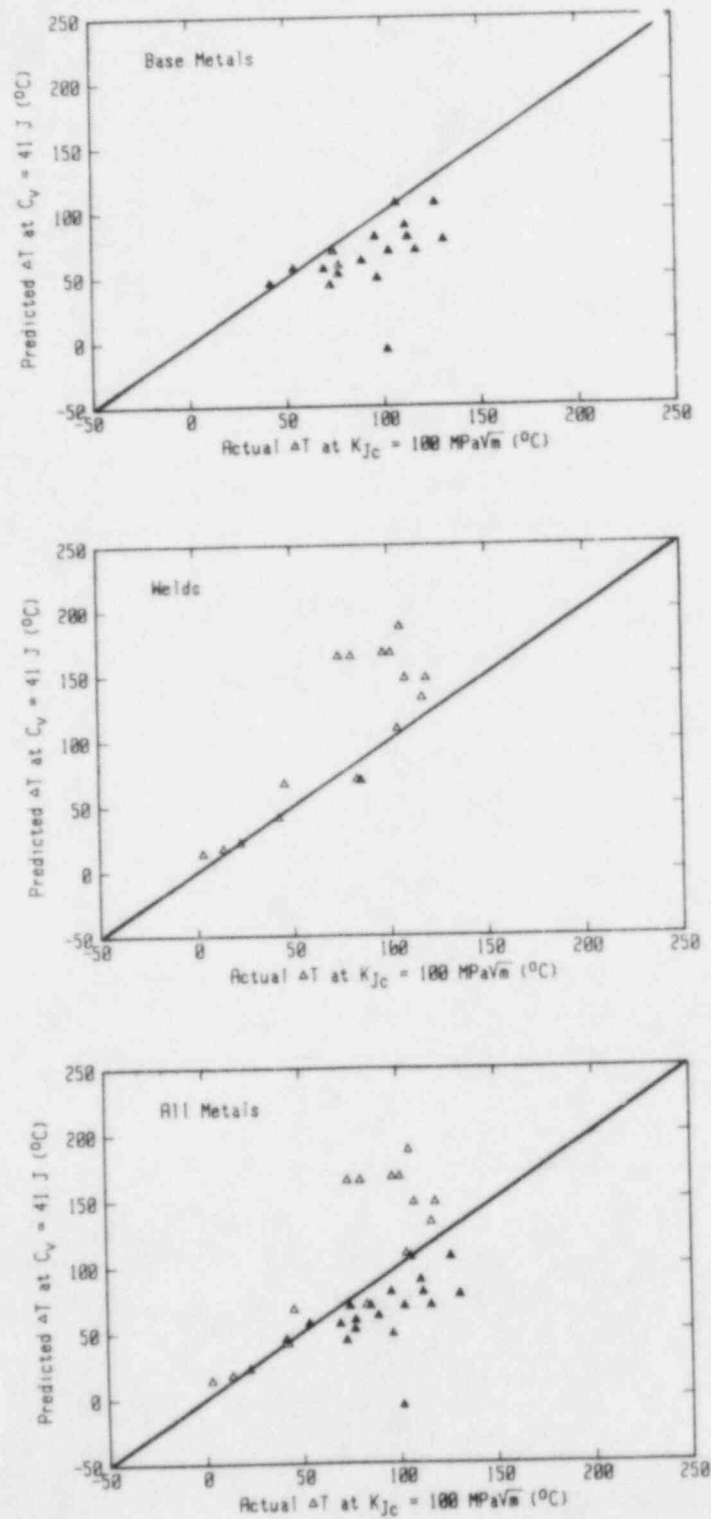


Fig. B-15 Comparison of $\Delta T(K_{Jc} @ 100 \text{ MPa}\sqrt{\text{m}})$ from the experimental data with values of $\Delta T(C_v @ 41 \text{ J})$ predicted using Regulatory Guide 1.99, Rev. 1 (Ref. 17).

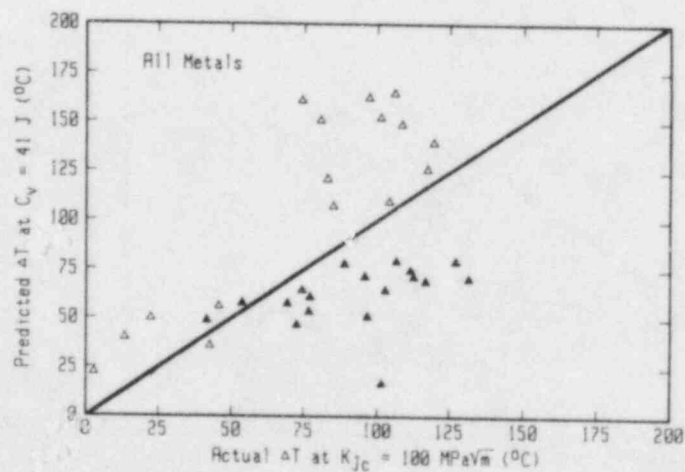
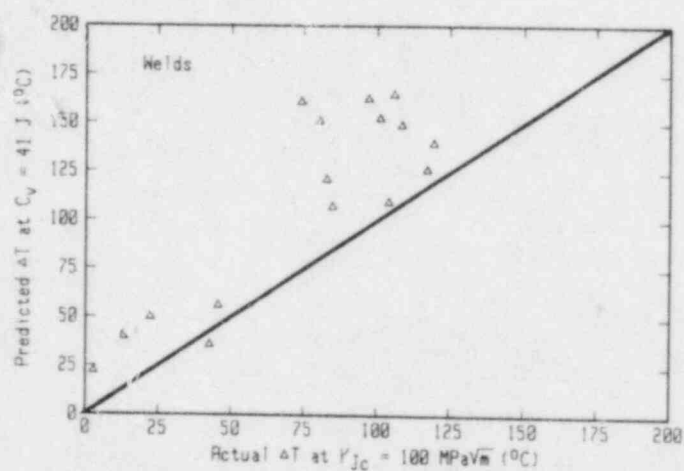
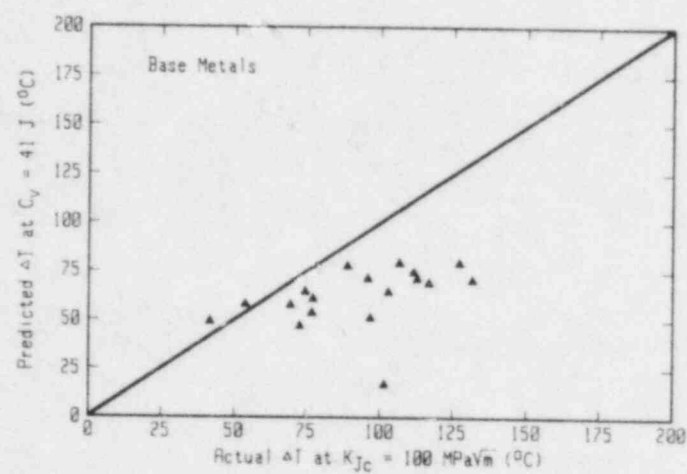


Fig. B-16 Comparison of $\Delta T(K_{Jc} @ 100 \text{ MPa}\sqrt{\text{m}})$ from the experimental data with values of $\Delta T(C_v @ 41 \text{ J})$ predicted using draft of Revision 2 to Regulatory Guide 1.99 (Ref. 18).

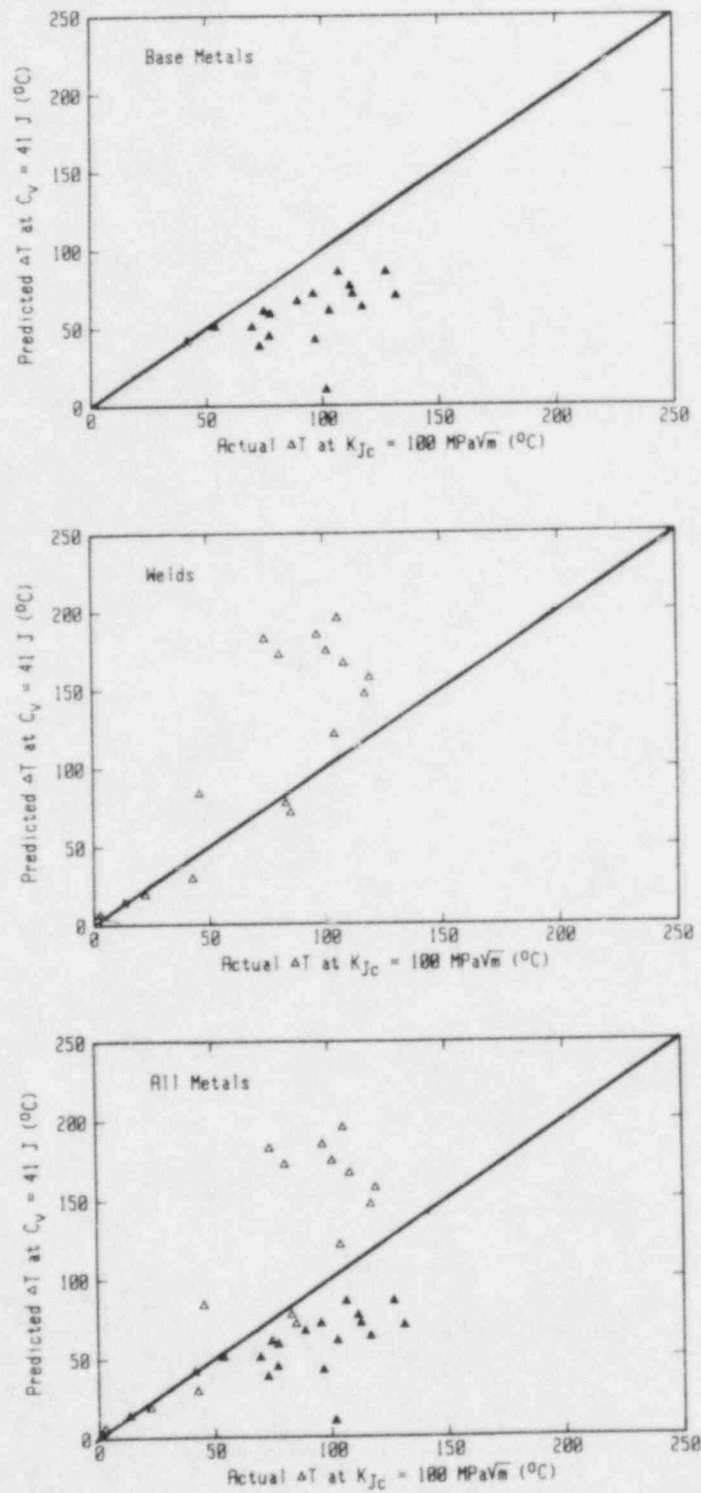


Fig. B-17 Comparison of $\Delta T(K_{JC} @ 100 \text{ MPa}\sqrt{\text{m}})$ from the experimental data with values of $\Delta T(C_V @ 41 \text{ J})$ predicted using NRC Screening Criteria (Ref. 19).

NRC FORM 335 (11-81)		U.S. NUCLEAR REGULATORY COMMISSION BIBLIOGRAPHIC DATA SHEET		1. REPORT NUMBER (Assigned by DDC) NUREG/CR-4395 MEA-2086	
4. TITLE AND SUBTITLE (Add Volume No., if appropriate) Correlation of C_v and K_{Ic}/K_{Jc} Transition Temperature Increases Due to Irradiation				2. (Leave blank)	
7. AUTHOR(S) Allen Hiser				3. RECIPIENT'S ACCESSION NO.	
9. PERFORMING ORGANIZATION NAME AND MAILING ADDRESS (Include Zip Code) Materials Engineering Associates, Inc. 9700-B George Palmer Highway Lanham, MD 20706-1837				5. DATE REPORT COMPLETED MONTH YEAR September 1985	
12. SPONSORING ORGANIZATION NAME AND MAILING ADDRESS (Include Zip Code) Division of Engineering Technology Office of Nuclear Regulatory Research U. S. Nuclear Regulatory Commission Washington, DC 20555				DATE REPORT ISSUED MONTH YEAR November 1985	
13. TYPE OF REPORT Technical Report				6. (Leave blank)	
15. SUPPLEMENTARY NOTES				8. (Leave blank)	
16. ABSTRACT (200 words or less) <p>Reactor pressure vessel (RPV) surveillance capsules contain Charpy-V (C_v) specimens, but many do not contain fracture toughness specimens; accordingly, the radiation-induced shift (increase) in the brittle-to-ductile transition region (ΔT) is based upon the ΔT determined from notch ductility (C_v) tests. Since the ASME K_{Ic} and K_{IR} reference fracture toughness curves are shifted by the ΔT from C_v, assurance that this ΔT does not underestimate ΔT associated with the the actual irradiated fracture toughness is required to provide confidence that safety margins do not fall below assumed levels.</p> <p>To assess this behavior, comparisons of ΔT's defined by elastic-plastic fracture toughness and C_v tests have been made using data from RPV base and weld metals in which irradiations were made under test reactor conditions. As well, comparison of ΔT's at various index levels gives indications of C_v, K_{Ic} and K_{Jc} curve shape change due to irradiation. Lastly, comparisons between measured $\Delta T(C_v)$ and values using various correlations or models are also made.</p>				10. PROJECT/TASK/WORK UNIT NO. 11. FIN NO. B8900	
17. KEY WORDS AND DOCUMENT ANALYSIS Notch ductility, fracture toughness, radiation embrittlement, β_{Ic} correction, nuclear pressure vessel steels and welds, test method correlations				14. (Leave blank)	
17b. IDENTIFIERS/OPEN-ENDED TERMS				19. SECURITY CLASS (This report) Unclassified	
18. AVAILABILITY STATEMENT Unlimited				20. SECURITY CLASS (This page) Unclassified	
				21. NO. OF PAGES 22. PRICE 5	

UNITED STATES
NUCLEAR REGULATORY COMMISSION
WASHINGTON, D.C. 20555

OFFICIAL BUSINESS
PENALTY FOR PRIVATE USE, \$300

FOURTH CLASS MAIL
POSTAGE & FEES PAID
USNRC
WASH. D.C.
PERMIT No. G-87

120555078877 1 1A1RF1R5
US NRC
ADM-DIV OF TIDC
POLICY & PUB MGT EC-PDR NUREG
F-801 DC 20555
WASHINGTON

NUREG/CR-4395

CORRELATION OF C_v AND K_{ic}/K_{jc} TRANSITION TEMPERATURE INCREASES
DUE TO IRRADIATION

NOVEMBER 1985